Gas Pipelines Corrosion Data Analysis and Related Topics

by

Daniel Lewandowski

A thesis submitted to the Delft University of Technology in conformity with the requirements for the degree of Master of Science.

Delft, The Netherlands

Abstract

Gas Pipelines Corrosion Data Analysis and Related Topics

by Daniel Lewandowski

Chairperson of Graduate Committee: *Prof. dr Roger M. Cooke*
Department of Mathematics

Graduate Committee: *Prof. dr Roger M. Cooke*
Ir. Eric Jager
Drs. Robert Kuik
Dr Dorota Kurowicka
Prof. dr Thomas A. Mazzuchi

In The Netherlands the grid of gas pipelines consists of over 11,000 km of steel pipes, most of the them laid in '60s. A large percentage of the grid reaches the age when corrosion of the pipelines is becoming increasingly important. Recently N.V. Nederlandse Gasunie, the leading Dutch gas company, has performed inspections of few of their pipelines. This thesis describes and analyzes with details the corrosion data collected during the inspection. The data includes information on percentage of metal loss and positions of the corrosion spots along the pipe. The preliminary analysis brings closer some statistical characteristics of the occurrence of corrosion and tries to find patterns in the data. Furthermore, there exists a Monte Carlo model which predicts failure frequency of gas pipelines given full characteristic of a pipe. Part of the thesis compares the results obtained by running the model with the actual data.

Acknowledgements

The author wishes to express sincere appreciation to the Delft University of Technology, where he has had the opportunity to work with Roger M. Cooke, *il miglior fabbro*, Dorota Kurowicka and Thomas A. Mazzuchi. Thanks to Eric Jager and Gerard Stallenberg from N.V. Nederlandse Gasunie for proposing the subject of this thesis, providing data and helpful explanations of issues related to the maintenance of gas pipelines. The author would also like to acknowledge Kasia, Paweł and Cornel for being good friends during these two years spent in Delft.

Last but not least, the author would like to acknowledge his parents and sister for their continuous support.

Contents

List of tables

List of figures

List of symbols

Input and output variables of the model introduced in Chapter 3 are listed and briefly described in Appendix B.

$E(X)$	mean value (expectation) of variable X
σ_X	standard deviation of variable X
$\rho(X,Y)$	product moment correlation of variables X and Y
$\rho_r(X,Y)$	rank correlation of variables X and Y
Ω	Ohm, unit of electric resistance
e	constant, base of a natural logarithm
$\ll$	relation symbol, significantly less then
F	frequency
P	probability
C	damage to pipeline coating
S	small pipeline damage
L	large pipeline damage
t_C	wall thickness removed by coating damage
t_S	wall thickness removed by small damage
t_L	wall thickness removed by large damage
d_0	default pipeline diameter
r_0	default soil resistivity
pH_0	default pH factor value
$p_1, p_2, \ldots, p_{14}$	linear terms in the Taylor expansion, Section 3.4
F_0	default frequency of damage to coating due to environment
CR_f	free corrosion rate, cathodic protection wholly non-functional
CR_{f0}	default free corrosion rate
CR_p	partial corrosion rate, cathodic protection partially functional
CR_{st}	stray current corrosion rate
cr	correlation ratio

List of abbreviations

Ω.cm	Ohm centimeter
km.yr	kilometer year
FCL	frequency of closed digs per km.yr
FOP	frequency of open digs per km.yr
MFL	magnetic flux leakage
LNG	liquified natural gas
CDE	coating damage due to environment
CP	cathodic protection system
SP	stray current protection system
$MTTF$	mean time to failure

Glossary of terms

%bit	%km with bitumen coating
%ebe	% of coating damages due to ground movement, root growth or chemical contamination; bitumen
%epe	% of coating damages due to ground movement, root growth or chemical contamination; polyethylene
b	birthyear
bs	%1km pipe near bond site
ch	%km with heavy industrial contamination
cps	year of cathodic protection (CP) installment
crf	free corrosion rate
crfz	default free corrosion rate
crp	corrosion rate when CP partially functional
crpe	pit corrosion rate if the pipe ground potential is -700 mV
crse	corrosion rate if there are unprotected stray currents
dia	diameter
dl	prob. of direct leak from 3rd parties
dpth	depth [m]
fcl	frequency of closed digs per km.yr
fclz	freq. of closed digs per km.yr; 0th order
fop	frequency of open digs per km.yr
fopz	freq. of open digs per km.yr; 0th order

grb	rate of occurrence of bitumen defects (per 100 km)
grp	rate occurrence of polyethylene defects (per 100 km)
hcone	freq. of hitting per km.yr; closed dig, no oversight
hconz	freq. of hitting per km.yr; closed dig, no oversight, 0th order
hcoye	freq. of hitting per km.yr; closed dig, oversight
hcoyz	freq. of hitting per km.yr; closed dig, oversight, 0th order
hoone	freq. of hitting per km.yr; open dig, no oversight
hoonz	freq. of hitting per km.yr; open dig, no oversight, 0th
hooye	freq. of hitting per km.yr; open dig, oversight
order	
hooyz	freq. of hitting per km.yr; open dig, oversight, 0th order
pcen	prob. of coating damage from environment
pcpfe	prob. that CP fails completely
pcppe	prob. that CP fails partially
pc3	prob. of coating damage from 3rd parties
ph	pH value
pl	prob. of large pipe damage
ps	prob. of small pipe damage
pspe	prob. that stray current protection fails at bond site
r	resistivity
rcon	perc. of repaired damages due to hits during closed digs without oversight
rcoy	perc. of repaired damages due to hits during closed digs with oversight
roon	perc. of repaired damages due to hits during open digs without oversight
rooy	perc. of repaired damages due to hits during open digs with oversight
rt	%km with heavy roots growth
rup54	perc. of direct leak which will be ruptures per km.yr; 5.4 mm wt
rup71	perc. of direct leak which will be ruptures per km.yr; 7.1 mm wt
t	pipe wall thickness [mm]
tl	material removed by large line damage [mm]
ts	material removed by small line damage [mm]
wf	%km with fluctuation under and above water table
wu	% km under water table
xbche	#defects per 100 km if chemical contamination; bitumen
xbde	#defects per 100 km if diameter = 36”; bitumen
xbrte	#defects per 100 km if heavy root growth; bitumen
xbwfe	#defects per 100 km if water table fluctuates; bitumen
xpche	#defects per 100 km if chemical contamination; polyethylene
xc	critical thickness fraction; coating damage

xl	critical thickness fraction; large damage
xpde	#defects per 100 km if diameter = 36"; polyethylene
xphe	pit corrosion rate if pH is raised by 2.3
xprte	#defects per 100 km if heavy root growth; polyethylene
xpwfe	#defects per 100 km if water table fluctuates; polyethylene
xre	pit corrosion rate if resistivity is a factor 10 lower
xs	critical thickness fraction; small damage
xwfe	pit corrosion rate if water table fluctuates
xwue	pit corrosion rate if water table is above pipe lines
yb	begin year for cumulative frequency of corrosion
ye	end year for cumulative frequency of corrosion

Introduction

Nature of industrial hazard

Industrialization and technological development are irreversible processes, which significantly influence human life and its quality. Aside from good and desirable consequences of these processes, there are also some visible side effects, like emission of toxical materials, noise, as well as hidden threats - industrial constructions are very complex and may involve seides of high emergency. All these dangers have been perceived and now there is a significant effort concentrated on eliminating or minimizing industrial risks. One of the sources of risk is transmission of hazardous substances, like oil or gas, in pipelines. Steel gas pipelines are exposed to many factors supporting growth of the corrosion. To be able to prevent this growth, many methods and techniques have been developed. These include passive prevention like bitumen or polyethylene coating, as well as active methods involving change of electrostatic characteristic of the pipe.

Goals of the research

This thesis concentrates on analysis of the corrosion data obtained by inspecting gas pipelines owned by N.V. Nederlandse Gasunie, Dutch gas company. Using MFL-pigs[1] (Magnetic Flux Leakage), also called "intelligent pigs", five pipelines were inspected. One of the pipelines have been reinspected and this data is also available. The data contains information on the wall thickness reduction, assumed to be caused by 3rd party digs or corrosion. The goal of this thesis is to bring closer a wide spectrum of safety and maintenance issues the gas industry, the Dutch gas industry in particular, must deal with. These

[1]For more detailed specification of MFL-pigs please refer to Chapter 2.

issues will be presented from a mathematical point of view. Firstly, Chapter 1 describes the safety regulations to which the gas pipelines operators are subject. The implication of those regulations is the requirement for appropriate maintenance of pipelines, including their inspections. Chapter 2 contains a small sample of the data collected during one of the inspections and general overview of all of the data sets provided by Gasunie. The actual data will be compared with the outputs of a probabilistic model of failure frequency of gas pipelines. The model was developed using a software program for uncertainty analysis with correlations written at Delft University of Technology, UNICORN, and is introduced with details in Chapter 3. Since the model is rather complicated, it might be interesting to study dependencies between input and output variables of the model. This will be done by sensitivity analysis. A general tool for this type of analysis is introduced in Chapter 4 and its application to UNICORN model is described in Chapter 5. Afterwards begins the actual analysis of the Gasunie's corrosion data. In Chapter 6 the data is visualized and compared to the model output, which allows us to evaluate performance of the model and eventually to recommend some future extensions of the model. Chapter 7 deals with determining the corrosion rate based on the data, since this is a hot topic now. Besides this, some additional tasks have been performed including writing a software application on the basis of UNICORN. The new front end is designed to run only the model introduced in Chapter 3. It will be presented with screen shots in the same chapter. Appendix A contains the help file for this front end and in Appendix B the reader will find the implementation of the model in UNICORN, with descriptions and definitions of input parameters and output formulas. Appendix C contains the MatLab code used in preliminary analysis of the data (Chapter 6).

The provided data proved to be very useful. Direct comparison with the UNICORN model outputs showed very good performance of the later in terms of predicting the failure frequency. Basically, for all of the inspected cases the actual data corresponded to 20^{th} – 80^{th} percentile of the distributions of failure frequency per km.yr. However, in most cases the results varied even less and were between 20^{th} and 45^{th} percentile of the distributions, what suggests a small tendency of the model to overestimate the frequency of failures.

The data sets reveal dissimilarities between the inspected pipelines. Pipeline A, A1 and B data report defects mostly located at the bottom of the pipelines,

whereas in case of Pipeline C, D and E data the defects are spread more uniformly, regardless if it is the top or the bottom of the pipeline. The Kolmogorov-Smirnov test allowed to distinct three groups of the pipelines. Data from pipelines in each of the groups can be regarded as drawn from the same underlying distribution. The first group are pipelines A, A1 and B, in the second one are Pipeline C and D. The last group consists of only Pipeline E.

Dutch gas industry

The first gas deposits in The Netherlands were discovered long before the Second World War. In 1933, the Batavian Petroleum Company (BPM, a subsidiary of Shell), decided to acquire rights for exclusive exploration of gas-rich fields in provinces of Groningen, Friesland, Drenthe, Overijssel and Gelderland. On 19 September 1947 the Dutch Petroleum Company (NAM) was set up, with BPM and Standard Oil Company (New Jersey), i.e. Esso, each taking a 50% share. At this time the whole natural gas production was located in the eastern part of The Netherlands. In 1962 the official natural gas supply by the NAM was one million cubic meters per day. On 18 October 1960 the NAM informed that the reserves in the Groningen gas field were greater than foreseen. A team from Esso proposed that the gas should initially be sold in the small users' market, in the public supply. Three gas companies - State Mines, Shell and Esso, signed a partnership which would sell the gas extracted to a limited company yet to be set up. This company would be responsible for purchasing, transporting and selling Dutch natural gas (and also other gases). The charter of the N.V. Nederlandse Gasunie was signed in the Old Wassenaar Castle on 6 April 1963. Shortly after that, Gasunie started to develop their network of large diameter natural gas pipelines.

Chapter 1

Gas pipelines safety regulations

In general, pipelines are recognized as a safe way to transport dangerous substances. However, pipelines accidents have occurred in Europe and worldwide, indicating that pipelines should be included within scope of the Seveso II Directive. This legislation regulates safety requirements imposed on companies dealing with hazardous materials. There was no general agreement on this issue, noweven, and pipes were excluded from the directive. Currently the European Council is discussing about introducing a separate legislation for pipeline transport. Basically, safety of the transport of dangerous substances in pipelines is regulated by national legislation and regulations, which can vary significantly even among the member states of EU. All major incidents related to gas pipelines in The Netherlands are investigated by a independent governmental body, the Dutch Transport Safety Board.

1.1 Gas safety guidelines and recommendations

Gas pipeline safety assessment and management concentrates on the release of the transported medium (leakage, rupture) from a pipeline. There are four well-known books describing methods and recommendations in designing and maintaining gas pipelines. Methods for determining and processing probabilities are described in the *Red Book (CPR 12E)*. The study of the physical effects from releases of hazardous materials is described in *Yellow Book (CPR 14E)*. The *Green Book (CPR 16E)* contains methods of determining the possible damage to people. Finally, risks due to transport of hazardous substances via

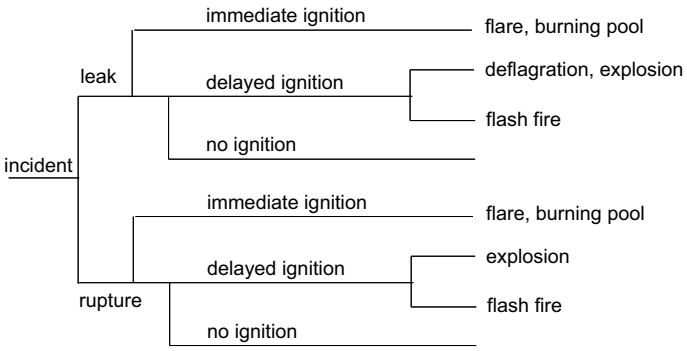

Figure 1.1: Example of incident scenarios for flammable media.

pipelines (and other installations) in The Netherlands are calculated according to the guide *Guidelines for quantitative risk assessment (CPR 18E)*, so-called *Purple Book*. All four books make up a guideline to the safety studies and are widely applicable in the pipeline industry, gas pipeline industry especially. The supervisory body is in this case the Committee for the Prevention of Disasters (CPR). This institution defines some safety requirements (CPR 1999) that must be met at the stage of designing a new pipeline:

> *The design must seek to reduce the environmental risk (probability and effect of leakage) presented by the system to an acceptable minimum:*
>
> - *in defining the route, minimum distances from occupied buildings (location classification) must be maintained;*
> - *the physical design of the system, including additional facilities connected or related to the system, must be such as to limit the effects of leakage.*

1.2 Risk assessment

Risk assessment for pipelines must answer a number of questions. First of all, we need to find the mode of escape and dispersion of the medium from a pipe. This is particularly important, when the transported medium is flammable, explosive and/or toxic. Furthermore, an analysis of possible accident scenarios must be carried out.

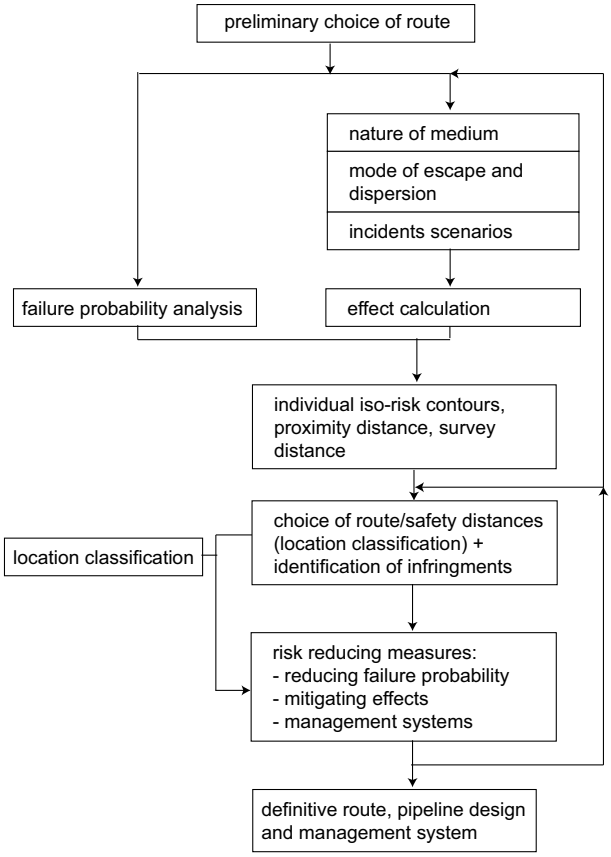

Figure 1.2: Hypothetical safety evaluation path.

There should be a safety evaluation carried out prior to creating a new pipeline. The same should be done for existing pipelines if there is a change in the (CPR 1999):

- piped medium
- maximum operating pressure
- maximum operating temperature
- area adjacent to the pipeline as a result of physical planning decisions

> *This safety evaluation must be based on an analysis of the individual risk and an evaluation of the design, the organizational and technical measures and the nature of the surrounding area.*

Then based on this evaluation, final decision on the route is made (Figure 1.2).

Area	Location Classification
scattered residential housing or no residential housing	1
less important special premises	2
residential areas, recreational areas or industrial areas	3
apartment building or important special premises	4

Table 1.1: Location classification.

1.3 Location classification

We can see that, as with other potentially hazardous structures, the land-use planning must be performed in case of pipelines. Location classification is performed in order to be able to distinguish (CPR 1999):

- population density
- building density
- presence of sensitive sites which are centers of human activity
- level of industry activity and the economic value

All structures and installments in neighborhood of a pipeline must be classified into four categories mentioned in Table 1.1. The higher the location classification, the smaller acceptable risk.

The individual risk is the probability that a person will die by accident when he is at a certain location for a year. The iso-contour of the individual risk connects points with equal individual risk and is called the risk contour. The minimum acceptable distances are derived from analysis of the risk contours. There are two basic concepts applied to determine the acceptability of the assumed road for a pipeline:

proximity distance - the shortest distance between the center of the pipeline and residential buildings or special structures; coincides with the 10^{-6} iso-risk contour (max. permissible individual risk)

Nominal diameter	**Proximity distances [m]**			**Survey distances [m]**		
inch	20-50 bars	50-80 bars	80-110 bars	20-50 bars	50-80 bars	80-110 bars
2	4	5	5	20	20	20
4	4	5	7	20	20	25
6	4	5	7	20	25	30
8	7	8	10	20	30	40
10	9	10	14	25	35	45
12	14	17	20	30	40	50
14	17	20	25	35	50	60
16	20	20	25	40	55	75
18	$*$	20	25	45	60	70
24	$*$	25	25	60	80	95
30	$*$	30	35	75	95	120
36	$*$	35	45	90	115	140
42	$*$	45	55	105	130	160
48	$*$	50	60	120	150	180

$*$ - distance to be determined in consultation between the parties involved in the project

Table 1.2: Proximity and survey distances in meters.

survey distance - the distance measured on both sides from the center of the pipeline within a survey is made to identify the presence of residential buildings, special structures and recreational and industrial areas; coincides with the 10^{-8} iso-risk contour.

Research has shown that calculation of the iso-risk contours can be dispensed with gas pipelines if the values given in Table 1.2 are used for the proximity distance and the survey distance from buildings. Currently these values are under review. It is expected that these will change in the near future.

Gasunie has purchased population density data of The Netherlands, to be able to carry out quantitative risk assessment concerning influence of the population density on frequency of pipelines failures. Moreover, locations of new pipelines are consulted with the regional authorities using their population data.

For transport pipelines the minimum separation distance from the nearest installation must be at least equal to the survey distance. However, some departures from this requirement are allowed. This is the case, when shorter distance is justified on planning, technical or economic grounds, but it cannot be less then the proximity distance. For locations where the individual risk induced by the presence of a pipeline is between 10^{-6} and 10^{-8} per year, a careful assessment must be carried out of all of the interests involved. This includes primary effects of release of the medium transported by the pipeline like:

- environmental pollution
- combustion/explosion following ignition
- physical explosion
- toxicity

Secondary consequential damages caused by one of the above mentioned incidents must be taken into account as well. This can be for example flood, erosion, blockage of shipping routes.

1.4 Other risk minimizing factors

There are also some restrictions concerning depth cover of pipelines. Obviously, the deeper a given pipe is laid, the smaller probability of hitting during 3$^{\text{rd}}$ party digs. The minimum depth cover must have 80 cm and must be increased if there is a likelihood of:

- deep ploughing or deep excavation
- grading works

or lays beneath road surfaces. If providing the required depth of cover is difficult, then the pipe must be protected with a cover, mainly concrete one. In places where the pipe crosses ditches or watercourses, it must be laid to a depth of at least 60 cm, unless a concrete cover is applied.

Many regulations concern pipe wall thickness to protect against mechanical damage and corrosion (CPR 1999):

The specified minimum yield strength divided by the circumferential stress at design pressure must be equal to or greater than the wall thickness allowances for mechanical damage.

1.5 Inspection, reporting and maintenance policy

Risk contours are calculated based on the probability of a pipeline failure. Therefore it is very important to maintain a well-designed failure database, since the failure analysis is based on historical data. The data is collected by inspecting the pipelines.

Failure data shows that the most important factors causing pipelines damages are third party activities. This can be for example laying telecommunication cables, pitting foundations etc. It must be ensured that the underground gas pipelines are marked and gas supplier employee supervise earthworks, especially those using heavy machines.

Australian gas regulations (Gas Safety (Safety Case) Regulations 1999) states, that safety management system must specify a number of issues regarding gas pipelines. Among other things they are:

- technical standards used in the design, construction, installation and operation of the facility
- clear definition of organizational structure and responsibilities
- control systems like alarm systems, temperature and pressure measure systems, emergency shut-down systems
- machinery and equipment must be specified to ensure that the equipment is fit for the purpose
- specification of the response plans designed to address all reasonably foreseeable emergencies
- emergency communication system adequate to communicate within facility and with the relevant fire authorities and emergency service

- internal monitoring, auditing and reviewing to ensure appropriate implementation of safety policies, objectives and procedures specified in SMS
- gas incidents recording, investigation and reviewing
- training to ensure that all employees have proper skill, knowledge and experience

Other national legislation concerning risk management of the gas facilities is more or less constructed with the same pattern. For example, English national regulations specify detailed procedures of acting in case of incidents involving gas (Health and Safety: The Gas Safety (Installation and Use) Regulations 1998). If escape of gas from a pipe occurs, a gas supplier must within 12 hours of being so informed of the escape, prevent the gas escaping.

In 1998 the U.S. Research and Special Programs Administration published a proposal replacing most LNG (Liquefied Natural Gas) requirements for siting, design, construction, equipment and fire protection. It also proposed some minor amendments to operation and maintenance requirements for new and significantly altered facilities. Those changes were proposed in order to more accurately reflect current technology and practices in the LNG industry and replace the regulations from 1979.

Recently in the U.S. the Department of Transportation of the Office of Pipeline Safety prepared amendments to some safety regulations. In January 2000 new safety standards for the repair of corroded or damaged steel pipe in gas or hazardous liquid pipelines have been introduced. Another legislation act is making changes to the reporting requirements for hazardous liquid pipeline accidents. The rule lowers the current reporting threshold of 50 barrels to a new threshold of 5 gallons, and makes changes to the accident report form. The changes are necessary, because the existing reporting threshold and reporting form have been recognized as not sufficiently informative for efficient safety analysis. This rule is effective since 1 January 2002.

One of the main factors having great impact on frequency of gas pipelines failures is corrosion. Progressing corrosion reduces the pipe wall thickness, causing a strength to stress to drop significantly. Since the gas in a pipe is under heavy pressure, pipe failure is a direct implication of the weak strength. It is extremely important to have a system of inspecting pipelines in order

to prevent a gas leakage. There is no system of continuous monitoring so far. One of the most applicable methods of gas pipelines inspection is to let intelligent pig into the interior of the pipeline. Then the pig travels along the pipe, propelled by slowly flowing gas and collects corrosion data. The "intelligent pig" is a device full of sensors capable of measuring deviation in the pipe wall thickness and position of the deviations. This method ensures saving the pipe from uncovering, but it is still very expensive (order of hundred thousands euros per run). Therefore only few pig runs have been performed in The Netherlands so far, but new runs are planned. Gasunie owns 11,600 km of pipelines in The Netherlands and inspecting all of them would be too expensive for the company. Thus, some pipeline sections are chosen. This is a rather subjective choice, sometimes supported by failure frequency models. This thesis analyzes data collected by Gasunie during six pig runs. One of the pipes was inspected twice in a period of 18 months.

1.6 Future initiatives

In 1996 the U.S. Gas Research Institute (GRI) introduced pipeline safety program which aimed in development of three main areas of pipeline safety research: inspection, integrity and monitoring. Current inspection measurements are far from perfect, while the intelligent pigs are not capable to detect corrosion with certainty and only 25 – 30 % of the U.S. pipeline system can be inspected by this type of devices (the same holds for the Dutch pipeline system). Therefore there is a huge effort directed towards expanding the capabilities of current intelligent pigs, focusing on improvements in current magnetic flux leakage technology. New methods of pipeline monitoring are in development as well. An example can be airborne instrumentation designed to determine the level of cathodic protection, measure the depth of cover and detect leaks along a pipeline. Due to very fast technological progress many pipeline risk related issues need development and evaluation (GRI objectives):

- an assessment of technology applicable to the inspection of pipeline segments which are currently unpiggable
- an evaluation of the risk assessment and risk management systems being used by the natural gas industry in the U.S., Canada and Europe

- an analysis of promising near-term pipeline monitoring technologies
- development of a national damage prevention/one-call system and anatomical mapping standard
- development of risk management as an alternative to current prescriptive regulations

It seems to be likely, that the development of safety standards in Europe will go in the same way.

The United States have a very good pipelines risk management system. The first priority of the U.S. pipeline industry is the Office of Pipeline Safety, which develops regulations and other approaches to risk management to assure safety in design, construction, maintenance and emergency response of pipeline facilities. In The Netherlands the gas sector has a rather significant freedom in establishing safety regulations. Basically, the largest Dutch gas company, N.V. Nederlandse Gasunie, must meet the requirements imposed by the Dutch government, but they are consulted before the regulations take effect. Nowadays, Gasunie is working on a proposal of new regulations concerning safety of gas facilities.

Risk assessment of natural gas transmission systems can be simplified and accelerated by using computer programs. A very well-known example of such a software is PIPESAFE, which is a result of joint work of many international gas companies, including N.V. Nederlandse Gasunie.

Chapter 2

Description of the Gasunie data

2.1 MFL-pig

The pipelines were inspected by so-called "intelligent pigs", which return detailed information on metal loss along the pipeline. This device makes use of the magnetic flux leakage principle and can be applied to detect internal, midwall and external metal loss, cracks and construction defects of a pipeline. Moreover, it can detect pipeline features like valves, tees, anchors, repair shells or cathodic protection connections. The "intelligent pigs" must meet a number of requirements with regard to accuracy of measurements. The key element of the data used in the analysis is the metal loss expressed as a fraction of the original wall thickness. Metal loss less than 10 % cannot be detected with sufficient certainty, thus the smallest reported metal loss is 10 %. Measurements can deviate from the true value, but the deviation is limited by the numbers mentioned in Table 2.1

Depth of metal loss (% wall thickness)	Tolerance (% wall thickness)
10 - 20	5
21 - 30	7
31 - 40	9
> 40	10

Table 2.1: Accuracy of sizing depth of metal loss.

Other important information provided by MFL-pigs is the position of the metal loss on the pipeline. In case of large corrosion the pipe must be dig out

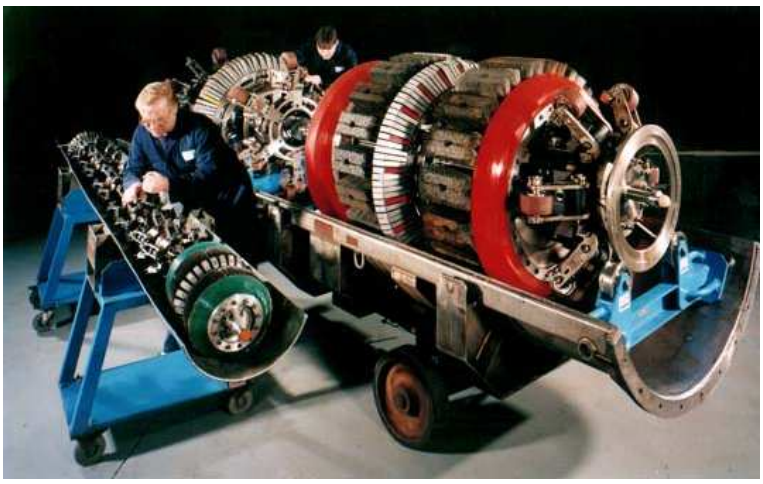

Figure 2.1: Small and large diameter "intelligent pig".

and repaired, which requires accurate information on location of the corrosion spot. Combining abilities of the MFL-pig with GPS (Global Positioning System) can provide a mapping accuracies to within 0.9 to 2.2 m or within 0.1 to 0.3 percent of the distance from the nearest reference point. Probability of detection of existing defects must be greater than or equal to 0.9. Accuracy of sizing length and width must be ≥ 90 %.

2.2 Overview of the Gasunie data

The analysis is based on the data collected during 6 inspections of Gasunie's gas pipelines. One of the pipelines has been reinspected after 18 months since the first inspection. In teh sequel the inspected pipelines will be referred to as pipeline A, B, C, D and E and in Table 2.2 the general characteristics of the pipelines are presented.

Pipeline A lays mostly in sand, in some places in peat. The same applies to Pipeline B. We don't have exact information on percentage of the pipelines laid in sand and peat. For both pipelines sand has been chosen as a soil type. For the first time Pipeline A was inspected in October 1999 and 65 metal loss events were found. The reinspection in April 2001 discovered 74 such events. Pipeline B was inspected in October 2000. The data reported 92 metal loss events with wall thickness reduction greater than or equal to 10 %. The original

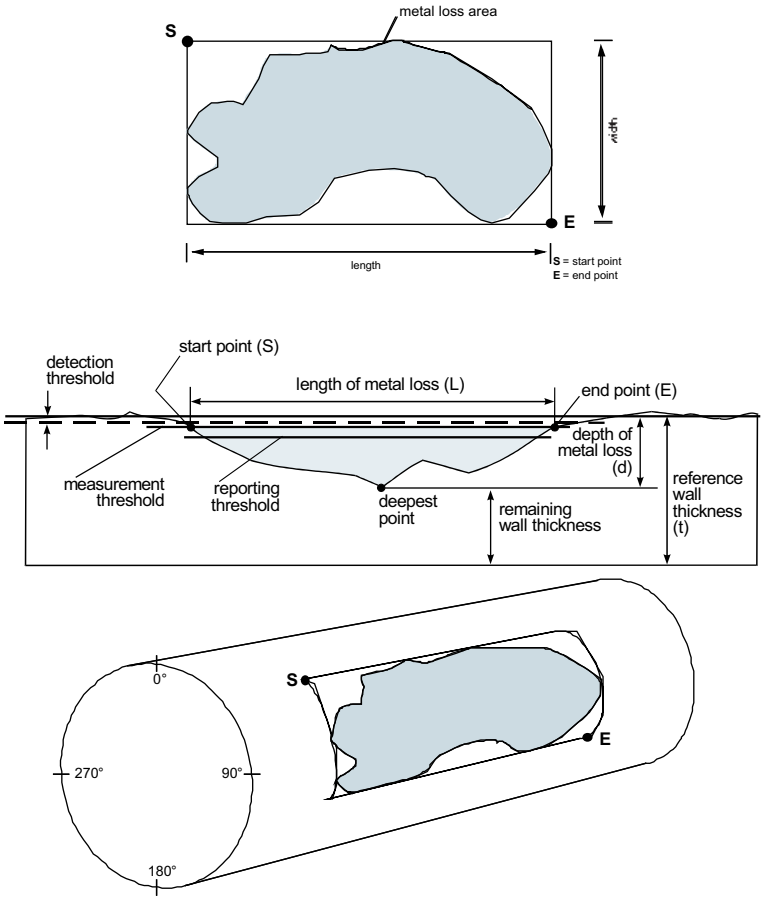

Figure 2.2: Overview of the measurements and parameters of MFL-pigs.

data included also defects with 0 % metal loss but, since it was not clear if their origin is metal loss or inaccurate detection they have been removed. Moreover, the data did not say anything about metal loss greater than 0 % and less than 10 %. The same procedure has been applied to the Pipeline C data, because it also included 0 % metal loss defects and after removing these 0 % metal loss defects, 85 defects in total remained. The first 100 km of this pipeline is laid in sand (74 defects), last 67 km long section is laid in clay (11 defects). The analysis for both types of soil has been performed separately. This pipeline was inspected in June 2001. A month later an inspection of Pipeline D was performed discovering 165 defects. Most recently, in April 2002, Pipeline E was inspected revealing 188 metal loss defects. This data includes also corrosion defects with the metal loss less than 10 %, perhaps due to the use of a new, more

Pipeline	Length [km]	Average year of installment	Diameter [inch]	Average wall thickness [mm]	Average depth cover [m]
A	69	1967	36	12.25	1.77
B	86	1965	36	11.77	1.9
C	168	1967	36	12.6	1.56
D	139	1966	24	7.87	1.45
E	50	1967	18	5.95	1.65

Table 2.2: General characteristics of the inspected pipelines.

Year of construction	Length of pipeline section with corresponding wall thickness	Wall thicknes	Distance from reference location	Position	Metal loss	Length	Width	Wall thickness
calendar year	m		m	hour	%	mm	mm	mm
1965	262.00	5.59	427.87	4:40	8	9	14	5.59
1965	558.80	5.59	686.35	7:50	11	16	14	5.59
1965	649.90	5.59	1031.57	10:00	24	14	21	5.59
1965	569.90	5.59	1993.63	8:40	9	9	15	5.59
1965	598.50	5.59	1993.71	8:00	24	19	14	5.59
1965	596.10	5.59	2113.07	12:50	19	9	20	5.59
1965	652.00	5.59	2255.3	1:10	8	9	14	5.59
1965	619.80	5.59	2263.26	9:50	7	21	22	5.59
1965	607.50	5.59	2397.59	11:50	16	18	16	5.59
1966	639.90	5.59	2571.41	3:30	3	84	76	5.59
1966	662.20	5.59	3299.71	9:50	10	21	14	5.59

Figure 2.3: Sample of the data collected during inspection of Pipeline E.

accurate MFL-pig. Those defects were not removed. The last two pipelines are laid in sand.

Each of the pipelines consists of a number of joined sections. During utilization of the pipe some of the sections have been replaced. Hence hardly any of the pipes preserves the same birth year (year of last inspection) and wall thickness of all of the sections. This fact holds for the inspected pipelines. For further analysis weighted average birth year, weighted average wall thickness and weighted average depth cover has been calculated and used in the analysis. Weights were calculated as the percentage of the pipeline length with given birth year, wall thickness and depth cover respectively. It must be noted that taking the average depth of cover is a quite significant simplification, since the frequency of damages to coating is not linear in the depth.

The data was provided in the form of MS Excel sheets. Figure 2.3 depicts

small sample of the data collected during the inspection of Pipeline E. The left part of the figure gives information on length of individual sections of the pipe with corresponding wall thickness. The right part describes places with reduced wall thickness. The spots can be easily located thanks to given distance from the reference location (location where the MFL-pig has been let into the interior of the pipeline) and position on the surface expressed as an hour (0:00 is top and 6:00 is bottom of the pipe). Furthermore, the data includes length and width of the spots, what help to orientate in their area.

Chapter 3

Description of the UNICORN model

This chapter is mostly based on the article "The Failure Frequency of Underground Gas Pipelines: A Model Based on Field Data and Expert Judgement" by D. Lewandowski & R.M. Cooke & E. Jager, to be published in *"Case Studies in Reliability and Maintenance" by W.R. Blischke & D.N.P. Murthy (eds)* (Lewandowski, Cooke & Jager 2002)

3.1 Introduction

This chapter presents a model predicting with uncertainty failure frequency of gas pipelines. It was developed by R.M. Cooke and E. Jager as a cooperative work of Delft University of Technology and N.V. Nederlandse Gasunie in 1995.

Previous studies (see for example Kiefner, Vieth & Feder 1990) focused on developing ranking tools which provide qualitative indicators for prioritizing inspection and maintenance activities. Such tools perform well in some situations. In The Netherlands, however, qualitative ranking tools have not yielded sufficient discrimination to support inspection and maintenance decisions. The population of gas pipelines in The Netherlands is too homogeneous. Moreover, as the status of current pipes and knowledge of effectiveness of current technologies is uncertain, it was felt that uncertainty should be taken into account when deciding which pipelines to inspect and maintain.

We therefore desire a quantitative model of the uncertainty in the failure

frequency of gas pipelines. This uncertainty is modelled as a function of observable pipeline and environmental characteristics. The following pipe and environmental characteristics were chosen to characterize a kilometer year of a pipeline (Basalo (1992), Lukezich, Hancock & Yen (1992), Chaker & (eds) (1989)):

Pipe Characteristics	Environmental Characteristics
1. pipe wall thickness	1. frequency of construction activity
2. pipe diameter	2. frequency of drainage, pile driving, deep plowing, placing dam walls
3. ground cover	3. percent of pipe under water table
4. coating (bitumen or polyethylene)	4. percent of pipe exposed to fluctuating water table
5. age of pipe (since last inspection)	5. percent of pipe exposed to heavy root growth
	6. percent of pipe exposed to chemical contamination
	7. soil type (sand, clay, peat)
	8. pH value of soil
	9. resistivity of soil
	10. presence of cathodic protection
	11. number of rectifiers
	12. frequency of inspection of rectifiers
	13. number of bond sites

Although extensive failure data is available, the data is not sufficient to quantify all parameters in the model. Indeed, the data yield significant estimates only when aggregated over large populations, whereas maintenance decisions must be taken with regard to specific pipe segments. Hence, the effects of combinations of pipe and environmental characteristics on the failure frequency is uncertain and is assessed with expert judgment. The expert judgment method is discussed in "Expert Judgment in the Uncertainty Analysis of Dike Ring Failure Frequency" (Cooke and Slijkhuis). Fifteen experts participated in this study, from The Netherlands, Germany, Belgium, Denmark, The United Kingdom, Italy, France and Canada.

When values for the pipe and environmental characteristics are specified, the model yields an uncertainty distribution over the failure frequency per kilometer year. Thus the model provides answers to questions like:

- Given a 9 inch diameter pipe with 7 mm wall laid in sandy soil in 1960

with bitumen coating etc., what is the probability that the failure frequency per year due to corrosion will exceed the yearly failure frequency due to 3rd party interference?

- Given a 9 inch pipe with 7 mm walls laid in 1970 in sand, with heavy root growth, chemical contamination and fluctuating water table, how is the uncertainty in failure frequency affected by the type of coating?

- Given a clay soil with $pH = 4.3$, resistivity $4,000\ \Omega$.cm and a pipe exposed to fluctuating water table, which factors or combinations of factors are associated with high values of the free corrosion rate?

In carrying out this work three problems had to be solved:

- How should the failure frequency be modelled as a function of the above physical and environmental variables, so as to use existing data to the maximal extent?

- How should existing data be supplemented with structured expert judgment?

- How can information about complex interdependencies be communicated easily to decision makers?

In spite of the fact that the uncertainties in the failure frequency of gas pipelines are large, we can nonetheless obtain clear answers to questions like those formulated above.

3.2 Modelling pipeline failures

The failure of gas pipelines is a complex affair depending on physical processes, pipe characteristics, inspection and maintenance policies and actions of third parties. A great deal of historical material has been collected and a great deal is known about relevant physical processes. However, this knowledge is not sufficient to predict failure frequencies under all relevant circumstances. This is due to lack of knowledge of physical conditions and processes and lack of data. Hence, predictions of failure frequencies are associated with significant

uncertainties, and management requires a defensible and traceable assessment of these uncertainties.

Expert judgment is used to quantify uncertainty. Experts are queried about the results of measurements or experiments which are possible in principle but not in practice. Since uncertainty concerns the results of possible observations, it is essential to distinguish failure *frequency* from failure *probability*. Frequency is an observable quantity with physical dimensions taking values between zero and infinity. Probability is a mathematical notion which may be interpreted objectively or subjectively. Experts are asked to state their subjective probability distributions over frequencies and relative frequencies.

Under suitable assumptions, probabilities may be transformed into frequencies and vice versa. In this model the following transformations are employed. Let N denote the number of events occurring in one year in a 100-kilometer section of pipe. Number N is an uncertain quantity, and the uncertainty is described by a distribution over the non-negative integers. Let $\mathcal{N}$ denote the expectation of N. If we assume that the occurrence of events along the pipe follows a Poisson distribution with respect to distance, then $\mathcal{N}/100$ is the expected frequency of events in one kilometer of pipe. If $\mathcal{N}/100 \ll 1$, such that the probability of two events occurring in one kilometer in one year is very small, then $\mathcal{N}/100$ is approximately the probability of one event occurring in one kilometer in one year. $(1 - \mathcal{N}/100)$ is approximately the probability of no event occurring in one kilometer in one year, and the probability of no events in the entire 100 kilometers is approximately $(1 - \mathcal{N}/100)^{100}$.

The result becomes more accurate if we divide the 100 kilometers into smaller pieces. Using the fact that $\lim_{x\to+\infty}(1-\mathcal{N}/x)^x = \mathrm{e}^{-\mathcal{N}}$, we find that the probability of no event in 100 kilometers in one year is $\mathrm{e}^{-\mathcal{N}}$; the probability of no event in one kilometer in one year is $\mathrm{e}^{-\mathcal{N}/100}$. The probability of at least one event in one kilometer is $1 - \mathrm{e}^{-\mathcal{N}/100}$, and if $\mathcal{N}/100 \ll 1$, then this probability is approximately $\mathcal{N}/100$. To accord with more familiar usage, however, it is often convenient to suppress the distinction between small frequencies and probabilities.

3.2.1 Example of modelling approach

The notation in this section is similar to, but a bit simpler than that used in the sequel.

Suppose we are interested in the frequency per kilometer per year that a gas pipeline is hit (H) during third party actions at which an overseer from Gasunie has marked the lines (O). Third party actions are distinguished according to whether the digging is closed (CL; drilling, pile driving, deep plowing, drainage, inserting dam walls, etc) and open (OP; e.g. construction). Letting F denote frequency and P probability, we could write

$$\begin{aligned}\text{Frequency}\{\text{Hit and Oversight present per km.yr}\} &= F(H \cap O/\text{km.yr}) \\ &= F(CL/\text{km.yr})P(H \cap O|CL) + F(OP/\text{km.yr})P(H \cap O|OP). \quad (3.1)\end{aligned}$$

This expression seems to give the functional dependence of $F(H \cap O)$ on $F(CL)$ and $F(OP)$, the frequencies of closed and open digs respectively. However, eq. (3.1) assumes that the conditional probabilities of hitting with oversight given closed or open digs does not depend on the frequency of closed and open digs. This may not be realistic; an area where the frequency of 3$^{\text{rd}}$ party digging is twice the population average may not experience twice as many incidents of hitting a pipe. One may anticipate that regions with more 3$^{\text{rd}}$ party activity, people are more aware of the risks of hitting underground pipelines and take appropriate precautions. This was indeed confirmed by the experts.

It is therefore illustrative to look at this dependence in another way. Think of $F(H \cap O)$ as a function of two continuous variables, FCL = frequency of closed digs per kilometer year, and FOP = frequency of open digs per kilometer year. Write the Taylor expansion about observed frequencies FCL_0 and FOP_0. Retaining only the linear terms one can obtain

$$\begin{aligned}F(H \cap O/\text{km.yr}) &= F(FCL, FOP) = \\ &F(FCL_0, FOP_0) + p_1(FCL - FCL_0) + p_2(FOP - FOP_0) \quad (3.2)\end{aligned}$$

If $P(H \cap O|CL)$ and $P(H \cap O|OP)$ do not depend on FCL and FOP then eq. (3.2) is approximately equivalent to eq. (3.1). Indeed, put $p_1 = P(H \cap O|CL)$; $p_2 = P(H \cap O|OP)$, and note that $F(FCL_0, FOP_0) = p_1 FCL_0 + p_2 FOP_0$.

The Taylor approach conveniently expresses the dependence on FCL and FOP, in a manner familiar to physical scientists and engineers. Of course it

can be extended to include higher order terms. If we take the "zero-order term" $F(FCL_0, FOP_0)$ equal to the total number of times gas lines are hit while an overseer has marked the lines, divided by the number of kilometer years in The Netherlands, then we can estimate this term from data. Frequencies FCL_0 and FOP_0 are the overall frequencies of closed and open digs. Probabilities p_1 and p_2 could be estimated from data if we could estimate $F(FCL, FOP)$ for other values of FCL and FOP, but there are not enough hittings in the data base to support this. As a result these terms must be assessed with expert judgment, yielding uncertainty distributions over p_1 and p_2. Experts are queried over their subjective uncertainty regarding measurable quantities; thus they may be asked:

Taking account of the overall frequency $F(FCL_0, FOP_0)$ of hitting a pipe line while overseer has marked the lines, what are the 5, 50 and 95 percent quantiles of your subjective probability distribution for:

The frequency of hitting a pipeline while overseer has marked the lines if frequency of closed digs increases from FCL_0 to FCL, and other factors remaining the same.

In answering this question the expert conditionalizes his uncertainty on everything he knows, in particular the overall frequency $F(FCL_0, FOP_0)$. We configure the elicitation such that the "zero order terms" can be determined from historical data, whenever possible.

How do we use these distributions? Of course if we are only interested in the average situation in the Netherlands, then we needn't use them at all, since this frequency is estimated from data. However, it is known that the frequency of third party activity (with and without oversight) varies significantly from region to region. If we wish to estimate the frequency of hitting with oversight where $FCL \neq FCL_0$ and $FOP \neq FOP_0$, then we substitute these values into eq. (3.2), and obtain an uncertainty distribution for $F(H \cap O)$, conditional on the zero-order estimate and conditional on the values FCL, FOP. This is pure expert subjective uncertainty. If we wish, we may also include uncertainty due to sampling fluctuations in the zero-order estimate.

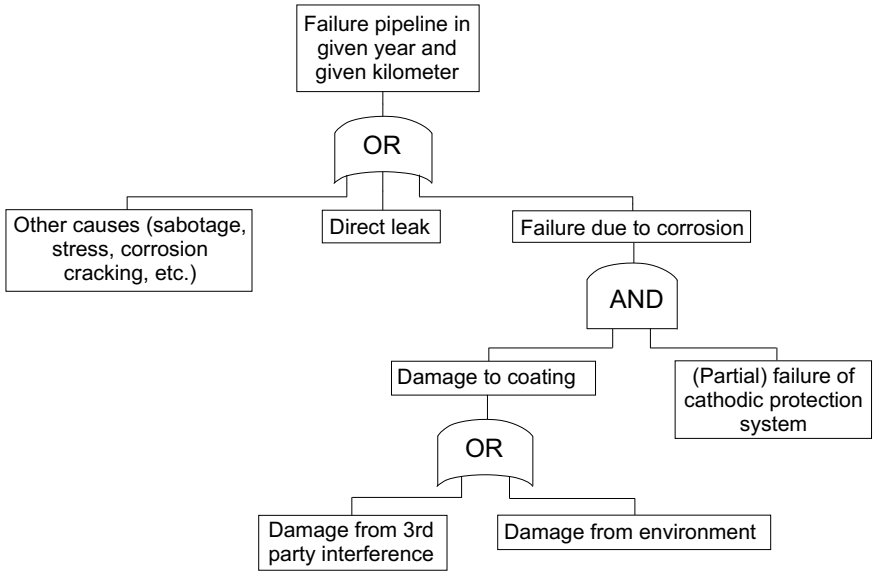

Figure 3.1: Fault tree for gas pipeline failure.

3.2.2 Overall modelling approach

The failure probability of gas pipelines is modelled as the sum of a failure probability due to third party actions and a failure probability due to corrosion[1]

$$\begin{aligned} P\{\text{failure of gas pipelines/ km.yr}\} = \\ P\{\text{failure due to 3rd parties/ km.yr}\} + \\ P\{\text{failure due to corrosion/ km.yr}\}. \end{aligned}$$

Both terms on the right hand side will be expressed as functions of other uncertain quantities and parameters. The parameters will be assigned specific values in specific situations, the uncertain quantities are assigned subjective uncertainty distributions on the basis of expert assessments. This results in an uncertainty distribution over possible values of $P\{\text{failure of gas pipelines/km·yr}\}$, conditional on the values of the known variables.

[1]The model does not include stress corrosion cracking or hydrogen induced cracking, as these have not manifested themselves in The Netherlands. Damage to pipelines during construction and installation is not modelled. Low probability scenarios like earthquake and flood have not been modelled, and 'exotic' scenarios like sabotage, war, malfeasance and the like are neglected.

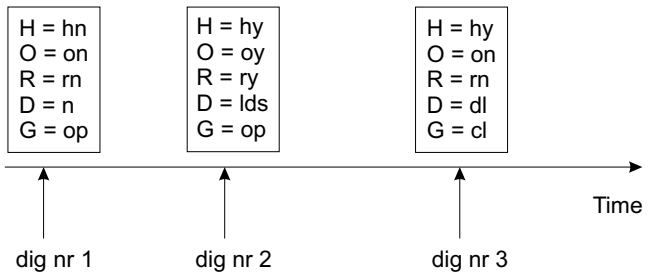

Figure 3.2: Digs as marked point process.

Failure due to corrosion requires damage to the pipe coating material, and (partial) failure of the cathodic and stray current protection systems. Damage to coating may come either from third parties or from the environment (Lukezich et al. 1992). The overall model may be put in the form of a fault tree as shown in Figure 3.1.

3.3 Third party interference

The model described here enables the calculation of uncertainty distributions over the probability per kilometer year of various damage categories, with or without repair, resulting from third party interference. The underlying probability model is a so-called "marked point process". Given one kilometer section of pipe, third party activities (within 10 meters of the pipe) are represented as a Poisson process in time. Each dig-event is associated with a number of "marks"; i.e. random variables which take values in each dig-event (Figure 3.2). The random variables and their possible values are shown in Table 3.1.

For each 1 km pipe section, the following picture emerges:
On the first dig the pipe was not hit, hence the damage was none ($D = n$) and no repair was carried out ($R = rn$). The second dig was an open dig with oversight; small line damage occurred, but was repaired. The third dig was closed without oversight, the line was hit and resulted in a direct leak. By definition, repair was unable to prevent leak, hence $R = rn$.

The one-kilometer pipe section is described by a number of parameters,

Variable	Meaning	Values	Interpretation
H	Pipe hit?	hy, hn	hityes, hitno
O	Overseer notified?	oy, on	overtsightyes, oversightno
R	Repair carried out?	ry, rn	repairyes, repairno
D	Damage?	n, $cd3$, lds, ldl, dl	none, coating damage, small line damage, large line damage, direct leak
G	Dig type?	op, cl	open dig, closed dig

Table 3.1: Marks for 3rd party digs.

which are assumed to be constant along this section:

- t: pipe wall thickness
- gc: depth of (ground) cover
- $f = (FOP, FCL)$: frequency of open and closed digs within 10 m of pipe

The values of these parameters will influence the distributions of the random variables in Table 3.1. Hence, we regard these as random variables, and their influence on other random variables is described by conditionalization. In any one-kilometer section the values for these variables can be retrieved from Gasunie data, and the distributions of other variables can be conditionalized on these values. From a preliminary study (Geervliet 1994) it emerged that pipe diameter and coating type were not of influence on the probability of hitting a pipe.

The damage types indicated in Table 3.1 are defined more precisely as:

- dl: direct leak (puncture or rupture)
- ldl: line damage large (at least 1 mm of pipe material removed, no leak)
- lds: line damage small (less than 1 mm of pipe material removed)

- $cd3$: coating damage without line damage due to 3rd parties

Every time a gas pipeline is hit, we assume that one and only one of these damage categories is realized. Hence, $D = n$ if and only if $H = hn$. By definition, if $D = dl$, then repair prior to failure is impossible.

We wish to calculate uncertainty distributions over the probability of unrepaired damage

$$P(D = z \cap R = rn|t, gc, f); \quad z \in \{cd3, lds, ldl, dl\}.$$

Letting $\sum_{HOG}$ denote summation over the possible values of H, O, G, we have

$$\begin{aligned} &P(D = z \cap R = rn|t, gc, f) = \\ &\quad \sum_{HOG} P(D = z \cap R = rn|H, O, G, t, gc, f) P(H, O, G|t, gc, f) = \\ &\quad \sum_{OG} P(D = z \cap R = rn|H = hy, O, G, t, gc, f) P(H = hy, O, G|t, gc, f), \end{aligned} \tag{3.3}$$

since third party damage can only occur if the pipe is hit.

For each of the four damage types, there are four conditional probabilities to consider, each conditional on four continuous valued random variables. To keep the model tractable it is necessary to identify plausible simplifying assumptions. These are listed and discussed below. The expressions "X depends only on Y" and "X influences only Y" mean that given Y, X is independent of every other random variable.

1. D depends only on (H, G, t)
2. R depends only on $(H, G, O \text{and} D \in \{cd3, lds, ldl\})$
3. gc influences only H
4. gc is independent of f
5. G is independent of f
6. (H, O, G) is independent of t given (gc, f).

Assumptions $1, 3, 4$ and 5 speak more or less for themselves. Assumption 2 says the following: if the pipe is hit and the damage is repairable $(D \neq dl)$

then the probability of repair depends only on the type of dig and the presence of oversight; it does not depend on the type of repairable damage inflicted. Assumptions 1 and 2 entail that D and R depend only on $(H, G, O, t, D \in \{cd3, lds, ldl\})$.

To appreciate assumption 5, suppose the uncertainty over $f = (FOP, FCL)$ is described by an uncertainty distribution, and consider the expression $P(FOP, FCL|G = cl)$. Would knowing the type of dig in a given 3rd party event tell us anything about the frequencies of open and closed digs? It might. Suppose that either all digs were open or all digs were closed, each possibility having probability 1/2 initially. Now we learn that one dig was closed; conditional on this knowledge, only closed digs are possible. Barring extreme correlations between the uncertainty over values for FOP and FCL, knowing $G = cl$ can tell us very little about the values of FCL and FOP. Assumption 5 says that it tells us nothing at all.

To illustrate how these assumptions simplify the calculations, we consider the event $(D = cd3 \cap R = rn)$; which we abbreviate as $(cd3 \cap rn)$. We can show that eq. (3.3) is now equal to

$$P(cd3 \cap rn|t, gc, f) = \sum_{OG} P(rn|hy, O, G)P(cd3|hy, G, t)P(O, hy|G, f)P(G)P(gc|hy)/P(gc).$$

Proof.
Using elementary probability manipulations and assumptions 1 and 2

$$\begin{aligned} &P(cd3 \cap rn|hy, O, G, t, gc, f)P(hy, O, G|t, gc, f) = \\ &\quad P(cd3 \cap rn|hy, O, G, t)P(hy, O, G|t, gc, f) = \\ &\quad P(cd3|rn, hy, O, G, t)P(rn|hy, O, G, t)P(hy, O, G|t, gc, f) = \\ &\quad P(cd3|hy, G, t)P(rn|hy, O, G)P(hy, O, G|t, gc, f). \end{aligned}$$

Reasoning similarly with assumptions 3, 4, 5 and 6, and using Bayes' theorem

$$\begin{aligned} P(hy, O, G|t, gc, f) &= P(hy, O, G|gc, f) \\ &= P(gc, O, G|hy, f)P(hy|f)/P(gc|f) = \\ &= P(gc|O, G, hy, f)P(O, G|hy, f)P(hy|f)/P(gc|f) = (\star) \end{aligned}$$

$$\begin{aligned}(\star) &= P(gc|hy)P(O,G|hy,f)P(hy|f)/P(gc)\\ &= P(gc|hy)P(O,hy|G,f)P(G|f)/P(gc)\\ &= P(gc|hy)P(O,hy|G,f)P(G)/P(gc).\end{aligned}$$

□

Similar expressions hold for damage types *lds* and *ldl*. For *dl*, the term $P(rn|hy,O,G)$ equals one as repair is not possible in this case. The terms

$$P(cd3|hy,G,t),\ P(G|hy),\ P(G),\ P(gc|hy) \text{ and } P(gc)$$

can be estimated from data; the other terms are assessed (with uncertainty) using expert judgment. The uncertainty in the data estimates derives from sampling fluctuations and can be added later, although this will be small relative to uncertainty from expert judgment. The term

$$P(gc|hy)/P(gc) = P(H = hy|gc)/P(H = hy)$$

is called the "depth factor"; it is estimated by dividing the proportion of hits at depth *gc* by the total proportion of pipe at depth *gc*. $P(G = cl|hy, cd3)$ is estimated as the percentage of coating damages from third parties caused by closed digs; $P(G = cl|hy)$ is the percentage of hits caused by closed digs, and $P(G)$ is the probability per kilometer year of a closed dig. This probability is estimated as the frequency of closed digs per kilometer year, if this frequency is much less than 1 (which it is).

The term $P(rn|hy,O,G)$ is assessed by experts directly when the terms $P(O,hy|G,f)$ are assessed using the Taylor approach described in section 3.

To assess the probability (with uncertainty) of ruptures due to third parties, experts assess, for two different wall thickness, the percentages of direct leaks which will be ruptures. Let RUP71 and RUP54 denote random variables whose distributions reflect the uncertainty in these percentages for thickness 7.1 and 5.4 mm respectively. We assume that RUP71 and RUP54 are comonotonic[2]. Putting

$$RUP54 = RUP71 + r(7.1 - 5.4),$$

we can solve for the the linear factor r, and for some other thickness t.

$$RUPt = RUP71 + r(7.1 - t)$$

[2]That is, their rank correlations are equal to one.

gives an assessment of the uncertainty in the probability of rupture, given direct leak, for thickness t. This produces reasonable results for t near 7.1. For $t > 10$ mm it is generally agreed that rupture from third parties is not possible (Hopkins, Corder & Corbin 1992).

3.4 Damage due to environment

In dealing with damage to coating due to environmental factors per kilometer year, we revert to the frequency notation, as this frequency can be larger than one. For both bitumen (bit) and polyethylene (pe) coatings, the probability of environmental damage depends on the pipe diameter (d), on the soil type (st) and on the percentage of the pipe exposed to fluctuating water table (wt_f). Bitumen coating is also sensitive to the proportion of the one-kilometer length exposed to tree roots (rt) and chemical contamination (ch). The effects of these factors are captured with a first order Taylor expansion whose linear terms $p_3, \ldots, p_{10}$ are assessed by experts

$$F(bit) = F_0(bit) + p_3 \cdot (d - d_0) + p_4 \cdot wt_f + p_5 \cdot rt + p_6 \cdot ch + st \cdot bit, \quad (3.4)$$

$$F(pe) = F_0(pe) + p_7 \cdot (d - d_0) + p_8 \cdot wt_f + p_9 \cdot rt + p_{10} \cdot ch + st \cdot pe. \quad (3.5)$$

Knowing the percentage of the pipeline with bitumen coating $\%bit$ we can calculate the overall frequency of coating damage per kmyr due to environment regardless the coating type

$$F = \%bit\ F(bit) + (1 - \%bit)F(pe).$$

To determine the probability of at least one coating damage per kilometer, these frequencies are divided by 100 to determine the frequency per 10 meter section. As these frequencies will be much less than 1, and assuming that damage to different 10 meter sections are independent, we have

$$P\{\text{at least 1 coating damage per km}\} = 1 - (1 - F/100)^{100}. \quad (3.6)$$

On substituting eq. (3.4) and eq. (3.5) into eq. (3.6), we obtain the probabilities per kmyr of bitumen and polyethylene coating damage per km year, due to environmental factors, notated $P(CDE_{bit})$ and $P(CDE_{pe})$.

chemical contamination of soil	pipe diameter	oversight
soil type (clay, sand, peat)	pipe inspection	repair
soil resistance	stray currents	acidity
pipe thickness	tree roots	pipe age
water table	third party actions	

Table 3.2: Factors influencing failure due to corrosion.

3.5 Failure due to corrosion

3.5.1 Modelling corrosion induced failures

The modelling of failure due to corrosion is more complicated than that of failure due to third parties. The probability of failure due to corrosion depends on many factors as listed in Table 3.2.

Corrosion can be viewed as the tendency of a metal to revert back to its natural and more stable state as an ore. The end result of corrosion involves a metal atom being oxidized, whereby it loses one or more electrons. The lost electrons are conducted through the bulk metal to another site where they are reduced. If we assure an electric field in the neighborhood of a pipeline, we prevent the pipe from emitting the electrons and limit the corrosion. Practically, this problem is solved by installing the cathodic protection system. A broad outline of such a system is depicted in Figure 3.3. The connections of rectifiers with pipeline are located about every 2 km.

The model described here uses only pit corrosion. Given these factors, the corrosion rate is assumed constant in time (Camitz & Vinka 1989).

For a pipeline to fail due to corrosion, two lines of defense must be breached. First the coating must be damaged, and second, depending on location, the cathodic or stray current protection system must not function as intended. Coating damage may be caused either by third party actions or by environmental factors. Both cathodic and stray current protection systems have been in place since 1970.

We first elaborate the model for pipelines installed after 1970. Assuming that the coating has been breached, pit corrosion will reduce the pipe wall thickness until a critical value is reached, at which point the pipe fails. This critical wall thickness, that is the thickness at which failure occurs, is expressed

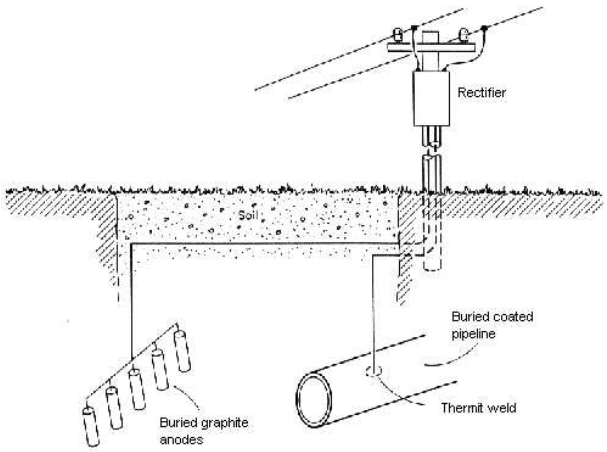

Figure 3.3: Overview of cathodic protection system.

as a fraction x of the original wall thickness minus the pipe material removed during the damage event. The fraction x depends on the pressure of the gas in the pipeline, and on the geometry of the pipe damage, and this relationship has been established by experiment. In this model, x is introduced as a parameter whose value depends only on the damage type, thus we distinguish x_C, x_S and x_L for (only) coating damage, small and large pipe damage respectively. Coating damage is either caused by 3$^{\text{rd}}$ parties ($cd3$) or by the environment (cde).

A length of pipe can be inspected for corrosion, and if corrosion is found, the pipe is uncovered and repaired. Hence, after such inspection the pipe is as good as new. The effective birthday (eb) of a pipe section is the calendar year of the last inspection.

Given a corrosion rate (CR) and a damage type, we define the effective life of a pipe section as the time required for the corrosion to reduce wall thickness to the critical wall thickness. Letting t denote the original pipe wall thickness, and $t_C = 0$, $t_S = 0.5$ mm, $t_L = 2$ mm denote the pipe wall thickness removed by damage type i, $i \in \{C, S, L\}$:

$$EL(CR, i) = x_i(t - t_i)/CR. \tag{3.7}$$

In this equation, CR is uncertain and x_i, t_i are parameters with uncertain indices. $EL(CR, i)$ is the time a pipe survives given corrosion rate CR after sustaining damage type i, $i \in \{C, S, L\}$.

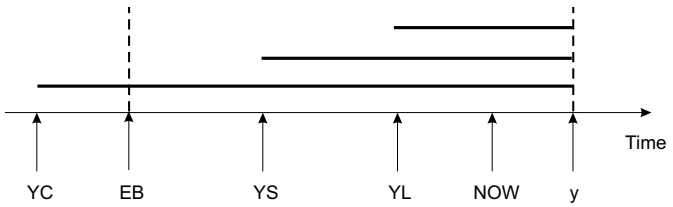

Figure 3.4: Effective lives and critical years for three damage types for fixed corrosion rate.

Suppose we are interested in the event "first failure of a one-kilometer length of gas pipeline occurs in calendar year y". For each given value of CR, there are three years, $y_C(CR)$, $y_S(CR)$ and $y_L(CR)$ such that damage type i in year y_i, somewhere on this one-kilometer length of pipe, causes failure in year y. y_i is called the critical year for damage type i. The situation is pictured in Figure 3.4.

Referring to Figure 3.4, we see that failure due to damage type C is impossible; the pipe isn't old enough in year y. If small damage (S) occurs in year y_S, and not before, and if large damage has not occurred before y_L, then the pipe fails in y due to small damage in y_S. The probability of this is

$$(1 - P_S)^{y_S - eb} P_S (1 - P_L)^{y_L - eb},$$

where we write $P_S = P(lds)$, $P_L = P(ldl)$, $P_C = P(cd3) + P(cde) - P(cd3 \cap cde)$. However, if y is "next year" then we already know that the pipeline has not already failed due to corrosion from small or large pipeline damage. Hence, we should conditionalize on the event "no small damage before y_S and no large damage before y_L". In this case, the probability of failure in year y due to small damage is simply P_S, and the probability of failure due to corrosion is, neglecting higher order terms, $P_S + P_L$ (all of these probabilities are conditional on CR).

If y is in the future, and we conditionalize on our knowledge that no failure has occurred up to now, with $T = y -$ now, $T < y_S - eb$, then the probability of failure due to corrosion between now and year y is (again, conditional on CR and neglecting small terms)

$$(1 - P_S)^T (1 - P_L)^T (P_S + P_L).$$

In general, let

$$q_i(eb, y, \text{ now }, CR) = min\{(y_i(CR) - eb), (y - 1 - \text{ now})\}$$

denote the number of years between y and now in which a failure due to damage type i could have caused failure between now and year $y - 1$, conditional on CR, and let

$$1_i \;=\; \begin{cases} 1, & \text{if } \; y_i(CR) > eb \\ 0, & \text{otherwise} \end{cases}$$

then (sum and product are over $i \in \{C, S, L\}$)

$$P_{f|cr}(CR, eb, y, now, P_C, P_S, P_L, t, x_C, x_S, x_L) = \prod (1 - P_i)^{q_i} \sum 1_i P_i \quad (3.8)$$

is approximately the probability of failure in year y due to corrosion, given CR. $P_{f|CR}$ is an uncertain quantity since the arguments written in capital letters represent uncertain quantities.

3.5.2 Pit corrosion rate

The free rate of pit corrosion CR_f [mm/yr] is modelled to depend on the soil type (clay, sand, peat), the soil resistance (r), the acidity (pH) and the proportion of pipeline under the water table, and fluctuating under and above the water table (wt_u, wt_f). CR_f is the rate of corrosion which would be obtained if the cathodic protection were not present. Using a zero-order corrosion rate with arguments r_0, pH_0, $wt_{u0} = wt_{f0} = 0$; we apply the linear approximation (supported by experiment)

$$CR_f = CR_{f0} + p_{11}(r - r_o) + p_{12}(pH - pH_0) + p_{13} \cdot wt_f + p_{14} \cdot wt_u. \quad (3.9)$$

The linear terms $p_{11}, \ldots p_{14}$ are assessed with expert judgment. All of the terms in eq. (3.9) depend on soil type.

We distinguish three states of the cathodic protection system:

- CP_f: wholly non-functional, $CR = CR_f$
- CP_p: partially functional (pipe-soil potential outside prescribed range), $CR = CR_p$

- CP_{ok}: wholly functional as prescribed; $CR \sim 0$.

Before the cathodic protection system was installed in 1970, only state CP_f was available. CR_p is determined via expert judgment as a fraction of CR_f. $P(CP_i)$ is the fraction of one-kilometer pipe length for which cathodic protection is in state i, $i \in \{f, p, ok\}$. Since the factors affecting the cathodic protection do not change from year to year, we assume that the states CP_f and CP_p affect the same portions of pipe each year.

Stray currents can induce corrosion against which cathodic protection is ineffective. In 1970 a protection system of bonds was installed to drain off strong stray currents in locations where these are known to occur. Each bond is inspected once a month hence if a bond has failed the stray current corrosion rate CR_{st} has been operative on the average for one half month. In the neighborhood of a bond, the corrosion rate before 1970 due to stray currents is CR_{st}, and after 1970 it is assumed to be $CR_{st}/24$. If bs is the proportion of a one-kilometer length of pipe in the neighborhood of a bond sites and $P(SP)$ is the probability that the stray current protection system fails at one site, then $bs \cdot P(SP)$ is the probability that CR_{st} (before 1970) or $CR_{st}/24$ (after 1970) obtains, given that damage has occurred somewhere in the pipe section.

Unconditionalizing equation (3.9) on CR, we obtain the probability of failure per kilometer year due to corrosion for pipe installed after 1970

$$P_{cor>70} = P_{f|cr}(CR_f)P(CP_f) + P_{f|cr}(CR_p)P(CP_p) + P_{f|cr}(CR_{st}/24)bsP(SP) \quad (3.10)$$

This is an uncertain quantity whose distribution is the uncertainty distribution for the failure frequency for a one-kilometer length of gas pipeline with specified pipe and environment parameter values.

For pipelines whose effective birthday is before 1970,

$$x_i(t - t_i) - (y - 1970) \cdot CR$$

is the thickness of pipe wall, under damage type i, exposed to corrosion at the rate obtaining before protection systems were installed. Let

$$1_{i,CR} = \begin{cases} 1, & \text{if } y - x_i(t - t_i)/CR > 1970 \\ 0, & \text{otherwise} \end{cases}$$

If $1_{i,CR} = 1$, then $y_i > 1970$; if $y_i < 1970$ then we must account for the absence of protection systems. We compute the effective life as follows

$$\begin{aligned} EL(CR_f, i) &= x_i(t - t_i)/CR_f, \\ EL(CR_p, i) &= 1_{i,CR_p} x_i(t - t_i)/CR_p, \\ &+ (1 - 1_{i,CR_p})(x_i(t - t_i) - (y - 1970)CR_p)/CR_f, \\ EL(CRst, i) &= 1_{i,CR_{st}} x_i(t - t_i)24/CR_{st} \\ &+ (1 - 1_{i,CR_{st}})(x_i(t - t_i) - (y - 1970)CR_{st}/24)/CR_{st}. \end{aligned} \tag{3.11}$$

The probability $P_{cor<70}$ is obtained by using eq. (3.11) instead of eq. (3.7) in eq. (3.8).

3.6 Results for ranking

3.6.1 Case-wise comparisons

Two types of results can be obtained with the model. First, we can perform case-wise comparisons. By specifying parameter values for two or more types of kilometer-year sections of pipelines, the uncertainty distributions for the frequency of failure can be compared. In Figure 3.5 compares three cases, namely

- bitumen coated pipe laid in 1975 in sand
- bitumen coated pipe laid in 1975 in clay
- polyethylene coated pipe laid in 1975 in sand

Percentiles of the subjective uncertainty distribution are shown horizontally; the logarithm of the failure frequency per kilometer year is plotted vertically (the absolute values are proprietary). Other parameters are the same in all cases, and those describing the frequency of 3rd party intervention are chosen in accord with the generic values retrievable from the Dutch data. Each graph plots the frequency per kilometer year of failure against the percentiles of the uncertainty distribution for the failure frequency. Each graph shows three curves, a curve corresponding to failure due to corrosion ($corlk$), a curve corresponding to failure due to 3rd party interference ($3leak$), and a curve corresponding to the sum of these two ($leak$).

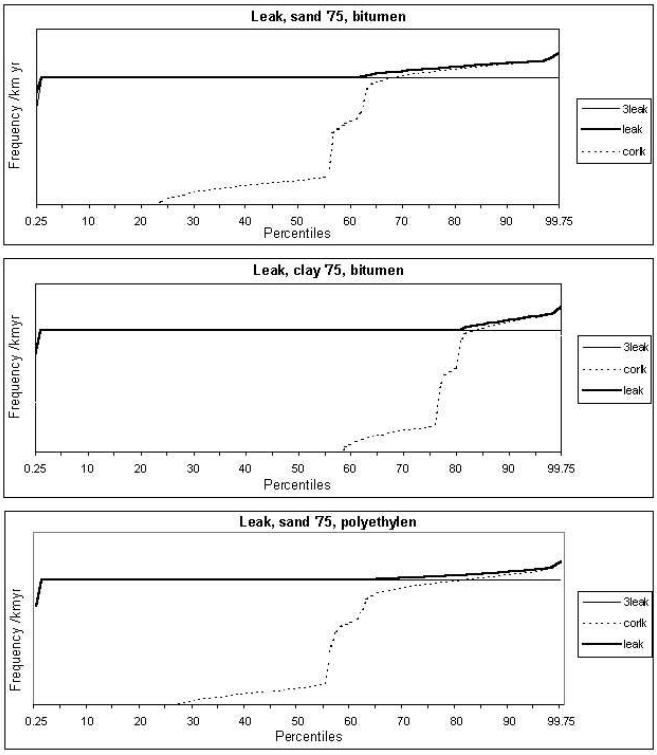

Figure 3.5: Uncertainty distributions for three cases.

Because of the choice of 3rd party interference frequencies, the curves for failure due to 3rd party interference are constant - this means that there is no uncertainty regarding this failure frequency. The curves for failure due to corrosion are not constant. In the first graph (bitumen in sand), we see that the 66th percentile of the uncertainty distribution for failure due to corrosion corresponds to the same failure frequency as 3rd party intervention. In other words, there is a 0.66 probability that the frequency of failure due to corrosion will be lower than that due to 3rd party intervention.

In the second graph (bitumen in clay) we find a probability of 0.85 that the frequency of failure due to corrosion will be lower than that due to 3rd party intervention. In the third graph (polyethylene in sand), we find a probability of 0.77 that the frequency of failure due to corrosion will be lower than that due to 3rd party intervention. In the second graph, note that the failure frequency curve for corrosion drops off more rapidly than in the third graph. This means that very low values are more likely for bitumen coated pipe in clay than for

polyethylene coated pipe in sand.

Comparisons of this nature can only be made on the basis of fully specified cases. We cannot conclude, for example, that "bitumen in clay is about the same as polyethylene in sand". The comparisons in Figure 3.5 depend on the values of all other environmental and pipe variables. Thus, changing the amount of root growth, the soil resistivity the age and thickness of the pipe,or any of the other parameters, might produce very different pictures.

Finally, we note that the failure frequency due to corrosion is highly uncertain. Nevertheless, clear comparisons may be made by taking this uncertainty into account.

3.6.2 Importance in specific case

As mentioned in the introduction, we use a Monte Carlo simulation to compute the uncertainty distribution of the failure frequency for a given pipeline and environmental characteristics. When we focus on a particular kilometer of pipe, i.e. a particular set of values for all the parameters in the model; we may ask "which factors are important for the failure frequency in this specific case?" Since this failure frequency is uncertain, we are really asking "which factors are important for the uncertainty in failure frequency in this case?"

To gain insight into this type of question a new graphic exploratory tool has been developed, termed "cobweb plots"[3]. These plots enable the user to gain insight into complex relations between interdependent uncertain quantities.

We illustrate by considering the uncertainty in failure due to corrosion in a bitumen coated pipe laying in sand for five years without cathodic protection.

The variable *corlk* or "leak due to corrosion" is potentially influenced by the following variables:

- crf: free corrosion rate
- crp: corrosion rate under partial functioning of cathodic protection
- crse: corrosion rate from stray currents
- ps: frequency of small unrepaired pipeline damage

[3]Wegman (1990) introduced a similar technique, though without conditionalization.

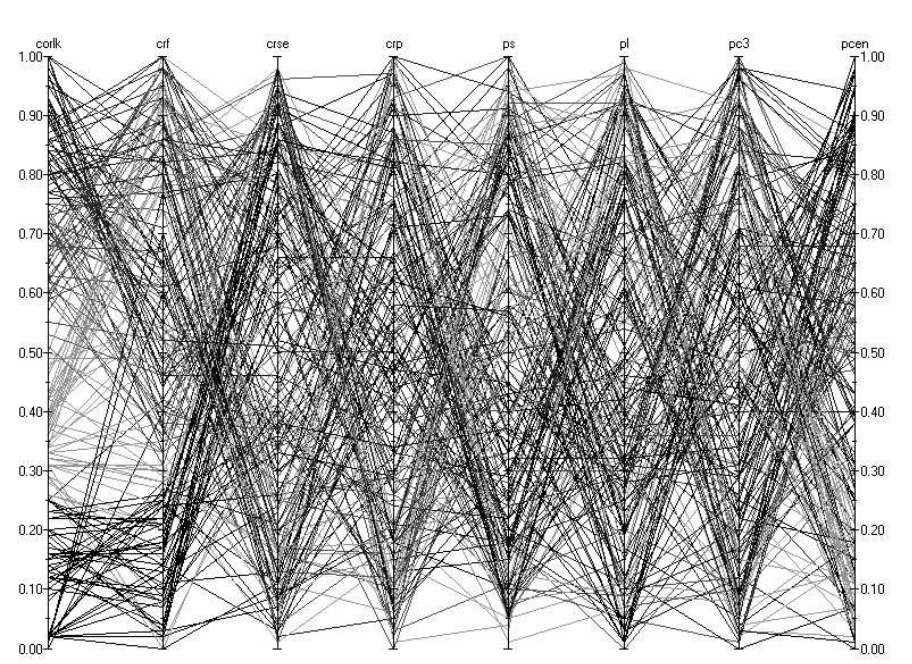

Figure 3.6: Unconditional cobweb plot.

- pl: frequency of large unrepaired pipeline damage
- pc3: frequency of coating damage from 3rd parties
- pcen: frequency of coating damage from environment

The uncertainty distribution for *corlk* is built up by considering a large number of "scenario's", where each scenario is made by sampling values from all input variables. In each scenario, unique values are assigned to all the above variables. We are interested in how the high and low values of *corlk* co-vary with high and low values of the above variables.

Cobweb plots allow the user to explore this co-variation. Suppose we plot all the values of the above variables on parallel vertical lines, with high values at the top and low values at the bottom. Each individual scenario assigns exactly one value to each variable; if we connect these values we get a jagged line intersecting each variable-line in one point. Suppose we plot jagged lines for each of 200 scenarios; the result will suggest a cobweb. It may be difficult to follow the individual lines; it is therefore convenient to "filter" or "condi-

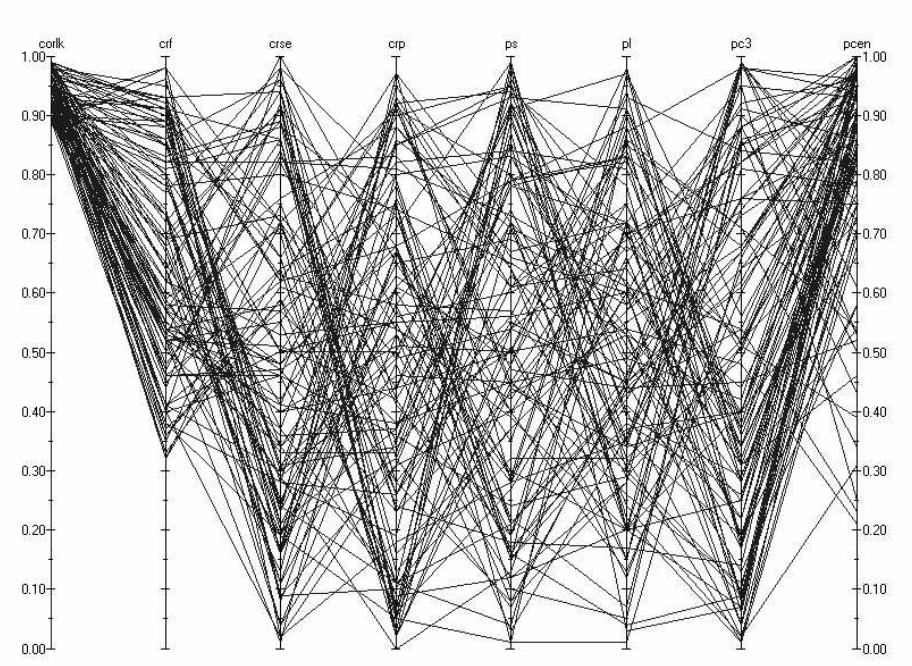

Figure 3.7: Cobweb plot conditional on high values of *corlk*.

tionalize" on sets of lines. For example, we might conditionalize on all lines passing through high values of *corlk* and see where these lines intersect the other variables.

The first cobweb plot (Figure 3.6) shows lines for 500 scenarios. The second cobweb plot (Figure 3.7) conditionalizes on high values of *corlk*: we see that these are associated with high values of crf and with high values of *pcen*. Variables *crp* and $crse$ are not affected by this conditionalization; by assumption, there is no cathodic protection in this case. The third cobweb plot (Figure 3.8) conditionalizes on low values of *corlk*. We see that these are strongly associated with low values of crf and with $crse$ but not associated with other variables. We may conclude that damage from the environment is important for high values of failure frequency due to corrosion, but not for low values. This sort of behavior occurs quite often; the variables that are associated with high values of some target variable are not the same as the variables associated with low values of the target variable.

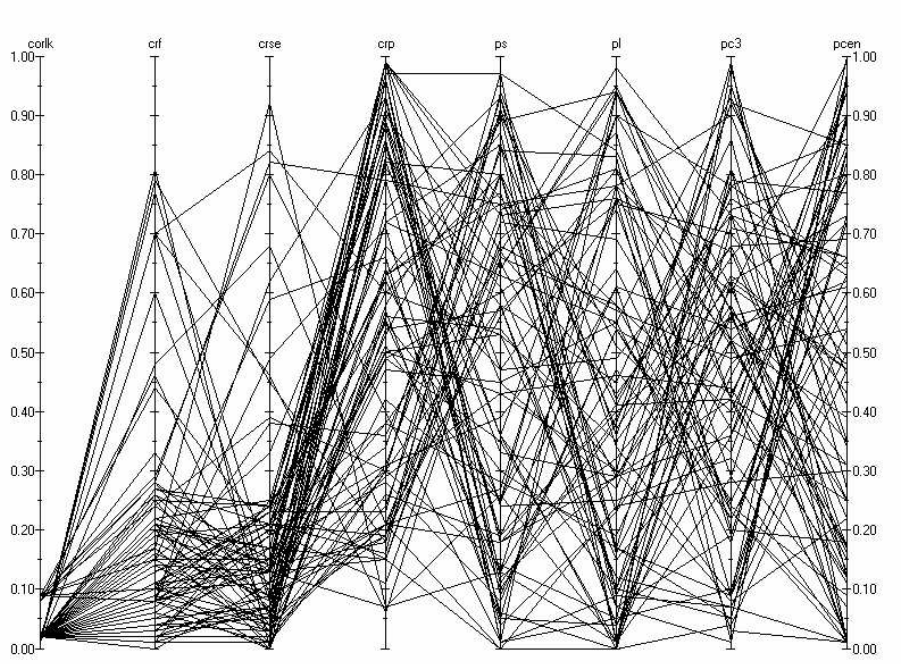

Figure 3.8: Cobweb plot conditional on low values of *corlk*.

3.7 Conclusions

We collect a number of conclusions.

- A ranking tool has been developed which uses failure data and structured judgment.
- The tool characterizes pipe sections according to some 20 pipe characteristics and environmental characteristics
- The tool predicts failure frequencies per kilometer year, and gives uncertainty bounds
- These predictions allow distinctions to be made between pipe sections with different characteristics, and these distinctions are not swamped by uncertainties, despite the fact that the uncertainties are large
- For most pipes, the risk due to corrosion is significantly less than the risk due to 3rd party interference

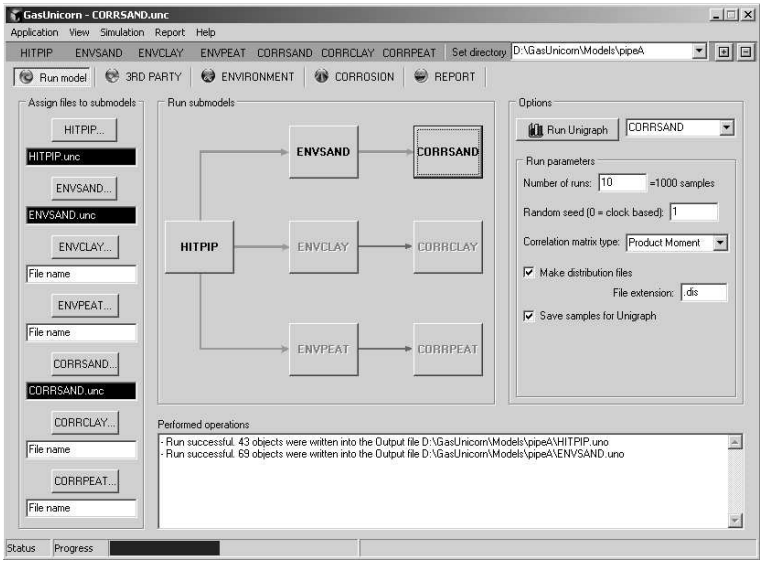

Figure 3.9: Main window of GasUnicorn, new interface for UNICORN.

- The depth of ground cover is of significant influence for the frequency and severity of 3rd party damage.

More detailed sensitivity analysis will be described in chapters 4 and 5.

3.8 Implementation

The whole theory presented in this chapter has been implemented in UNICORN, software package developed at Delft University of Technology. This program uses Monte Carlo methods for dealing with uncertainties and gives a possibility to incorporate dependencies between input variables.

For convenience, the model has been split into three submodels, each of them forming a separate section. First, we calculate the probability of coating damage, small damage, large damage and direct leak caused by 3rd party interference (we call this submodel HITPIP), then we calculate the probability of coating damage due to corrosion and corrosion rate (ENVSAND, ENVCLAY or ENVPEAT, depends on soil type). Outputs of these two submodels are used by the third submodel (CORRSAND, CORRCLAY or CORRPEAT) to determine overall failure frequency of gas pipelines. Definitions of input parameters and functions are available in Appendix B.

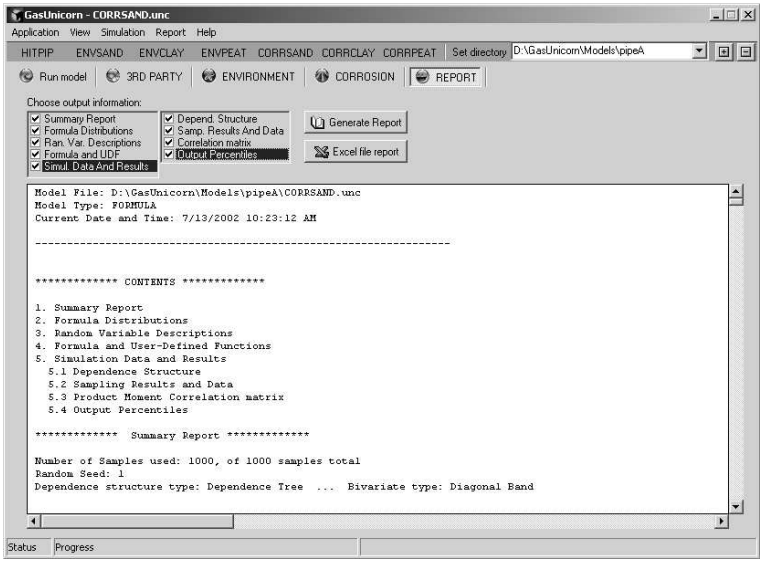

Figure 3.10: Report created by GasUnicorn based on the results of last simulation.

3.9 UNICORN frontend for the model

UNICORN is a very advanced tool for modelling uncertainty with correlations. Its current development even extends capabilities of this software. The program has a modular structure, where the core of the software is contained in a stand-alone dynamic library file called from freely designed interface. Many of the functions offered by UNICORN require trained users. For this reason a new frontend for UNICORN has been developed under contract with N.V. Nederlandse Gasunie designed specifically for the model brought closer in this chapter and temporarily is called *GasUnicorn*. This allows to greatly simplify the process of running the model. Figure 3.9 presents the main windows of the new interface.

Basically the functional division mentioned in the previous section is preserved in the new interface. All the submodels are loaded and run separately. This software allows to perform all basic commands on files including loading, changing and saving parameters. It is not intended to change the model's functions in this software though. For this purpose the full version of UNICORN must be used. After successful running of one of the submodels a report is created containing a detailed information on outputs. Figure 3.10 shows an

example of such a report. All samples can be saved into a file. This allows to produce so-called cobweb plots, representation of high dimensional distributions[4]. New feature introduced in this software is a capability to export the report to a MS Excel file.

Appendix A describes running UNICORN with the new interface.

[4]See section 3.6.2 for details.

Chapter 4

Bayesian sensitivity analysis

This chapter is based on the article "Bayesian Sensitivity Analysis" by D. Lewandowski & R.M. Cooke (Lewandowski & Cooke 2001)

4.1 Introduction

As Bayesian models become more popular and more complex, it issues of appraising model performance, and identifying important parameters receive more attention.

Classically, a parameter is identifiable if there is a function of the data which converges almost surely to the value of this parameter. A distinctive feature of Bayesian methods is that we can easily learn from data about parameters which in a classical sense are *not* identifiable. In particular, the posterior distribution can differ from the prior, without having a Dirac distribution as its limit. This simple remark means that sensitivity, sensitivity to data, and the consequences of sensitivity must be rethought from a Bayesian perspective.

In this chapter we discuss a number of issues that arise in Bayesian model criticism and sensitivity analysis. Methods are suggested for identifying important parameters and for analysing the impact of data versus prior information.

These ideas are illustrated with an analysis of the two stage hierarchical model used the Swedish Nuclear Inspectorate's data processing (Pörn 1990)[1]. This model is designed to utilize failure data from similar plants to update

[1]Prof. R.E. Barlow was instrumental in the development of this model and served on the PhD thesis committee

failure rates at a given plant. Relevant questions concern the sensitivity to hyperparameters, the sensitivity to data, and the impact of information from other plants.

4.2 Sensitivity in hierarchical models

We are interested in characterizing the sensitivity of aspects of a model to the data. Loosely, if a parameter "does not listen to the data" then it is weakly identifiable in a Bayesian sense. This is relevant for model criticism for two reasons. First, if other quantities of interest depend on weakly identifiable parameters, then this might be a cause of concern as these quantities would remain strongly dependent on the prior distribution. Second, weakly identifiable parameters might be eliminated in a more parsimonious model.

We consider a generic two stage model with parameter vector $\lambda = (\lambda_1, ..., \lambda_n)$, hyperparameter vector $\theta = (\alpha, \beta, \gamma, \dots)$, data matrix $X = X_{ij}$ with row i associated with λ_i, and some distribution g over θ containing constants K. In general it is assumed that the components of λ are independent given θ, and that given λ_i the data $X_{i,\cdot}$ is independent of $(\theta, X_{j,\cdot}), j \neq i$.

Among the questions of interest are:

- Which parameters are sensitive to the data?
- Which parameters are sensitive for a given parameter?
- Can the computation of sensitivities be done efficiently?

4.2.1 Which parameters are sensitive to the data?

This question can be answered by computing the relative information of a parameter's posterior with respect to its prior. Letting $(\lambda_i|X)$ denote a random variable with distribution equal to the conditional distribution of λ_i given X, and assuming densities exist, we could compute

$$I((\lambda_i|X); \lambda_i) = \int f(\lambda_i|X) \ln \left(\frac{f(\lambda_i|X)}{f(\lambda_i)} \right) d\lambda_i. \tag{4.1}$$

Note that if λ_i follows the improper prior $d\lambda_i$, then

$$-I((\lambda_i|X); \lambda_i) = H(\lambda_i|X) = -\int f(\lambda_i|X) \ \ln f(\lambda_i|X) \ d\lambda_i. \tag{4.2}$$

where H denotes the entropy.

4.2.2 Which parameters are sensitive for a given parameter?

Having determined the sensitivity of parameters to data, we now examine the sensitivity of parameters to each other. There are many ways of doing this and the best method will depend on the specific case at hand. The simplest idea is to regress the parameter of interest, say λ_i onto other parameters, indexed as ψ

$$\lambda_i = \sum_{\psi} \frac{\rho(\lambda_i, \psi)\sigma_{\lambda_i}}{\sigma_\psi}\psi + Error. \tag{4.3}$$

In many cases the relationship between λ_i and ψ is exponential rather than linear and eq. (4.3) might be replaced by log linear regression

$$\ln(\lambda_i) = \sum_{\psi} \frac{\rho(\ln(\lambda_i), \psi)\sigma_{\ln(\lambda_i)}}{\sigma_\psi}\psi + Error, \tag{4.4}$$

or by rank regression

$$F_i(\lambda_i) = \sum_{\psi} \rho(F_i(\lambda_i), F_\psi(\psi))F_\psi(\psi) + Error, \tag{4.5}$$

where F_* denotes the cumulative distribution function of its argument. Equation (4.5) regresses the quantile function of λ_i on the quantile functions of the ψ's. The quantile function of a continuous random variable is of course uniform on $[0, 1]$ with variance $1/12$. The *rank correlation* $\rho(F_i(\lambda_i), F_\psi(\psi))$ is also denoted $\rho_r(\lambda_i, \psi)$.

The expressions (4.3), (4.4) and (4.5) can be evaluated either in the prior or in the posterior joint distributions. The former two can be evaluated on-the-fly, as their computation involves only moments. The rank regression coefficients cannot be evaluated on-the-fly as we must first determine the cumulative distribution function, and this is typically known only at the end of a simulation.

4.2.3 A more general notion of sensitivity.

We consider a function $G = G(X, Y)$ of random vectors X and Y with $\sigma_G^2 < \infty$. In analogy with the above, we may ask for which function $f(X)$

with $\sigma^2_{f(X)} < \infty$ is $\rho^2(G, f(X))$ maximal? The answer is given in the following proposition.

Proposition 4.2.1. *Let $G = G(X, Y)$ with $\sigma^2_G < \infty$; then*

(i) $Cov(G, E(G|X)) = \sigma^2_{E(G|X)}$,

(ii) $max_{f;\, \sigma^2_{f(X)} < \infty} \rho^2(G, f(X)) = \rho^2(G, E(G|X)) = \frac{\sigma^2_{E(G|X)}}{\sigma^2_G}$.

Proof.
(i) $Cov(G, E(G|X)) = E(E(GE(G|X)|X)) - EGE(E(G|X)) = E(E^2(G|X)) - E^2(E(G|X))$.
(ii) Let $\delta(X)$ be any function with finite variance. Put $A = \sigma^2_{E(G|X)}$, $B = \mathrm{Cov}(E(G|X), \delta(X))$, $C = \sigma^2_G$, and $D = \sigma^2_\delta$. Then

$$\begin{aligned} \rho^2(G, E(G|X) + \delta(X)) &= \frac{(A+B)^2}{C(A+D+2B)}, \\ \frac{\sigma^2_{E(G|X)}}{\sigma^2_G} &= \frac{A}{C}, \\ \frac{(A+B)^2}{C(A+D+2B)} \leq \frac{A}{C} &\iff B^2 \leq AD. \end{aligned}$$

The latter inequality follows from the Cauchy-Schwarz inequality. This is similar to a result by Whittle (1992). □

The quantity $\frac{\sigma^2_{E(G|X)}}{\sigma^2_G}$ is called the *correlation ratio*, and may be taken as the general sensitivity of G to X. Note that the correlation ratio is always positive, and hence gives no information regarding the direction of the influence. If we take $f(X) = X$ then we will notice, that according to Proposition 4.2.1, the product moment correlation $\rho^2(G, X) \leq \rho^2(G, E(G|X))$, but in case of a strong nonlinearity this is not a good estimation. The more the relation between X and $E(G|X)$ (thus implicitly between X i G) is nonlinear, the greater the difference between $\rho^2(G, X)$ and $\rho^2(G, E(G|X))$. It is easy to show that

$$0 \leq \frac{\rho^2(G, X)}{\rho^2(G, E(G|X))} \leq 1,$$

and this fraction is equal to 1 if $E(G|X) = k \cdot X$, where k is a constant. Thus it can be regarded as a sort of a measure of nonlinearity.

The following propositions explore some properties of the correlation ratio. The first is straightforward, the second uses Proposition 4.2.1.

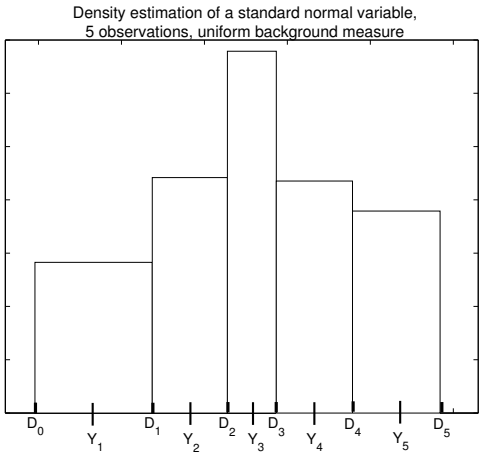

Figure 4.1: Density approximation with 5 observations.

Proposition 4.2.2. *Let $G(X,Y) = f(X) + h(Y)$ with $\sigma_f^2 < \infty$, $\sigma_h^2 < \infty$ and X, Y are not both simultaneously constant ($\sigma_G^2 > 0$). If X and Y are independent then*

$$\rho^2(G, E(G|X)) + \rho^2(G, E(G|Y)) = 1.$$

Proposition 4.2.3. *Let $G = G(X,Y)$ with $Cov(E(G|X), E(G|Y)) = 0$; then*

$$\rho^2(G, E(G|X)) + \rho^2(G, E(G|Y)) \leq 1.$$

Proof.

$$\begin{aligned} \rho(E(G|X), G - E(G|Y)) &= \frac{Cov(E(G|X), G - E(G|Y))}{\sigma_{E(G|X)}\sqrt{\sigma_G^2 - \sigma_{E(G|Y)}^2}} \\ &= \frac{\sigma_{E(G|X)}}{\sqrt{\sigma_G^2 - \sigma_{E(G|Y)}^2}} \leq 1 \\ \sigma_{E(G|X)}^2 + \sigma_{E(G|Y)}^2 &\leq \sigma_G^2 \end{aligned}$$

□

4.2.4 Can the computations be done efficiently?

The computations frequently use Monte Carlo methods. Efficiency in this context usually means on-the-fly. That is, we would like to perform all necessary calculations on a sample, then discard the sample and proceed to the

next sample. A computation which involves operations on the entire sample is not efficient.

For reasons of simplicity we first discuss an on-the-fly method of computing the entropy as defined in (4.2). Values for λ_i are generated by simulation and are plotted on the real line as $Y_1 \dots Y_N$ (see Figure 4.1)[2]. We approximate the density as a step function whose steps occur at the midpoints D_i between Y_i, and Y_{i+1}. We set $D_0 = Y_1 - (Y_2 - Y_1)/2$, and $D_N = Y_N + (Y_N - Y_{N-1})/2$.

Each point has equal probability, namely $1/N$. The density above the point Y_i is therefore estimated as

$$P_i = \frac{1}{N(D_i - D_{i-1})}.$$

The entropy is then computed as

$$H \approx (-1/N) \sum_{i=1}^{N} \ln \left(\frac{1}{N(D_i - D_{i-1})} \right).$$

The relative information (4.1) is computed in a similar fashion. The prior density of λ_i is approximated as a step function with value $f(Y_i)$ between points D_{i-1}, D_i, where f is the prior density

$$I((\lambda_i|X); \lambda_i) \approx (1/N) \sum_{i=1}^{N} \ln \left(\frac{1}{N(D_i - D_{i-1}) f(Y_i)} \right). \tag{4.6}$$

These quantities can be computed on-the-fly. If the computation has been done for N samples, adding one additional sample requires only a local adjustment. We can also group the samples, such that we consider k adjacent samples and estimate the density over such a k-tuple starting with Y_i as $k/(N(D_{i+k} - D_{i-1}))$. Grouping the samples in this way a larger "local adjustment" in (4.6), but gives better results.

To illustrate, the entropy of 1000 samples from the standard normal distribution has been computed on 20 iterations. The results are shown as computed above, and also after grouping the data points by 2's, by 5's and by 10's (see Figure 4.2). The Entropy of the standard normal is 1.419. If we truncate the standard normal to $[-3.3]$ corresponding roughly the above density approximation with 1000 samples, the entropy integral is 1.4056.

[2]Although we must retain the ordered sample in memory, we do not perform operations on the whole sample; in this sense we are still on-the-fly.

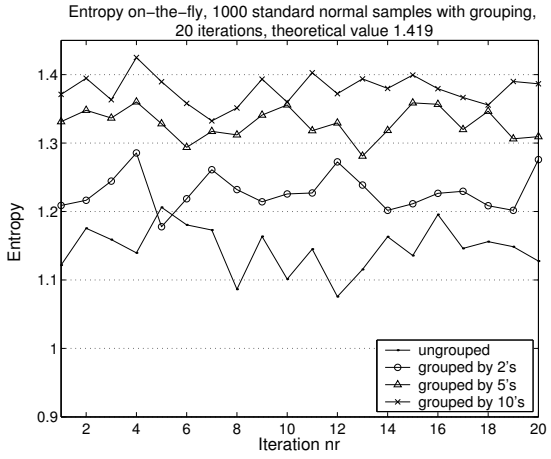

Figure 4.2: Entropy, 1000 standard normals, 20 iterations.

We see that the results are stable, though the ungrouped data tend to be a bit jittery, thus producing a lower entropy value than the theoretical value.

The same pattern emerges in computing the relative information on the fly. Figure 4.3 shows 20 iterations of 1000 samples for calculating $I(X|Y)$, where X is standard normal, and Y is normal with mean 5 and standard deviation 3. The distribution of X is treated as the posterior in (4.6). The theoretical value is 2.043. Again, the estimator with ungrouped data is stable but overestimates the relative information due to sample jitter.

A. O'Hagan (personal communication) has recently proved that the bias in computing entropy with ungrouped data is asymptotically equal to $\gamma - 1 + \ln(2)$, where γ is Euler's constant. Thus, for a sufficiently large sample, we can remove this bias and obtain better results.

Computing correlation ratio cr may be difficult in some cases. However, if we can sample Y' from the conditional distribution $(Y|X)$ independently of Y, and if the evaluation of G is not too expensive, then the following simple algorithm may be applied (Homma 1990):

1. Sample (x, y) from (X, Y),

2. Compute $G(x, y)$,

3. Sample y' from $(Y|X = x)$ independent of $Y = y$,

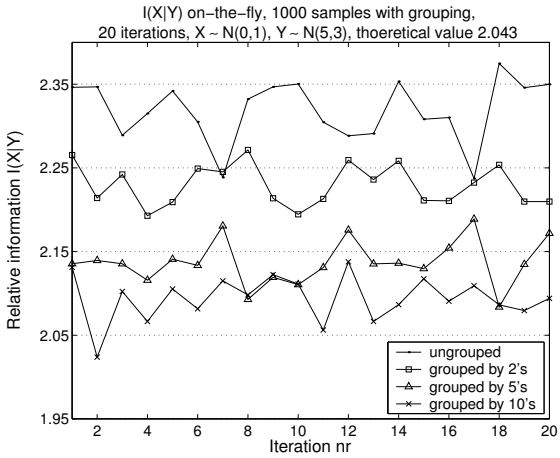

Figure 4.3: $I(X|Y)$ 1000 samples, 20 iterations, X=N(0,1), Y = N(5,3).

4. Compute $G' = G(x, y')$,

5. Store $Z = G \cdot G'$,

6. Repeat.

The average value of Z will approximate $E(E^2(G|X))$, from which the correlation ratio may be computed as

$$cr(G, X) \approx \frac{E(E^2(G|X)) - E^2(G)}{\sigma_G^2}.$$

Of course, if Y and X are independent, then this algorithm poses no problems. If Y and X are not independent, then it may be difficult to sample from $(Y|X)$. In this case there is no alternative to the "pedestrian" method: save a large sample, compute $E(G|X = x_i \pm \varepsilon)$ for suitable $x_1, ...x_n$, and compute the variance of these conditional expectations. To do this for a large number of variables can be slow.

4.3 Example, the SKI model

A Bayesian model for dealing with plant-to-plant variability has been adopted by the Swedish Nuclear Inspectorate SKI (Pörn 1990). This model has been reviewed by Cooke, Dorrepaal & Bedford (1995) and discussed by Hofer &

Peschke (1999) and Meyer & Hennings (1999). Hora & Iman (1990) describe a similar model. We consider a collection of classes of components (plants). Each class consists of components which are considered identical for the purposes of lifetime estimation, and which are used in a specific plant under plant-specific conditions. Different plant specific conditions lead to different Rate of Occurrence of Failure (ROCOF). Since we would like to use data from given plants to make inference about the ROCOF in another plant, we have to assume something about the underlying relationship between the ROCOF's of the various plants. In Pörn's model, these ROCOF's are treated as independent realisations of random quantities with the same distribution.

Specifically:

1. The pattern of failures at each plant is supposed to follow a Poisson process. At plant i, we have x_i failures in an operating time of T_i. The plant specific ROCOF is λ_i, which is a realisation of the random variable Λ.

2. Λ follows a mixed gamma distribution

$$P(\lambda_i|\theta) = G(\lambda_i|\alpha,\beta)(1-c) + G(\lambda_i|1/2,1)c.$$

   α and β are unknown shape and scale parameters, and c is a random variable taking values in $[0,1]$. According to (Pörn 1990), c is a contamination parameter mixing $G(\lambda_i|\alpha,\beta)$ with a relatively vague gamma to "add a pinch of uncertainty". The uncertainty over values of θ is modelled by assuming that θ is a random vector.

3. $\lambda_1, \ldots, \lambda_n$ are independent realizations of Λ.

4. Given $(\lambda_1, \ldots, \lambda_n)$, $(x_1, \ldots, x_n)$ are independent.

5. Given λ_i, x_i and $(\theta, \lambda_1, \ldots \lambda_{i-1}, \lambda_{i+1}, \ldots, \lambda_n)$ are independent.

A consequence of the dependence structure here is that data (x_i, T_i) from plant i can only influence our beliefs on the value of λ_j $(j \neq i)$ through its influence on our beliefs on the value of θ.

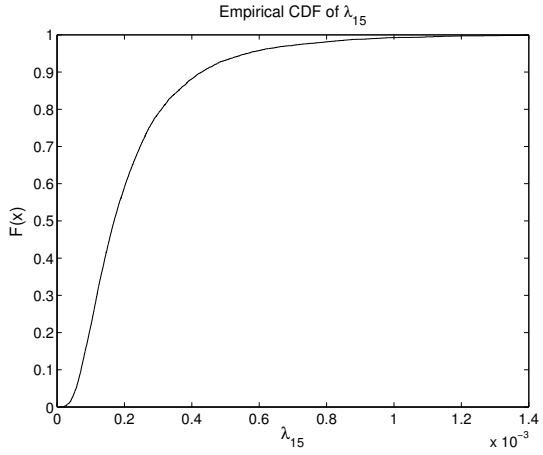

Figure 4.4: Cumulative distribution function of λ_{15}.

Inference under Pörn's model Suppose that we have data (x_i, T_i) from plants $i \in \{1, \ldots, n+1\}$. Suppose that we have chosen a prior distribution for the hyperparameters $P(\alpha, \beta, c)$, and that we wish to have an updated distribution of λ_{n+1}. Note that we have information on λ_{n+1} from two directions:

1. The influence of all of the data on our beliefs of the value of θ, and
2. The influence of the plant-specific data (x_{n+1}, T_{n+1}) on our beliefs over the value of λ_{n+1}.

It will be noted that the data (x_{n+1}, T_{n+1}) is used twice in this procedure. According to Pörn (1990) the effect of this double counting is small.

Under the assumptions of Pörn's model, it can be shown that the likelihood function of $\theta = (\alpha, \beta, c)$ given the data (x_i, T_i) $(i = 1, \ldots, n)$ is proportional to

$$\prod_{i=1}^{n} [A\,(1-c) + B\,c\,] \tag{4.7}$$

$$A = \frac{\Gamma(x_i+\alpha)}{\Gamma(x_i+1)\Gamma(\alpha)} \left(\frac{\beta}{\beta+T_i}\right)^{\alpha} \left(\frac{T_i}{\beta+T_i}\right)^{x_i}$$

$$B = \frac{\Gamma(x_i+1/2)}{\Gamma(x_i+1)\Gamma(1/2)} \left(\frac{1}{1+T_i}\right)^{1/2} \left(\frac{T_i}{1+T_i}\right)^{x_i}$$

The terms under the product operator in formula (4.7) will be denoted p_i. Each p_i represents an update of the hyperpriors based only on the data from plant

Plant	Nr Failures	Operating Hours
1	2	17600
2	1	17600
3	3	10700
4	1	10700
5	0	29500
6	0	29500
7	4	15000
8	1	15000
9	1	22000
10	1	22000
11	0	4600
12	0	4600
13	1	5600
14	0	5600
15	3	5000

Table 4.1: Swedish nuclear plant centrifugal pump data.

	λ_{15} [failures/hour]
5%	$8.0 \cdot 10^{-5}$
50%	$2.3 \cdot 10^{-4}$
95%	$6.3 \cdot 10^{-4}$
mean	$2.8 \cdot 10^{-4}$

Table 4.2: Results for λ_{15}.

i. The likelihood of λ_{n+1} given x_{n+1} is easily seen to be

$$P(x_{n+1}|\theta) = e^{-\lambda_{n+1}T_{n+1}} \frac{(\lambda_{n+1}T_{n+1})^{x_{n+1}}}{\Gamma(x_{n+1}+1)}.$$

Thus, the posterior distribution of λ_{n+1} given data (x_i, T_i) $(i = 1, ..., n+1)$ is

$$G(\alpha + x_{n+1}, \beta + T_{n+1})(1-c) + G(1/2 + x_{n+1}, 1 + T_{n+1})c, \qquad (4.8)$$

where $\theta = (\alpha, \beta, c)$ follows a distribution proportional to the product of the prior $P(\alpha, \beta, c)$ and (4.7).

This model may be computed by analytical methods, or with Monte Carlo integration. In the later case we sample the hyperpriors and apply acceptance-

rejection to produce samples of (4.7).

Figure 4.4 shows posterior cumulative distribution function of λ_{15} which was obtain using data from all plants.

Data in Table 4.3 is analyzed in (Pörn 1990) and in a mathematical review (Cooke et al. 1995), to which we refer for the prior distributions and details on the inference model. Table 4.3 shows the results in (Pörn 1990) for the updated distribution of the failure rate for plant 15 using the data of Table 4.3.

4.4 Sensitivity results

We are interested in λ_{15} after updating on the data from all plants. In particular, we are interested in how sensitive λ_{15} is to the data from plant 15 (i.e. p_{15}), how sensitive it is to the data from other plants, and how sensitive it is to the hyperparameters. In these calculations, the posterior distribution was obtained with acceptance-rejection sampling. All sensitivity results concern the posterior distribution. Based on 9521 posterior samples the posterior mean and variance of λ_{15} are (compare Table 4.3):

i) $E(\lambda_{15}) = 2.22\text{E-}04$

ii) $Var(\lambda_{15}) = 3.26\text{E-}08$

The acceptance-rejection method rendered the on-the-fly algorithm impractical, and correlation ratios were computed with the pedestrian method.

Table 4.4 presents sample based correlations, rank correlations, and correlation ratio's. All these refer to the posterior distribution. Evidently, the information from some plants are more important than from others. Plants $2, 8, 9, 10$ have the biggest influence on the function λ_{15}. The posterior parameter β is associated with the largest correlation ratio. Note that the correlation ratio is always greater than ρ^2; the size of this difference is an index of the non-linearity of the regression function $E(\lambda_{15}|X)$.

We ask, which features of the data at plant i are driving these results. The variance of p_i is directly related to the amount of data available at plant i. Figure 4.5 shows no obvious relation between the correlation ratio with λ_{15} and variance of p_i $(i = 1, \ldots, n)$. Note that the posterior variance will be inversely proportional to the square of T_i, so that p_5, p_6 have the highest posterior variances.

X	$\rho(\lambda_{15}, X)$	$\rho_r(\lambda_{15}, X)$	$\rho^2(\lambda_{15}, X)$	$\rho_r^2(\lambda_{15}, X)$	$\rho^2(\lambda_{15}, E(\lambda_{15}\|X))$
p_1	-0.19	-0.14	0.0361	0.0196	0.0558
p_2	-0.47	-0.55	0.2209	0.3025	0.234
p_3	0.28	0.44	0.0784	0.1936	0.113
p_4	-0.33	-0.31	0.1089	0.0961	0.119
p_5	0.02	-0.04	0.0004	0.0016	0.0185
p_6	0.02	-0.04	0.0004	0.0016	0.0185
p_7	0.29	0.46	0.0841	0.2116	0.123
p_8	-0.44	-0.50	0.01936	0.25	0.208
p_9	-0.48	-0.59	0.2304	0.3481	0.247
p_{10}	-0.48	-0.59	0.2304	0.3481	0.247
p_{11}	-0.29	-0.36	0.0841	0.1296	0.102
p_{12}	-0.29	-0.36	0.0841	0.1296	0.102
p_{13}	-0.04	0.05	0.0016	0.0025	0.0162
p_{14}	-0.27	-0.35	0.0729	0.1225	0.1415
α	-0.33	-0.45	0.1089	0.2025	0.153
β	-0.39	-0.59	0.1521	0.3481	0.251
c	0.09	0.03	0.0081	0.0009	0.0207

Table 4.3: Correlation ratios for λ_{15}.

The key to understanding the sensitivities of Table 4.4 is given in Figure 4.6. The "mean time to failure" MTTF of a plant i is the operating time T_i divided by the number of failures x_i. If this time is bigger than the inverse expectation of λ_{15} (4444) then the function p_i is strongly negatively correlated with λ_{15}. The greater this difference the greater is the absolute value of the correlation (both product moment correlation and rank correlation). Notice, that if plant i has a MTTF smaller than MTTF of λ_{15} then the correlation is positive. Although the mean lifetime at plant 3 is only a little smaller than 4444, p_3 and λ_{15} are quite strongly correlated. We know that $\rho^2(\lambda_{15}, p_i) \leq \rho^2(\lambda_{15}, E(\lambda_{15}|p_i))$ (Proposition 4.2.1). Thus if a MTTF of a plant i is much different from the inverse of the expectation of λ_{15} then p_i has greater influence on λ_{15}. Note the effect of the sign of the correlation.

Variables α, β and c are hyperparameters. We use data from the plants to update our belief in these variables. In the posterior distribution, we see that β is the most important parameter, and α is more important than 10 of the 14 plants. This indicates that the final result is still strongly driven by the

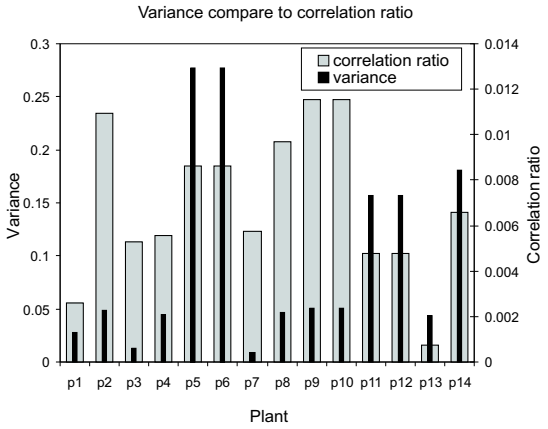

Figure 4.5: Variance of p_i compared to correlation ratio between λ_{15} and p_i.

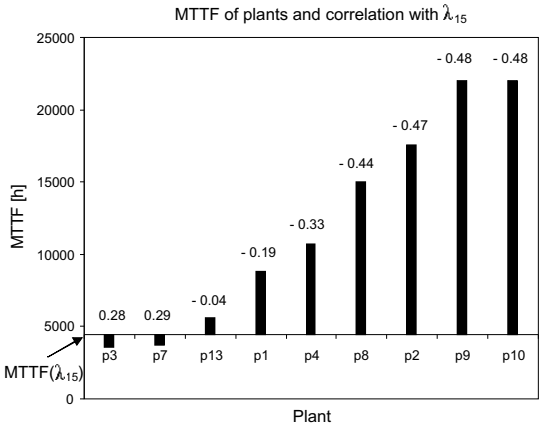

Figure 4.6: The MTTF of the plant i compared to the inverse of expectation of λ_{15} (MTTF of λ_{15}) and the correlation between λ_{15} and p_i.

hyperparameters. It must be noted that the distributions of the p_i also depend on the hyperparameters; however we should hope that their influence dies off rapidly as the data from all plants is gathered. After all, the data represents a total of 188,600 operating hours. The parameter c, on the other hand, does not play a significant role. The persistence of hyperparameters α and β observed here confirms the conclusion of Cooke et al. (1995), obtained with a much more laborious analysis.

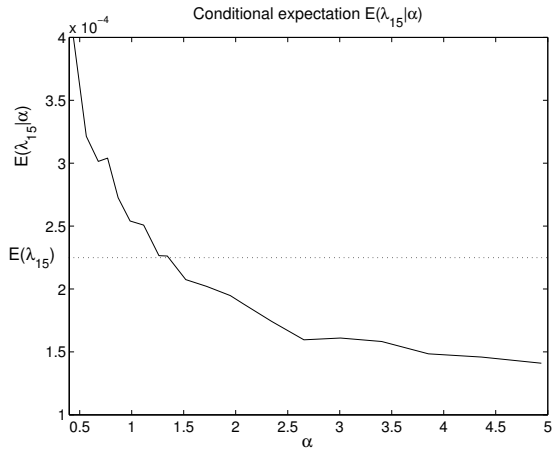

Figure 4.7: Dependence between $E(\lambda_{15}|\alpha)$ and α compared to $E(\lambda_{15})$

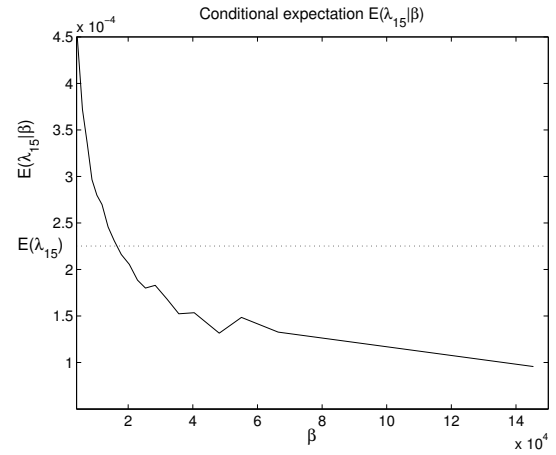

Figure 4.8: Dependence between $E(\lambda_{15}|\beta)$ and β compared to $E(\lambda_{15})$

The rank correlation $\rho_r(\lambda_{15}, \beta)$ is negative. Thus, small values of β tend to arise in combination with large values of λ_{15}. This is illustrated in Figure 4.8 which shows that the regression $E(\lambda_{15}|\beta)$ is decreasing.

The variable c is applied to add "a pinch of uncertainty" and it is a pinch indeed. c does't play a significant role in this model.

Consider Figure 4.7. Parameter β is a function inter alia of α. Thus, α influences λ_{15} through itself and β, and we might expect that α has greater influence on λ_{15} than β. However, $Var(E(\lambda_{15}|\alpha))$ is less than $Var(E(\lambda_{15}|\beta))$.

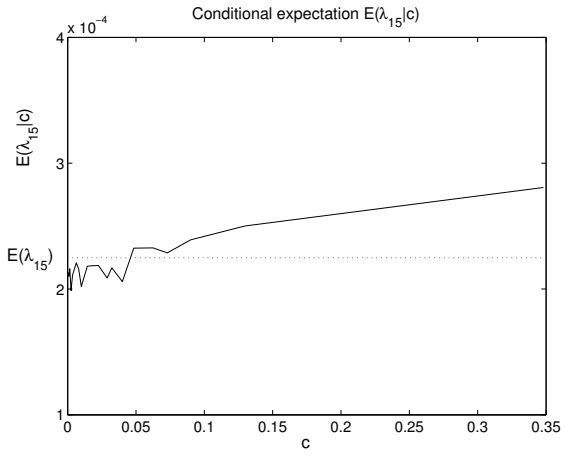

Figure 4.9: Dependence between $E(\lambda_{15}|c)$ and c compared to $E(\lambda_{15})$

Figures 4.7 and 4.8 show that the regression of λ_{15} on α and β is not linear. This recommends the use of the correlation ratio as a measure of dependence. The relative unimportance of c is illustrated in Figure 4.9, where we see that the conditional expectation of λ_{15} given c does not differ greatly from the unconditional expectation of λ_{15}.

4.5 Conclusions

Sensitivity analysis and model criticism are active topics at the moment. The Bayesian approach allows these issues to be raised and analysed in a natural way. By analysing the sensitivity of a parameter of interest to data and to prior parameters, we can judge the relative importance of prior assumptions.

There are many ways to quantify sensitivity using entropy based concepts or regression based concepts. We have argued that the correlation ratio is particularly attractive in this regard, although it cannot always be computed on-the-fly, and may be difficult to compute analytically.

The SKI two stage Hierarchical Bayes model is a very interesting case because, (i) it is an important application (ii) it has been studied and reviewed extensively, and (iii) it is complicated enough that quantitative measures of sensitivity greatly contribute to understanding the model. The main conclusions regarding the persistence of hyperparameters α and β reached by Cooke

et al. (1995) by laborious re-computations, are obtained quite simply in Table 4.4. Moreover, we also gain insight into the features of the data which drive the parameter of interest (Figure 4.5).

Chapter 5

Sensitivity analysis of the UNICORN model factors

The previous chapter presented a commonly used measure of sensitivity of output results to input parameters. This measure is called the correlation ratio and denoted by cr. It will be applied to the Unicorn model that has been studied in Chapter 3. The correlation ratio does not have a property of symmetry ($cr(G, X) \neq cr(X, G)$). Since we want to know how the input variable changes values of its function, we take G as the conditioned function and X as the conditioning variable. Thus we calculate $cr(G, X)$.

The model consists of 3 submodels and dependencies in each submodel will be analyzed separately. This analysis is not the easy task though. The problem described by the model has so many dimensions, that checking impact of all of the parameters on the output is simply a very time-consuming task. Therefore we concentrate on some chosen in advance parameters, which will describe a hypothetical family of gas pipelines. For instance, we can be interested in answering the following question - *To what extent the inputs influence the frequency of leakage per kmyr of a pipe laid in sand in 1965? The pipeline has a bitumen coating and 36 inch diameter.* This is a part of the specification of Pipeline A. Taking also values of the rest of the parameters derived from characteristics of this pipeline, allows to replace the above question with this one - *Which factors drives the failure frequency of Pipeline A and which ones have the greatest influence on this frequency?.* We no longer regard a non-existing pipeline. Now the number of the defects indicated in the Pipeline

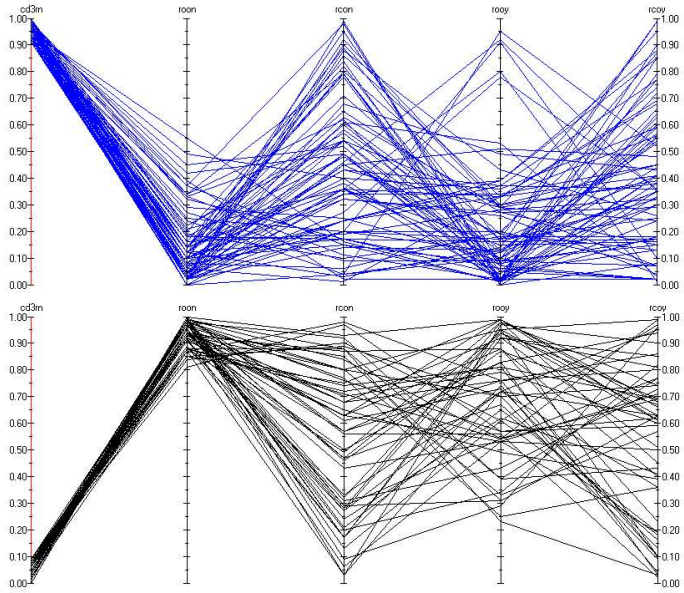

Figure 5.1: Cobweb plots of the variables of HITPIP submodel.

A data is rather a sample from the distribution of the number of defects of a virtual pipeline having the same characteristics as Pipeline A. This makes the sensitivity analysis even more important. The best documented is the information on pipelines A and B, which includes full characteristics of the soil type in which the pipelines were laid. Since those two pipelines are very similar as regards physical dimensions and environmental characteristics, we shall concentrate on the sensitivity analysis for model with specification of pipeline A. For comparison, the soil type will be replaced with clay with typical values of some parameters like pH factor and resistivity.

5.1 Sensitivities in modelling of damage due to 3^{rd} party digs

The submodel HITPIP evaluates the probability of coating damage *cd3rn*, small damage *ldsrn* and large damage *ldlrn*, as well as the probability of a direct leak *dl*. Two main user selected parameters are thickness and depth of the pipeline. Consider a set of parameters given in Appendix B for this submodel.

Conditioning variable	Conditioned variable		
	cd3rn	ldsrn	ldlrn
roon	**0.84**	**0.85**	**0.84**
rcon	0.06	0.06	0.06
rooy	0.13	0.14	0.13
rcoy	0.03	0.03	0.04

Table 5.1: Correlation ratios for outputs of HITPIP submodel.

Inputs *hooye*, *hcoye*, *hoone* and *hcone* representing experts' assessment of the frequency of hitting a pipeline do not contribute in the model, because this particular set of values takes into account only the zero order terms while calculating outputs. Notice that *fop* and *fopz* are equal, similarly *fcl* and *fclz* (Appendix B describes the abbreviations used in this chapter). From the remaining inputs important are percentages of the hits of the pipeline that are repaired *rooy*, *rcoy*, *roon* and *rcon*. The source for these variables were experts. Table 5.1 contains the correlation ratios of the output (conditioned) variables given conditioning variables. The probability of a direct leak is not analyzed here, since in this case it explicitly depends on depth and frequency of ruptures and is not uncertain.

The most influencial input variable is the percentage of hits during open digs without oversight *roon*, regardless the output variable. The formulas of *cd3rn*, *ldsrn* and *ldlrn* do not differ significantly from each other and there is no surprise in almost equality of the correlation ratios. Figure 5.1 agrees with the numbers in Table 5.1. It clearly shows a strong negative correlation between *cd3rn* and *roon*. Intuitively, the greater the percentage of repaired damages, the lower the frequency of damages that can initiate corrosion. The mean value of *roon* is not very big (0.461) and is less than the mean value of *rooy* which is equal to 0.84. Nevertheless, the great impact of variable *roon* on the models outputs can be explained by large value of the associated constant *hoonz*, frequency of hitting per kmyr during open digs with no oversight. This frequency is at least twice as large as the other frequencies - *hooyz*, *hcoyz* and *hconz*. Remarkable is the fact that $\rho^2(cd3rn, roon) \approx cr(cd3rn, roon)$. According to proposition eq. (4.2.1), this means, that the relation between $cd3rn$ and $roon$ is almost fully linear and this is also depicted in Figure 5.2. We see that the conditional expectation $E(cd3rn|roon)$ is almost linear in $roon$.

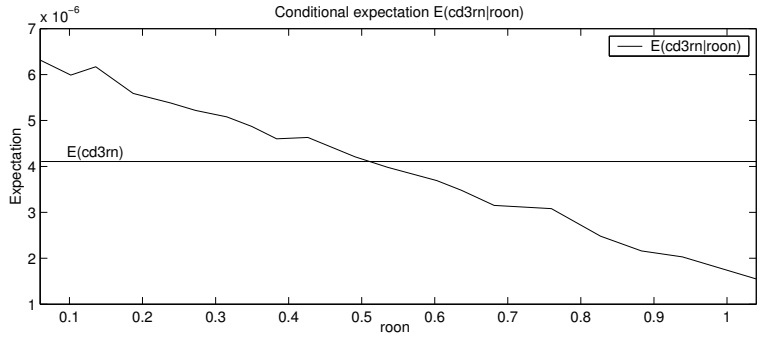

Figure 5.2: Conditional expectation $E(cd3rn|roon)$.

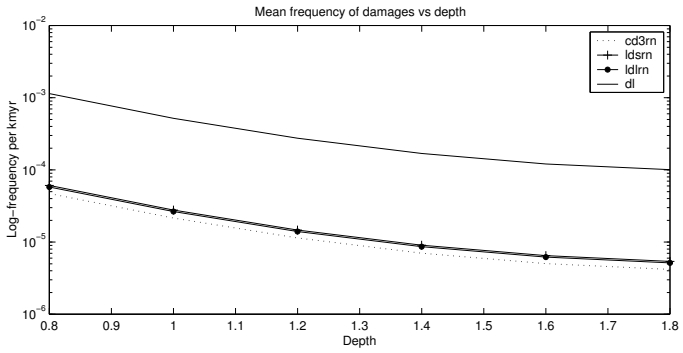

Figure 5.3: Influence of depth cover on frequency of damages due to 3^{rd} party digs.

The same holds for $cr(ldsrn, roon)$ and $cr(ldlrn, roon)$.

To avoid damages of pipelines due to 3^{rd} party digs, they are laid as deep as possible. In practise the depth cover varies from about 0.8 m to 1.8 m. Figure 5.3 shows that the increasing of the depth cover from 0.8 to 1.8 meter decreases the frequency of hitting by the factor of 10. The depth cover has absolutely no influence on the correlation ratios given in Table 5.1.

Correlation ratio	Value	
	$r = 200000$	$r = 50000$
cr(crf, xwf)	0.48	0.08
cr(crf, xwu)	**0.57**	0.08
cr(crf, xph)	0.02	0.02
cr(crf, xr)	0.02	**0.82**

Table 5.2: Influence of environmental characteristics on the corrosion rate in sand.

5.2 Sensitivities in modelling environmental factors

Three most important output variables of ENVSAND model are *pcde*, *crf* and *crp*. Variable *crf*, free corrosion rate, is influenced by the resistivity and *pH* of the soil, and percentage of the pipeline exposed to impact of water. As stated in section 3.5.2, the corrosion rate is calculated using the following formula (notation the same as in Appendix B)

$$crf = crfz + xr(r - 200000) + xph(pH - 5.7) + xwf \cdot wf + xwu \cdot wu.$$

Since values of the resistivity and *pH* are not comparable (they represent two different physical quantities), it is hard to compare their impact on final corrosion rate. Much easier is to evaluate the influence of the percentage of the pipeline where the water table is fluctuating under and above the pipe *wf* and the percentage of the pipeline under the water table *wu*. If we set them to be equal we can find which of the mentioned environmental characteristics supports growth of the corrosion to a larger extent. First let us look closer at the situation, where $wf = wu = 0.2$ and resistivity $r = 200000$, $pH = 5.7$. Hence the resistivity and *pH* are equal to the default values and don't influence the default corrosion rate $crfz$. The second column of Table 5.2 contains the correlation ratios for this case. The most influencial factors are *xwf* and *xwu*. The correlation ratios between *crf* and *xph* and *xr* are included only for the sake of completeness. The mean value of the corrosion rate in this situation is 1.48 mm/yr. If we change value of the resistivity of sand to 50 kΩ.cm, keeping the rest values of the parameters the same, a different picture emerges. The mean value of the corrosion rate rises to 3.98 mm/yr. With lower resistivity,

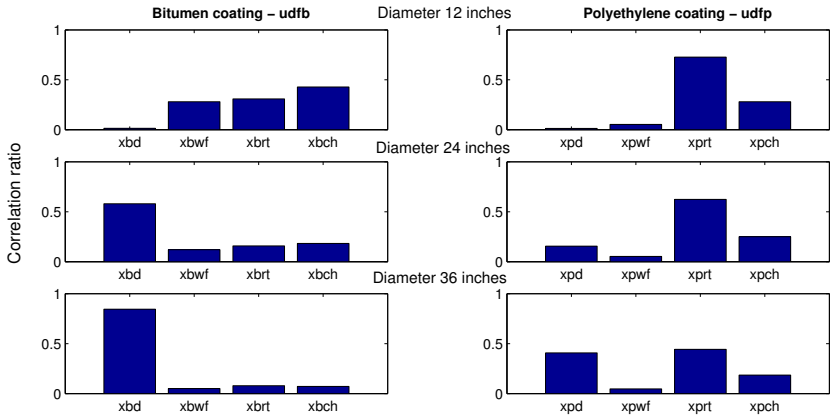

Figure 5.4: Correlation ratio between *udfb* and *udfp* and input factors.

the electrons are emitted by the steal pipe at higher rate. This results in higher corrosion rate. The importance of the resistivity is quantitatively confirmed by the correlation ratio $cr(crf, xr)$ (third column of Table 5.2). Since the correlation ratio is a measure of relative importance, the influence of *xwf* and *xwu* significantly drops compared to the resistivity. Notice that the conditions of Proposition 4.2.2 are met and the sums of the correlation ratios in each column of Table 5.2 are almost equal to 1. Small differences result from the method of calculating the correlation ratio.

The frequency of coating damages depends on the coating type (bitumen or polyethylene), diameter of the pipe (the influence is expressed by variables *xbd* or *xpd* obtained from experts, for bitumen and polyethylene respectively), percentage of the pipeline with fluctuating water table (*xbwf* or *xpwf*), percentage of the pipeline exposed to heavy root growth (*xbrt* or *xprt*) and percentage of the pipeline laid in chemically contaminated soil (*xbch* or *xpch*). To be able to compare the influence of coating type on this frequency it is assumed that 50 % of the pipeline is bitumen coated. The remaining part has a polyethylene coating. To calculate the frequency of bitumen coating damages we use the following formula which corresponds to eq. (3.4)

$$udfb = grb/(100 \cdot (1994 - 1968)) + xbd \cdot (dia - 12) + xbwf \cdot wf + xbrt \cdot rt + xbch \cdot ch.$$

We use a similar equation to calculate the frequency of polyethylene coating

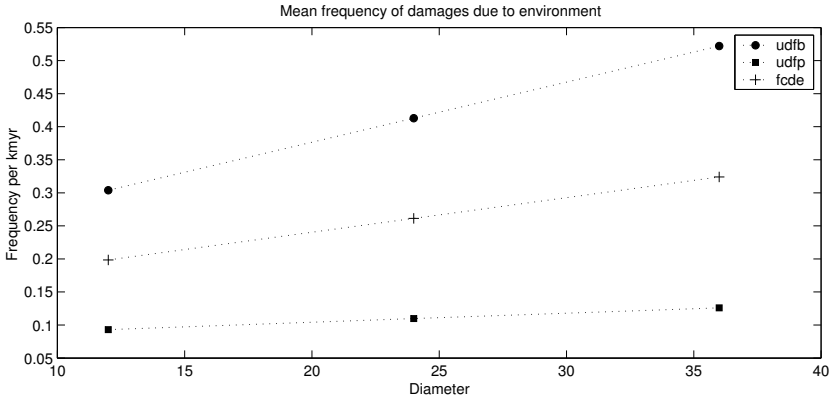

Figure 5.5: Mean frequency of coating damages due to environment.

damages

$$udfp = grp/(100 \cdot (1994 - 1968)) + xpd \cdot (dia - 12) + xpwf \cdot wf + xprt \cdot rt + xpch \cdot ch.$$

Given these two quantities we find the overall frequency of coating damages as follows

$$fcde = \%bit \cdot udfb + (1 - \%bit) \cdot udfp,$$

where $\%bit$ denotes the percentage of the pipeline with bitumen coating. As it has been stated above, in this analysis $\%bit = 0.5$.

Figure 5.4 depicts the correlation ratios between *udfb* and *xbd*, *xbwf*, *xbrt*, *xbch* in case of bitumen coating (left column). The column on the right hand side contain the same information but for polyethylene type of coating. Simultaneously, the six plots present influence of the diameter of the pipeline on the correlation ratios. In case of a 12 inches diameter pipeline, the most important factor appears to be the chemical contamination of the soil (bitumen) and root growth (polyethylene). Diameter does not affect the frequency of coating damages, because it is equal to the default value used in the formula of *udfb* and *udfp*. The more we increase the diameter, the more important becomes this factor at the cost of the others. But this is easily seen from the above formulas. We can see also that bitumen is more sensitive to fluctuating water table than polyethylene.

The frequency of coating damages due to environment increases with the increase of the diameter. Figure 5.5 shows this relationship. For larger percentage of bitumen coating this frequency would be closer to the upper line

Correlation ratio	Value	
	$r = 4k$	$r = 2k$
cr(crf, xwf)	0.45	0.08
cr(crf, xwu)	**0.51**	0.07
cr(crf, xph)	0.02	0.02
cr(crf, xr)	0.02	**0.83**

Table 5.3: Influence of environmental characteristics on the corrosion rate in clay.

udfb, otherwise it would be closer to the lower line *udfp*. This plot reveals that polyethylene has greater resistance to damages.

In this model the frequency *fcde* does not depend on the soil type. Hence the same conclusions hold for clay and peat. What certainly may change is the corrosion rate. Table 5.3 presents the correlation ratios between corrosion rate in clay and input variables. The results are only slightly different than the ones in Table 5.2. There is the same structure of dependencies as in sand. However the corrosion rate in clay is much smaller and for the default resistivity $r = 4$ kΩ.cm the mean value is 0.8 mm/yr. Decreasing the resistivity to $r = 2$ kΩ.cm rises this value up to 2.5 mm/yr. Hence, in case of normal environmental conditions, the most important for growth of corrosion factor is presence of water, regardless of whether the pipe is fully under the water table or fluctuating under and above of it.

5.3 Sensitivities in modelling the overall failure frequency in sand

Without doubt, modelling of the frequency of gas pipeline failures is the most complex task in the Unicorn model. This sensitivity analysis has been done for pipeline A specification (bitumen coating) and we shall evaluate the frequency of failure in year $ye = 1998$. Firstly, we must calculate the probability of failure in year *ye* due to corrosion given the corrosion rate *crf*, *crp* or *crse* (corrosion rate given unprotected stray currents). These probabilities are denoted by *pcrf*, *pcrp* and *pcrs* respectively. Influence of these quantities on the frequency of failures depends on percentage of the pipeline exposed to one of the three corrosion rates. Only the percentage of the pipeline at the bond

sites *bs* can be selected by the user. Thus implicitly, the user can influence the probability of the pipeline failure due to corrosion induced by the stray currents. To account that fact we consider two situations, where $bs = 0.8$ and $bs = 0.2$. Moreover, very important for the overall failure frequency is the birth year *b*, since the pipelines laid before 1970 were subjected to intense corrosion rate (cathodic protection was installed in 1970). Hence in total, we have 4 scenarios and the results of the analysis are in Table 5.4. For the pipeline laid in 1975 the most important factor is the probability of failure due to free corrosion rate. Only this corrosion rate is able to remove enough wall thickness and cause a leak within 23 years. The effective life of the pipeline given partially working cathodic protection or failure of the stray currents protection system is simply to long to cause a failure in 1998 (minimum is 29 years). Furthermore, the results are completely insensitive to *bs*. The mean of *corlk* is 0.0024 per km.yr.

For the pipeline laid in 1967 this number increases to 0.0164 per km.yr for $bs = 0.2$ and 0.0679 per km.yr if $bs = 0.8$. Because of the very complex interactions between the input variables, the sensitivity analysis gets very complicated. The probability of failure given fully non-working cathodic protection system *pcrf* is slightly higher than in the former case. But now the probability of the pipeline failure given partially working cathodic protection system *pcrp* is greater than zero, because 31 years is about the 30^{th} percentile of the distribution of the effective life. The probability of pipeline failure given stray currents protection system failure *pcrs* behaves similarly. Variable *pcrp* has a little bit larger values than *pcrf*. The probability of the failure of the stray currents protection system *pcrs* is constant and in 54 % of the scenarios higher than the probability of full failure of the cathodic protection. If we add, that in this specific case the percentage of the pipe in the neighborhood of bond sites is 20 to 80 times greater than the percentage of the pipeline exposed to free corrosion rate, we can understand why *pcrs* have became so important in this case.

Indirectly *corlk* may be influenced by the following variables:

pcen frequency of coating damage from environment

pc3 frequency of coating damage from 3^{rd} parties

ps frequency of small unrepaired pipeline damage

Correlation ratio	Value			
	$b = 1967$		$b = 1975$	
	$bs = 0.8$	$bs = 0.2$	$bs = 0.8$	$bs = 0.2$
cr(corlk, pcrf)	0.09	0.13	**0.71**	**0.71**
cr(corlk, pcrp)	0.62	0.56	0.03	0.03
cr(corlk, pcrs)	**0.96**	**0.88**	0.02	0.02

Table 5.4: Influence of the corrosion rate on the failure frequency due to corrosion in sand.

Correlation ratio	Value			
	$b = 1967$		$b = 1975$	
	$bs = 0.8$	$bs = 0.2$	$bs = 0.8$	$bs = 0.2$
cr(corlk, pcen)	0.10	0.13	**0.09**	**0.09**
cr(corlk, pc3)	0.02	0.02	0.03	0.03
cr(corlk, ps)	0.02	0.02	0.02	0.02
cr(corlk, pl)	0.02	0.02	0.01	0.01
cr(corlk, crf)	0.06	0.05	0.04	0.04
cr(corlk, crp)	**0.27**	**0.20**	0.02	0.02
cr(corlk, crse)	0.02	0.02	0.01	0.01

Table 5.5: Influence of some variables on the failure frequency due to corrosion in sand.

pl frequency of large unrepaired pipeline damage

crf free corrosion rate

crp corrosion rate under partial functioning of cathodic protection

crse corrosion rate from stray currents

The correlation ratio between *corlk* and these variables do not reveal any significant dependencies (Table 5.5). But we must account the fact that due to some transformation in the model, the dependencies have been weakened. Regardless of this fact, the cobweb plots may help to get insight into the relations between the above mentioned variables. Figure 5.8 shows the cobweb plot of the selected variables conditionalized on top 15 % of *corlk*. Thus we can find which factors drive high frequency of pipeline failures due to corrosion. There is an easily identifiable positive correlation between *corlk* and *pcen*, indicating that coating damages due to environment have a significant influence on the

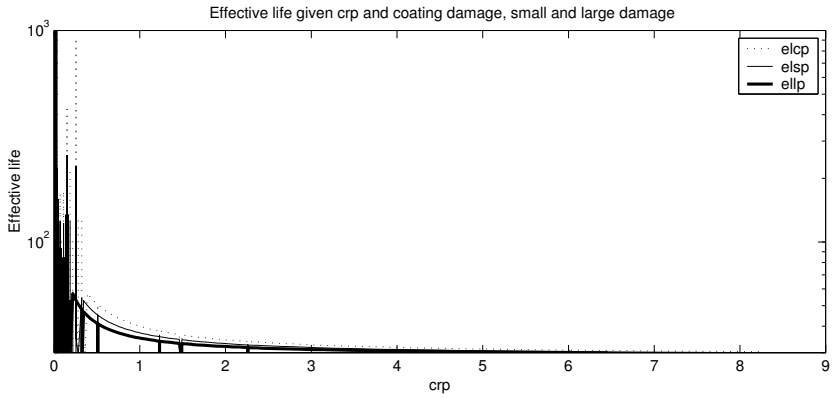

Figure 5.6: Effective life of the pipeline given partially working cathodic protection system.

high failure frequency. Variable *crp* has even greater impact on *corlk*. Although, there is a few percent of the scenarios from the top of the distribution of *crp* selected, the majority of them are in lower 26 % of the distribution. This is an interesting feature while low *crp* should increase the effective life of the pipeline, resulting in a lower frequency of the pipeline failures. The relationship between *crp* and effective life given coating damage *elcp*, small damage *elsp* and *ellp* is pictured in Figure 5.6. We can see that for small values of *crp* there is a large uncertainty involved. For larger values of *crp* we observe an expected decrease of the effective life.

Let us zoom to the area of the plot where the effective life has very large variance (Figure 5.7). This time the x-axis is labelled by index of the ordered statistics of *crp* instead of their values. We consider 300 out of 1000 ordered samples of *crp* and corresponding values of *elcp*. To make the picture more clearer *elsp* and *ellp* have not been plotted, but keep in mind that they act in exactly the same manner as *elcp*. There are very high peaks visible in the plot, 48 out of 266 values of *elcp* are larger than 57.3 years. This number of years corresponds to the value of *eclp* at 267^{th} ordered point of *crp* from which *elcp* starts to be smooth and decreasing in *crp*. Hence for the rest of these selected scenarios (exactly 218) the effective life *elcp* is about 30 years, meaning that the pipe reaches the age when the failure due to partial failure of the cathodic protection becomes highly likely. Note that 267^{th} ordered sample of *crp* is about its 26^{th} percentile and this agrees with the cobweb plot in Figure 5.8.

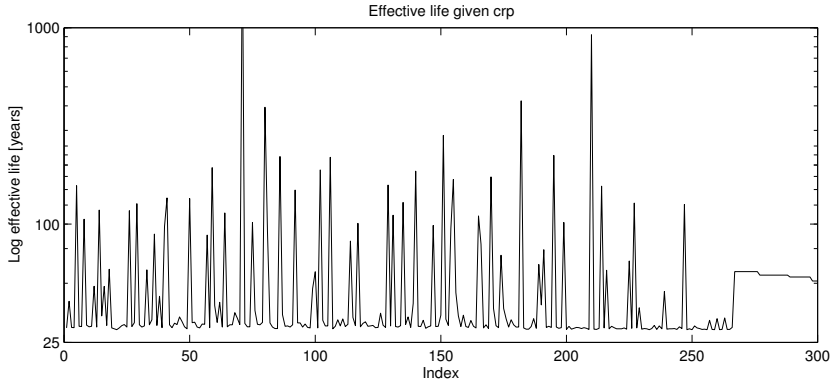

Figure 5.7: Effective life of the pipeline given partially working cathodic protection system for small values of crp.

Where does this unexpected feature come from? The effective life of the pipeline given partially working cathodic protection and coating damage is calculated with the following formula

$$elcp = (xc \cdot t - (j - 1970) \cdot crp)/crf + j - 1970$$

for pipeline which effective birthyear is before 1970 and

$$elcp = (xc \cdot t)/crp + j - 1970 \tag{5.1}$$

otherwise, where $xc = 0.9$ is the critical thickness fraction, $t = 12.26$ is the pipe wall thickness and $j = ye = 1999$ is year of inspection. We see that only two uncertain quantities appear in this equation, *crp* and *crf*. Samples of *crp* have been ordered, hence the only quantity which could cause those peaks is *crf*. If *crp* is less than or equal to 0.38 mm/year, then the effective live is so long that the pipe must have been placed in the ground before 1970 and then hence the pipeline was exposed to *crf* for years between effective birthyear and 1970. The 267^{th} ordered sample of *crp* is equal to 0.39 mm/year and that is why for this value and greater *elcp* is calculated using equation (5.1) where *crf* does not appear. Further analysis of the sample files created by Unicorn revealed that for those 267 scenarios, *crf* have very small values (less than 0.1 mm/yr) and this cause the observed peaks of *elcp*.

Coming back to Figure 5.8, the small amount of samples at the top of the distribution of *crp* is a result of the short effective life *elcp*, *elsp* and *ellp* for

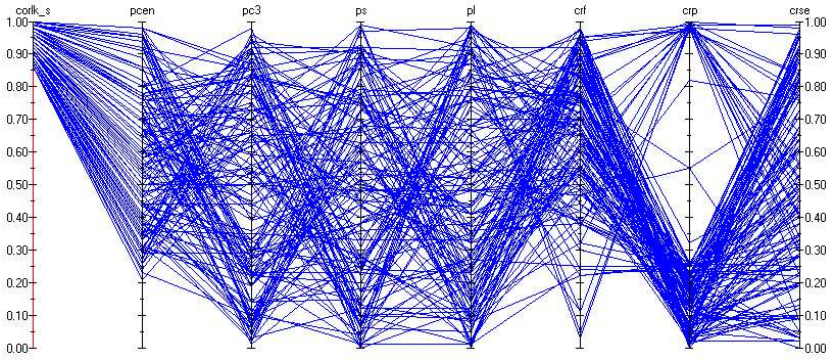

Figure 5.8: Cobweb plot of *corlk* and other variables conditionalized on high values of *corlk*, 31 year old pipeline laid in sand in 1967.

high values of *crp*. The effective life for intermediate values of *crp* is too long to cause a failure of the pipeline due to corrosion.

The analysis of the cobweb plot in Figure 5.9, where we conditionalize on lower 10 % of the values of *corlk*, is more straightforward. This time we see that the low values of *corlk* and *crf* are positively correlated and *pcen* has lost the ability to affect *corlk*. This might suggest that low frequencies of pipeline failures comes from sporadic failures of the pipeline exposed to the free corrosion rate. But this not quite correct. Notice that there is a gap in the distribution of *corlk* presented in the cobweb. Although lower 10 % of the distribution has been selected, all of the scenarios start from 0. This is because 15 % of the samples of *corlk* are equal to zero (this percentage drops to about 6 % for 80 years old pipeline). If *crf* is small and *crp* is not too large, then in result, the effective life of the pipeline will be too long to cause any failures within 31 years.

5.4 Sensitivities in modelling the overall failure frequency in clay

Clay is known as a soil type which supports corrosion growth to a smaller extent than sand. This will also be shown in the following pages.

Basically the same structure of dependencies as in sand emerges here (Table 5.6). The affects are weaker, and this happens due to the mentioned resis-

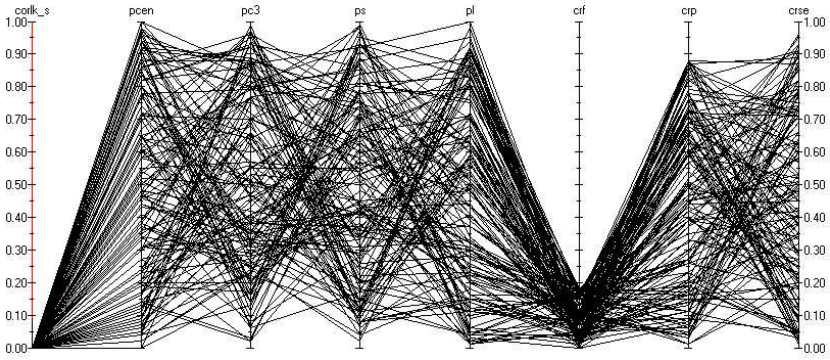

Figure 5.9: Cobweb plot of *corlk* and other variables conditionalized on low values of *corlk*, 31 year old pipeline laid in sand in 1967.

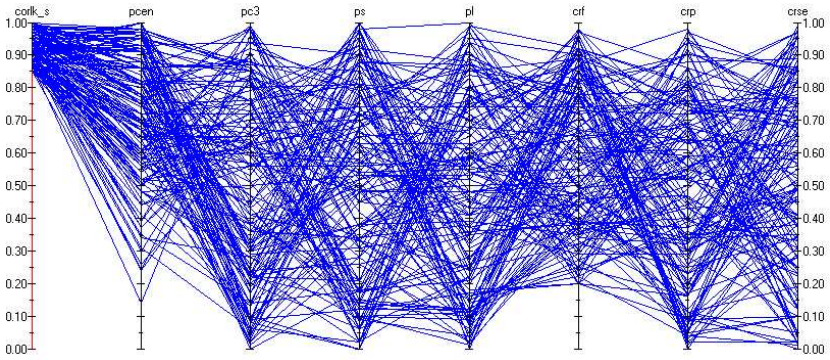

Figure 5.10: Cobweb plot of *corlk* and other variables conditionalized on high values of *corlk*, 22 year old pipeline laid in sand in 1975.

tivity of a steal pipeline to corrosion in clay. Again, the probability of stray currents protection system failure plays the most important role.

Table 5.7 contains the correlation ratios between *corlk* and some input variables. There is almost no impact of the inputs on this variable. Compared to Table 5.5, only *crf* became a little bit more influencial, the others stayed at the same or lower (*crp*) level of importance. The mean of *corlk* is much lower than this value in case of sand. For pipelines laid in 1967 and $bs = 0.8$ it is equal to 0.02263 per km.yr and this is about 3 times less than the corresponding value in sand. The difference gets smaller if $bs = 0.2$. Then the mean is 0.00727 per km.yr (about twice smaller). For pipelines laid in 1975 the mean of *corlk* does not change with change of *bs* and is equal to 0.00157 per km.yr (compared

Correlation ratio	Value			
	$b = 1967$		$b = 1975$	
	$bs = 0.8$	$bs = 0.2$	$bs = 0.8$	$bs = 0.2$
CR(corlk, pcrf)	0.08	0.14	**0.58**	**0.58**
CR(corlk, pcrp)	0.51	0.46	0.02	0.02
CR(corlk, pcrs)	**0.71**	**0.59**	0.02	0.02

Table 5.6: Influence of the corrosion rate on the failure frequency due to corrosion in clay.

Correlation ratio	Value			
	$b = 1967$		$b = 1975$	
	$bs = 0.8$	$bs = 0.2$	$bs = 0.8$	$bs = 0.2$
cr(corlk, pcen)	0.03	0.03	0.05	0.05
cr(corlk, pc3)	0.02	0.02	0.03	0.03
cr(corlk, ps)	0.03	0.02	0.02	0.02
cr(corlk, pl)	0.01	0.01	0.02	0.02
cr(corlk, crf)	0.08	0.08	**0.07**	**0.07**
cr(corlk, crp)	**0.10**	**0.07**	0.01	0.01
cr(corlk, crse)	0.02	0.02	0.02	0.02

Table 5.7: Influence of some variables on the failure frequency due to corrosion in clay.

to 0.00238 in sand).

The cobweb plots in Figure 5.11 shows slight association of high values of *corlk* and *crf*. Variables *pcen* and *crp* don't reveal a similar characteristic as in sand. Conditionalizing the cobweb on lower percentiles of *corlk* (see Figure 5.12) shows almost the same picture as the corresponding cobweb for pipeline laid in sand. But now as many as 47 % of the samples of *corlk* are equal to 0. The cause is the same as in case of sand - in 47 % of the scenarios the effective life of the pipeline is too long to cause failure. The gap can be easily seen in Figure 5.13. This proves also, that clay is a good soil type to lay the pipelines in, as the corrosion rate is very small.

Summarizing, the sensitivity analysis of the HITPIP model showed that the greatest influence on the frequency of damage to coating has the percentage of hitting gas pipeline during open digs without oversight *roon*. This is due to high frequency of this type of digs. In the future they could be eliminated by more frequent inspections from Gasunie of the digs. Sensitivities in the

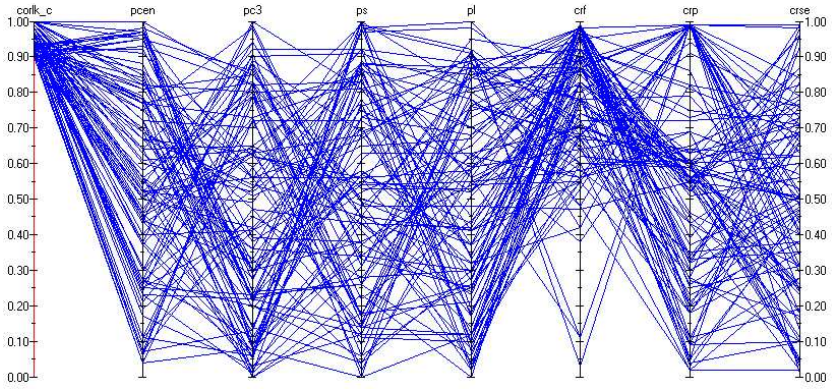

Figure 5.11: Cobweb plot of *corlk* and other variables conditionalized on high values of *corlk*, 31 year old pipeline laid in clay in 1967.

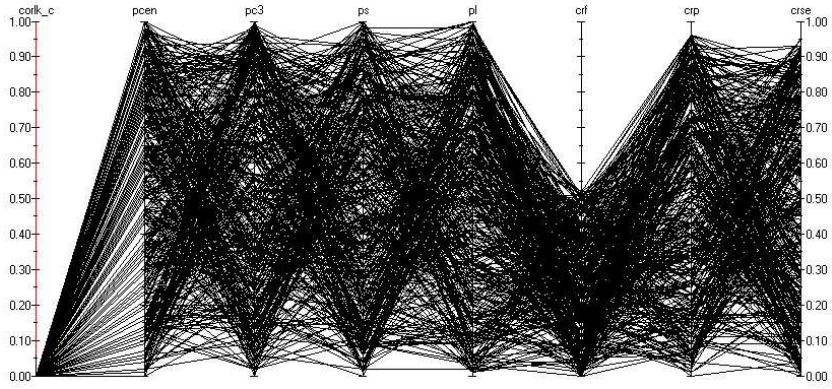

Figure 5.12: Cobweb plot of *corlk* and other variables conditionalized on low values of *corlk*, 31 year old pipeline laid in clay in 1967.

environmental part of the model must be analyzed individually for a specific set of input variables, because of the very complex interactions occurring there. The same holds for the analysis of the overall failure frequency. For sure, polyethylene is a much better coating material than bitumen. As regards these two types of materials, they both are sensitive to different damage initiating events. This should be taken into account when a new pipeline is designed.

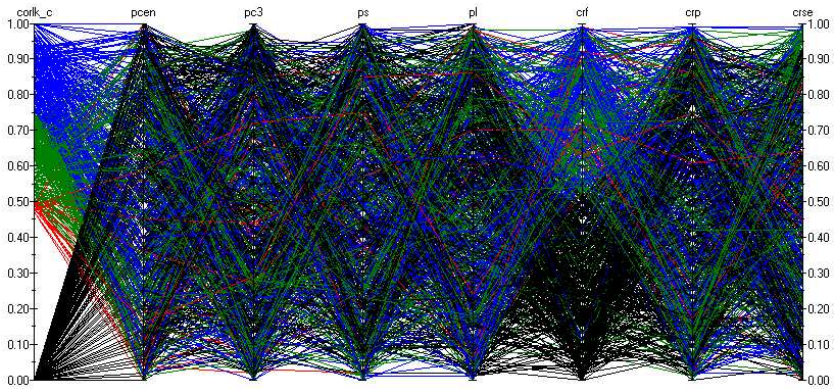

Figure 5.13: Cobweb plot of *corlk* and other variables, 31 year old pipeline laid in clay in 1967.

Chapter 6

Analysis of the corrosion data

This chapter studies information on inspected pipelines by visualizing the data. This will help to form a clearer picture of specific aspects of the corrosion problem the gas industry is dealing with. Pipeline A data will be analyzed separately, since this pipeline was inspected twice in course of 18 months.

The analysis methods have been implemented in MatLab. The code of the function is available in Appendix C.

6.1 Analysis of pipeline A data

The first inspection of Pipeline A was performed in October 1999, after 32 years since laying in the ground. In April 2001 the pipeline was reinspected.

Figure 6.1 presents two step functions constructed by plotting the total number of corrosion spots against distance from the reference location. This kind of plots allow to discover locations where the occurrence of metal loss is more likely than elsewhere. Line representing the number of corrosion spots found during reinspection in 2001 (Pipeline A1) is above the line representing the same number for inspection from 1999 (Pipeline A). This is correct, since the pipeline A1 data include the metal loss locations from the pipeline A data plus additional spots that have had appeared in time period of 18 months between the inspections. This plot shows also that many of the spots appear as clusters (high jumps of the lines).

The quantile-quantile plot shows almost linear relationship between the both data sets. There is only a difference in tails of the distributions (Fig-

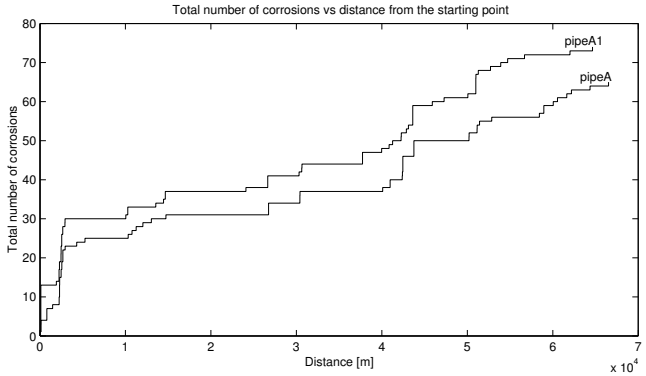

Figure 6.1: Total number of corrosion spots in Pipeline A and A1 data sets.

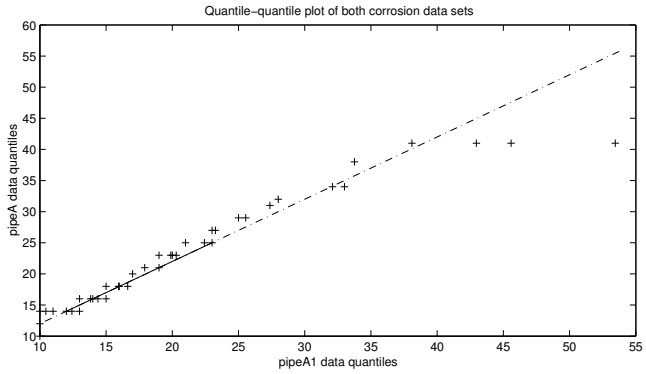

Figure 6.2: Quantile-quantile plot of Pipeline A and A1 data sets.

ure 6.2), because maximum metal loss in the pipeline A data is 44 %, whereas in 2001 the maximum is 55 %. The empirical distribution function plotted in Figure 6.3 also depicts that fact.

Figure 6.4 presents histograms of the corrosion data. During inspection in 2001 many new, small metal loss events have been observed. There were 5 such events in 1999 and this number increased to 20 in 2001. Assuming, that the MFL-pigs used for the inspections were accurate, 15 new corrosion spots have appeared within 18 months. This might seem to be a lot, since within 32 years since "birth year" only 66 corrosion events developed and suddenly after 18 month we have 15 new ones. But we must remember that only corrosion events with greater than 10 % of metal loss are reported. It could be that

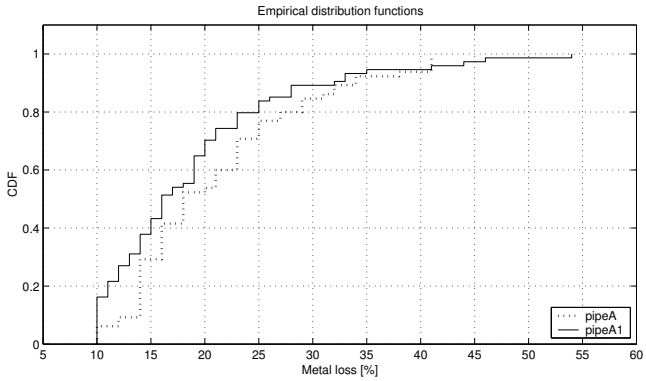

Figure 6.3: Empirical distribution functions of metal loss for Pipeline A and A1 corrosion data.

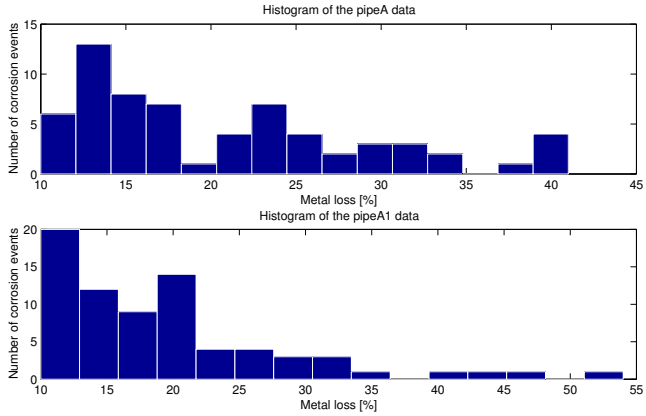

Figure 6.4: Histograms of corrosion events found during inspections in 1999 (pipeA) and 2001 (pipeA1).

in 1999 there were many small corrosion spots with the metal loss close to 10 % but not exceeding this value. A period of 18 months is enough time for corrosion to remove a few percent of the wall thickness what makes corrosion spots detectable.

Figure 6.5 presents histograms of the vertical positions of the metal loss events in polar coordinates. This allows to visualize the positions in a very intuitive way, where 0° and 180° labels represent top and bottom of the pipe respectively. According to Figure 6.5, the metal loss spots are located mainly at the bottom of the pipeline. This excludes 3$^{\text{rd}}$ party digs as a cause of the

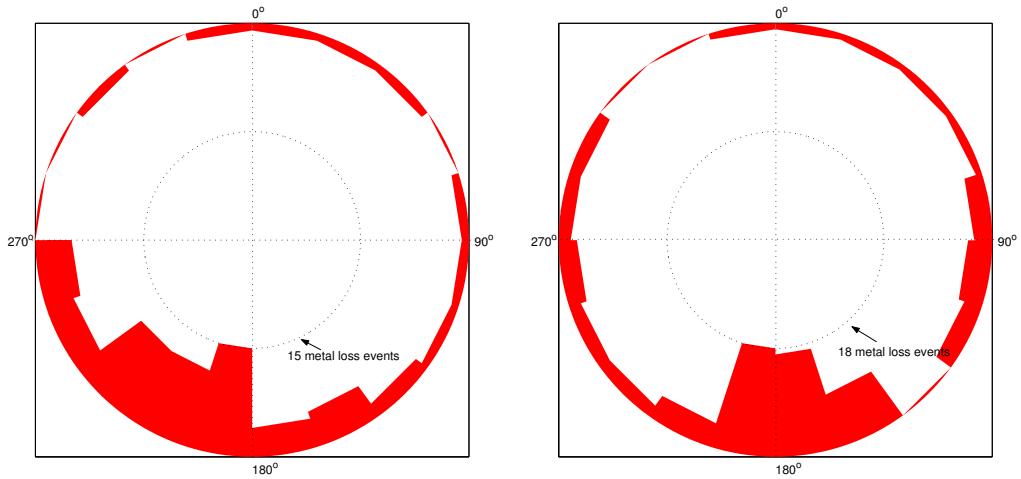

First inspection Second inpection

Figure 6.5: Vertical positions of the metal loss events on the surface of pipeline A.

metal loss. Very likely corrosion could start because of the damage of the coating during laying the pipe in the ground. Very curious is the fact, that in 1999 most of the spots were located between 180 and 270 degrees, whereas in 2001 it appeared to be 145–210 degrees. It might be an indication of not very accurate locating the metal loss locations by the MFL-pig.

6.2 Analysis of pipelines B, C, D and E data

This section analyzes the data from pipelines B, C, D and E. Similarly to the previous section let us start with plotting the total number of the metal loss events against the distance from the reference point. Pipelines B and C have the same diameter and wall thickness. They both are high pressure, large diameter pipelines. Pipelines D and E have smaller diameter and wall thickness (see Table 2.2 for details). Especially pipelines D and E reveal no sensitivity to location, what supports the assumption of the UNICORN model, saying that the distance between two successive corrosion spots is exponentially distributed and hence, the number of the spots in a segment of pipeline with given length follows a homogeneous Poisson process. In case of pipelines B and C we can again observe high jumps indicating clusters of corrosion spots.

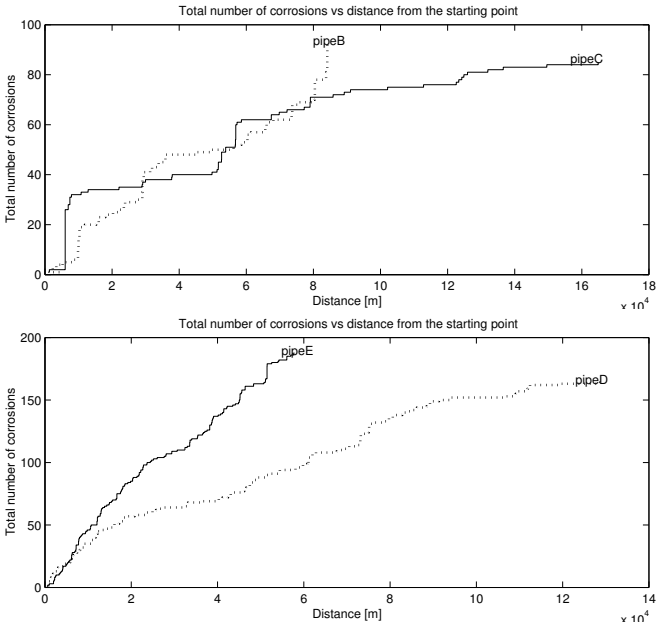

Figure 6.6: Total number of corrosion spots in pipeline B, C, D and E data sets.

Pipelines B, C and D corrosion data is left-truncated (see Figure 6.7). Only Pipeline E data provides information on corrosion events with less than 10 % of the wall thickness metal loss. This pipeline has been inspected most recently. Pipelines D and E definitely reveal different characteristics (susceptibility to corrosion) than the others. First of all, there is twice as many of the detected defects as in the other data sets. The reason for that could be smaller wall thickness of these pipes. If pipe E has the wall thickness equal to 5.95 mm, than 10 % of the metal loss is 0.595 mm. In case of pipe A 10 % of metal loss is 1.225 mm. Since the corrosion rate (metal loss due to corrosion in millimeters per km per year) is independent of the wall thickness, corrosion of pipe E will be detectable sooner than that one occurring in pipe A. The second factor making them distinctive is an almost complete lack of clusters of defects.

Figure 6.8 visualizes information on positions of corrosion spots on the surface of pipelines B, C, D and E. Pipeline B data reveals the same pattern as Pipeline A data. Most of the spots are located at the bottom of the pipelines. A completely different picture emerges from Pipeline C, D and E data. In these cases the spots are spread out almost uniformly regardless if it is the top

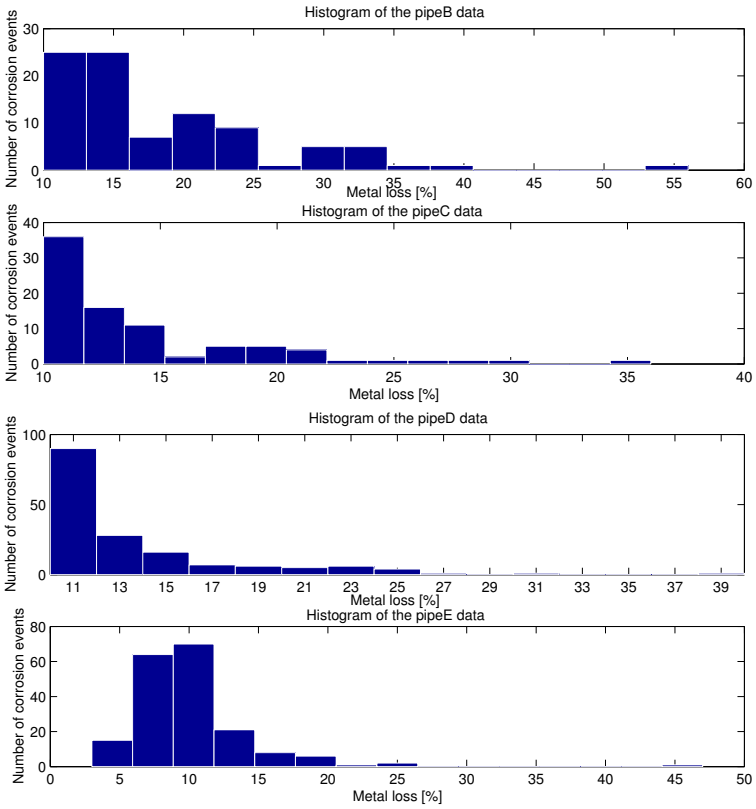

Figure 6.7: Histograms of corrosion events found during inspections of pipelines B, C, D and E.

or bottom of the pipeline. It might be that pipelines C, D and E are crossing highly urbanized areas and part of the defects could be initiated by 3rd party digs, but we don't have this kind of information. Further analysis did not reveal any particular dependency between distance from the reference point and vertical positions of the corrosion spots on surface of the pipelines.

6.3 Comparison of the UNICORN output with the actual data

One of the main purposes of this study is evaluation of the UNICORN model presented in Chapter 3. This model predicts, with uncertainty, failure frequency of gas pipelines. It has been designed specifically to the Dutch

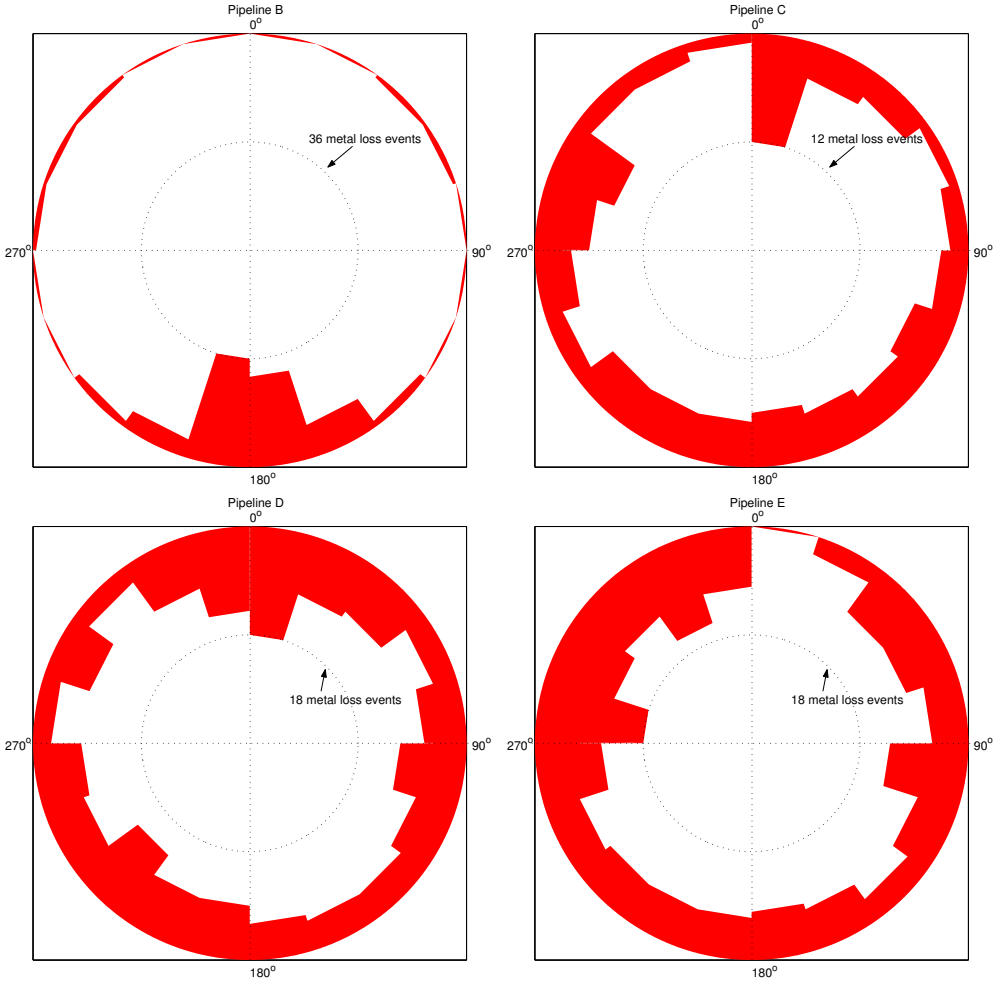

Figure 6.8: Vertical positions of the metal loss events on the surface of pipelines B, C, D and E.

conditions. One can ask how can we compare output of the model with the data, since there is no failure in the data! However what the model returns is, in fact, the frequency of exceeding a certain level of metal loss. This level is set by three parameters xc, xs and xl which are critical thickness fraction given that there was a coating damage (C), small damage (S, 0.5 mm of removed wall thickness) or large damage (L, 2 mm of removed wall thickness) respectively. By default $xc = 0.9$, $xs = 0.7$ and $xl = 0.6$. For instance, assume that there was a small damage in past; a telecommunication company laid their cables and scratched the pipeline. The parameter xs says that 70 % of the remaining wall

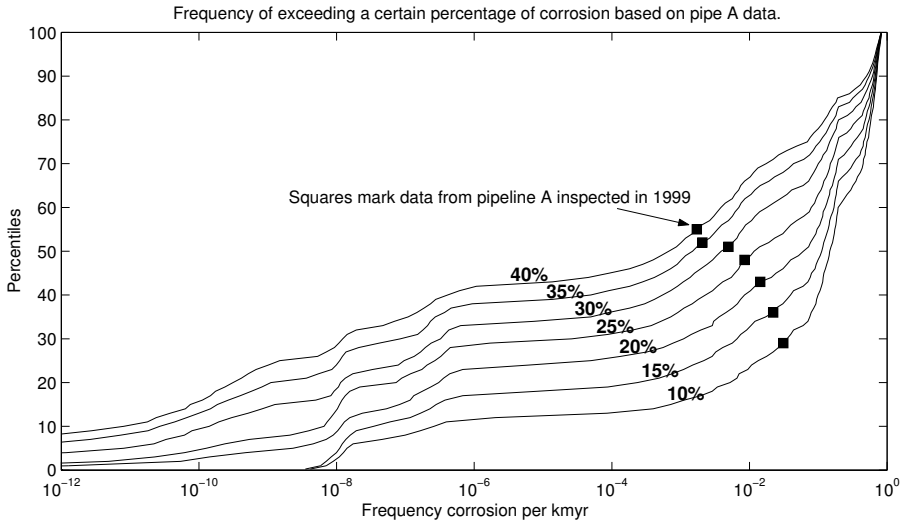

Figure 6.9: Comparison of the UNICORN output with the Pipeline A data inspected in 1999.

thickness (the initial thickness minus 0.5 mm) must be removed by corrosion in order to cause a leak. The values of $xc = 0.9$, $xs = 0.7$ and $xl = 0.6$ have been determined experimentally. We see that the UNICORN model output is simply the frequency of exceeding 90 %, 70 % and 60 % of metal loss. By manipulating these parameters, we could obtain frequency of exceeding any other percentage of metal loss, like 10 % to 40 %. And this frequency is implicitly given in the inspection data. The data includes total length of the pipelines and their age. We can determine the number of defects where the percentage of metal loss exceeds, say 20 %. In case of Pipeline A this number is 21. Dividing 21 by the length of Pipeline A (69 km) and its age (32 years) we obtain frequency of exceeding 20 % of metal loss per km.year. There is nothing simpler than plotting this frequency and distribution of the frequency of exceeding 20 % of metal loss from the UNICORN model together.

To obtain the corresponding distribution from UNICORN, we must set xc, xs and xl such that for each of the initiative events (coating damage, small damage and large damage) sum of the wall thickness removed by this event and later corrosion is equal to 20 %. Obviously $xc = 0.2$, since the pipe wall was untouched. Values of xs and xl will depend on the initial wall thickness, because 0.5 mm removed by small damage is about 4 % and 8 % of the initial

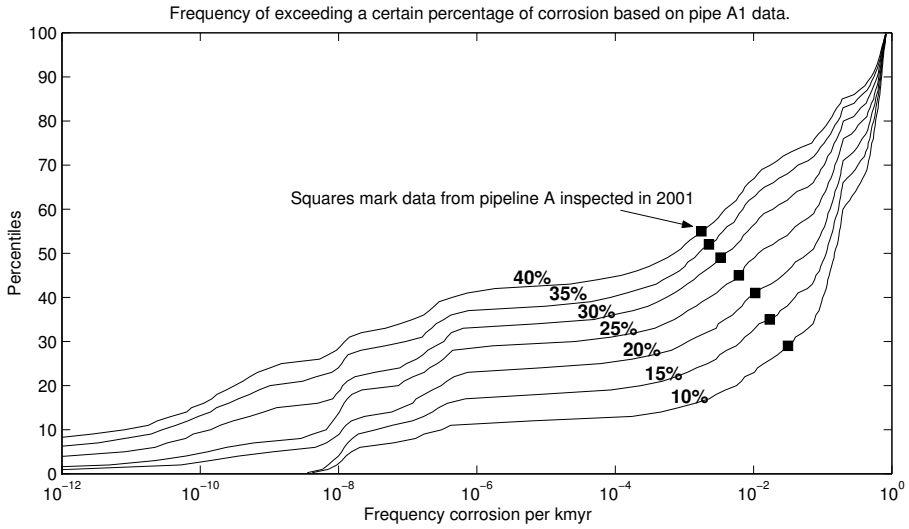

Figure 6.10: Comparison of the UNICORN output with the Pipeline A data inspected in 2001.

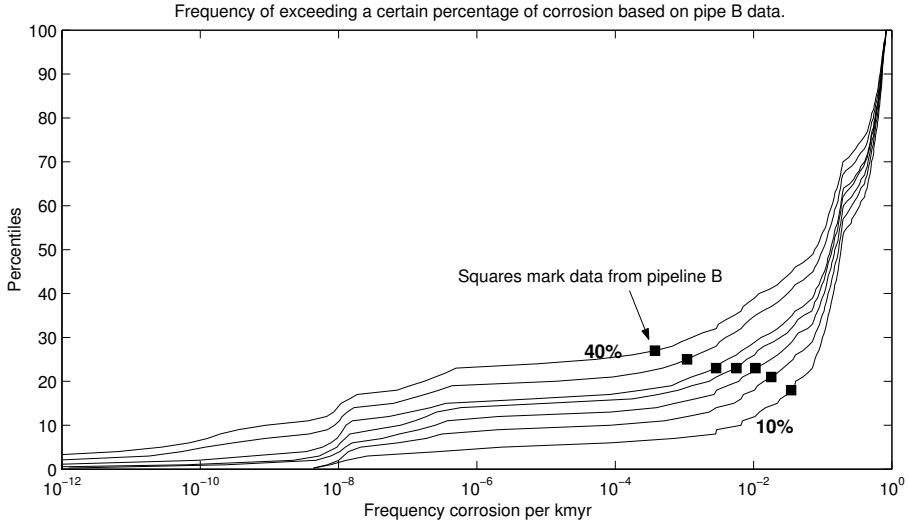

Figure 6.11: Comparison of the UNICORN output with the Pipeline B data.

wall thickness of Pipeline A and E respectively. The whole thing complicates in case of determining xl. 2 mm removed by large line damage is 33 % of the initial wall thickness of Pipeline E. We cannot set a negative value of this parameter in order to determine the frequency of exceeding 10 % of metal

loss. In such cases xl is set to be equal 0 and this is easily distinguishable, for instance in Figure 6.13, where the lines representing the frequency of exceeding 10 % and 15 % of metal loss starts from 10^{-8} on x-axis in contrast to the rest of the frequencies.

Figure 6.9 depicts results obtained by implementing the above reasoning. First the characteristics of Pipeline A have been incorporated into the UNICORN model. The resulting seven output distributions depicted in the figure corresponds to exceeding 10 % to 40 % of metal loss with step 5 %. The black squares mark the frequencies derived from the data. The data vary from 30^{th} to 56^{th} percentile of the UNICORN's output. This is a satisfactory result, since the data is in the range predicted by the model and very close to medians, which are ones of the main quantitative characteristics of a probabilistic distribution.

The same conclusion holds for the data from reinspection of Pipeline A in 2001 (Figure 6.10). There are 11 more defects compare to inspection from 1999, but the UNICORN model took this fact into account. A different picture emerges from Figure 6.11, where the model's predictions are overestimated compare to the data. This could be a problem of the model or the information on soil characteristics, like pH or resistivity might not be correct. However, even this result cannot disqualify the whole model.

The analysis of pipeline C data was more time-consuming and complicated because of the fact that first 100 km was laid in sand and the second part (last 67 km) was laid in clay. The two sections have been analyzed separately. The average weighted birth year of the first section is 1965. In case of the second section it is 1969 (this part was repaired many times in the past). Moreover the characteristics of the soil, in which the pipe was laid is unknown. Therefore the analysis was performed for two different characteristics of the soil. Nevertheless, it is still dangerous to draw some strong conclusions from this analysis, since the real characteristic of the soil may be completely different from those assumed.

First let's concentrate on analysis of the first 100 km of pipeline C. Figure 6.12 contains plots of the distributions returned by the model assuming two different characteristics of sand. The first set of values comes from the information we have on Pipeline A and B. Set 2 was used during development of the model in 1995. The values of the individual parameters are in Table 6.1.

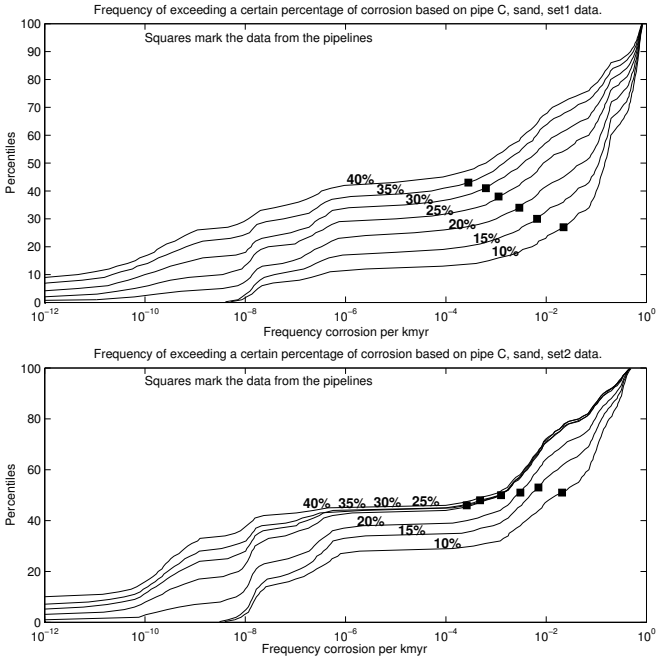

Figure 6.12: Comparison of the UNICORN output with the Pipeline C data (first 100 km of the pipeline laid in sand).

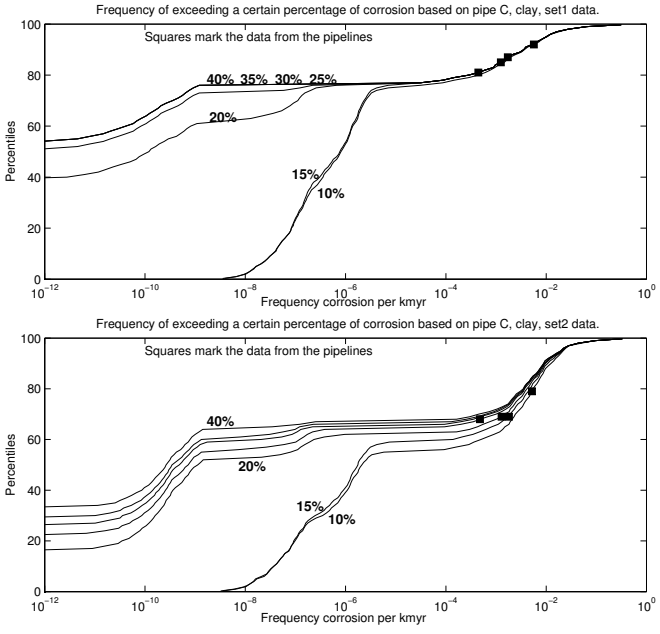

Figure 6.13: Comparison of the UNICORN output with the Pipeline C data (last 67 km of the pipeline laid in clay).

Parameter	Set 1	Set 2	Description
wf	0	10	percentage of 1km pipeline with fluctuation under and above water table
rt	0	10	percentage of 1km pipeline with with heavy roots
ch	0	10	percentage of 1km pipeline with with heavy industrial contamination
wu	95	20	percentage of 1km pipeline under water table
r	10 kΩ.cm	50 kΩ.cm	resistivity
bs	0.8	0.4	percentage of 1km pipeline near bond site

Table 6.1: Two characteristics of sand applied to the UNICORN model.

The same values have been used also to the analysis of the Pipeline D and E data.

We see that for Set 1 of the values the model a little bit overestimates the data. However for set 2 the data is almost equal to the medians of the distributions revealing a significant unanimity. The story looks completely different if we look at the last 67 km of Pipeline C laid in clay. In this case we also perform analysis for two soil characteristics, but with different value of resistivity to better fit the typical values of resistivity in clay. In set 1 the resistivity is equal 4 kΩ.cm and in set 2 this parameter has value 6 kΩ.cm. Now the data is heavily underestimated (see Figure 6.13), especially in case of values of the model parameters taken from Set 1. Remarkable is fact that about 60–70 % of the mass is concentrated at very low values of frequency of corrosion exceeding 10 % to 40 % loss of wall thickness. There are only four squares marking data, because there was no metal loss greater than 30 % of the wall thickness.

The analysis of pipelines D and E shows little difference between the results for those two pipelines. In both cases failure frequencies derived from data are about 15^{th} to 25^{th} percentiles of the model's output distributions obtained by assuming values of the parameters from Set 1 (Figures 6.14 and 6.15). For values from Set 2 the predictions are better and the corresponding data equal to 33^{rd} to 43^{rd} percentiles of the UNICORN's output.

Set 2 of values decreases the corrosion rate. Why is that? Let's consider

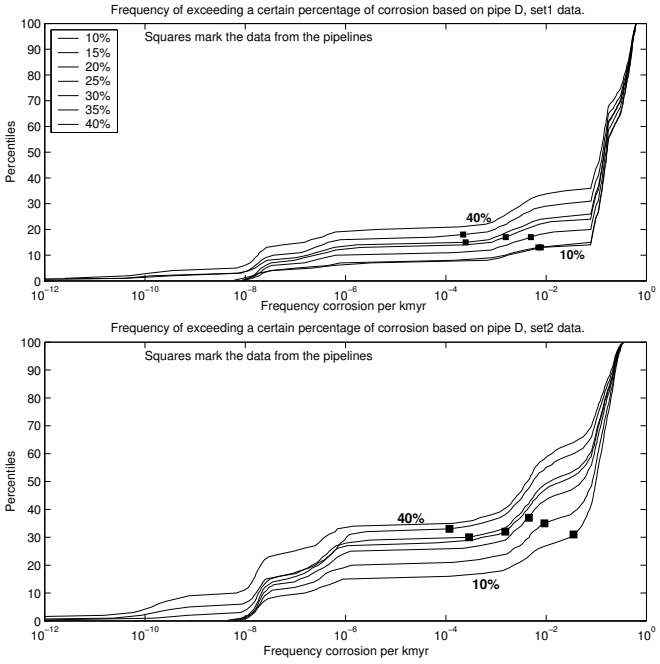

Figure 6.14: Comparison of the UNICORN output with the Pipeline D data.

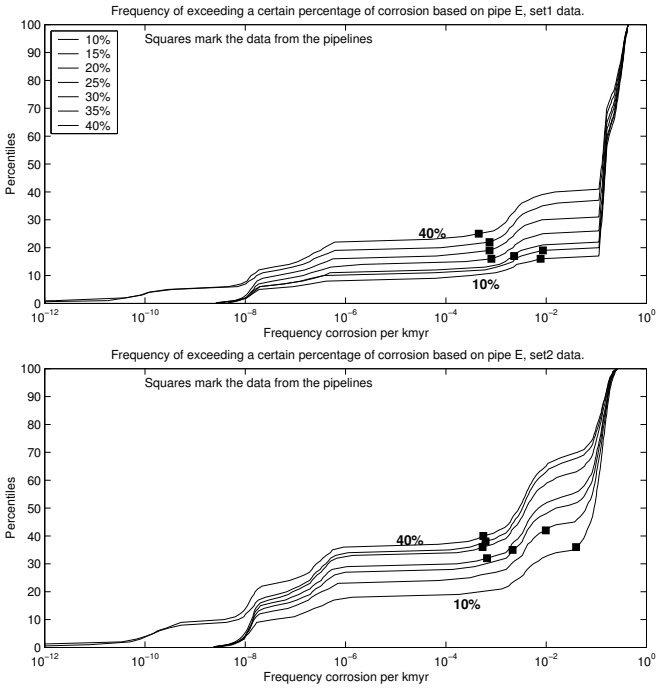

Figure 6.15: Comparison of the UNICORN output with the Pipeline E data.

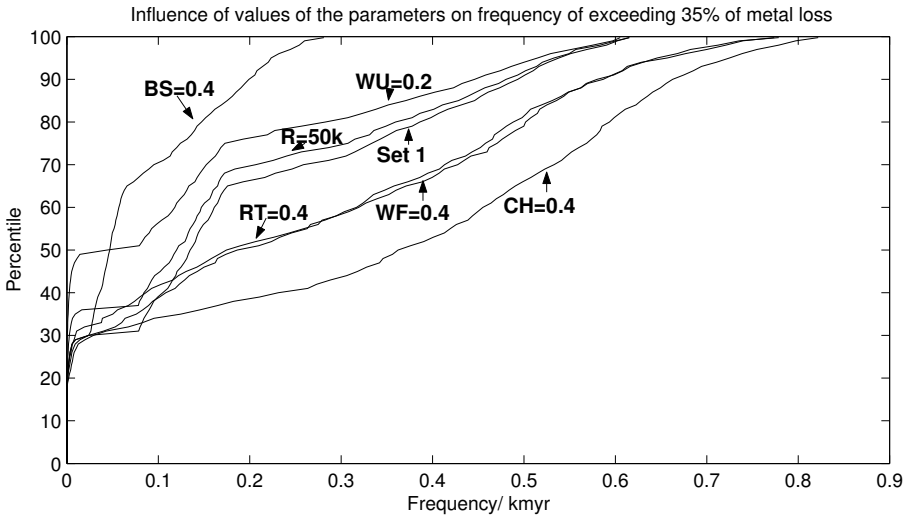

Figure 6.16: Influence of values of the parameters on frequency of exceeding 25 % of metal loss.

the following situation. First we perform a run of the UNICORN model using values from Set 1. The rest of the parameter values correspond to the specification of pipeline D. Setting $xc = 0.35$,$xs = 0.3$ and $xl = 0.06$ causes the output distribution to represent the frequency of exceeding 35 % of the metal loss due to corrosion. Now change one value of a parameter at time, for example increase wf from 0 to 0.4 and keeping the rest of the parameters as in set 1, perform another run. Figure 6.16 depict results obtained by changing values of the parameters to $bs = wf = rt = ch = 0.4$, $wu = 0.2$ and $r = 50$ kΩ.cm, of course each of them separately. The x-axis has a linear scale in contrast to Figures 6.9–6.15. Increasing percentage of the pipe length fluctuating under and above water table (wf) and exposed to heavy root growth (rt) and chemical contamination (ch) causes the corrosion rate to increase implying higher frequency of defects. Among these three parameters ch influences the frequency to the largest extent (the distribution has a longer tail, than the one obtained with the standard values of the parameters taken from Set 1). Resistivity does not seem to influence significantly the frequency. Decreasing the percentage of the pipeline under the water table from 95 % to 20 % decreases also the failure frequency. This clearly shows that presence of the water supports the growth of the corrosion. Bond sites are particulary open to corrosion, because

of stray currents that may occur in such places. In 1970 a system preventing occurrence of strong stray currents but the probability that this system will fail is very high (0.95). Hence the larger portion of the pipe is in the neighborhood of the bond sites, the higher corrosion rate and frequency of failure. In the model this portion is set by value of the parameter bs. The model's predictions show here proper behavior. The frequency distribution obtained for $bs = 40$ % is concentrated on lower values than the one obtained for $bs = 80$ % (see Figure 6.16).

The analysis in this chapter showed that in some aspects the data reveal significant dissimilarities between the inspected pipelines. First of all, the Pipeline A and B data report only defects located at the bottom of the pipelines, whereas in the Pipeline C, D and E data the metal loss defects are located also at the top of the pipelines. It seems that Pipeline D and E data are the most accurate ones. They both have smaller diameter and thickness than the other pipelines and this makes the defects easier to detect. Together they provide information on over 350 metal loss events and give information justifying the assumptions of the UNICORN model (the occurrence of events along the pipe follows the Poisson distribution with respect to distance). The Kolmogorov-Smirnov test tests whether two data sets differ significantly. This test proved that there is no sufficient grounds for rejecting the hypothesis that the Pipeline A and B corrosion data come from the same underlying distribution. We can include also Pipeline A1 data in this group. However, any of these data sets differ significantly from Pipeline C, D and E data. The test for lack of a significant difference between the Pipeline C and D data returned $p - value = 0.996$ indicating that the empirical distribution functions of the percentage of metal loss reported by these data sets are almost identical. This is a very strong evidence of a similarity of these two data sets. Pipeline E differs significantly from the rest of the data, because it is the only data set that includes the metal loss events with less than 10 % of removed material. Comparison of the data with the UNICORN output showed a rather good performance of the model. In case of the modelling of the frequency of failures of a pipeline laid in sand it overestimates the results a little bit, but this doesn't disqualify the model.

Chapter 7

Corrosion rate

Determining the corrosion growth rate of steel pipelines is a hot topic now. Until now there was no corrosion data available. Nowadays, there exists a technology capable to collect this kind of data. Mainly we have the MFL-pigs in mind here. This device have been used by Gasunie to inspect their pipelines. Pipeline A data might be particularly useful in determining the corrosion rate. This pipeline was inspected for the first time in 1999. Eighteen months later the pipeline has been reinspected. We shall name the data collected during the reinspection as Pipeline A1.

Ideally, to find the distribution of the corrosion rate per km.yr, we would have to determine the same corrosion spots in both data sets and then check the difference between the metal losses. This difference would be the corrosion rate per kilometer per 18 months, which can be easily transformed to corrosion rate per km.yr. Thus, the first task is to determine the same corrosion spots.

Figure 7.1 visualizes locations of the corrosion spots reported in both data sets. We can clearly see locations of the new spots like at 5.5^{th} km or 24^{th} km of the pipeline. Puzzling is the fact, that some of the spots observed in 1999 were not report in 2001 (for instance at 5^{th} km or 60^{th} km of the pipeline). Likely, this is caused by inaccurate locations of the spots given by the MFL-pig. To have perfect distinction of the corresponding spots 3 measurements must agree - two reported defects must be at the same location and position and the metal loss reported in the 1999 data must be at most equal to the metal loss detected in the 2001 data. These three conditions are not met simultaneously by the provided data.

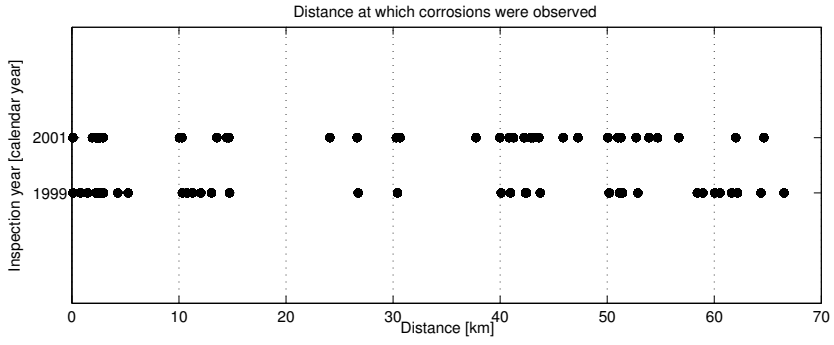

Figure 7.1: Location of the corrosion spots.

	A	B	C	D	E	F
1	Pipeline A			Pipeline A1		
2	Location	Position	Metal loss	Location	Position	Metal loss
3	43746.41	6:50	41	43618.23	05:50	21
4	43746.56	6:50	41	43618.3	05:40	14
5				43618.4	05:50	44
6						
7						
8	43747.45	7:20	29	43619.23	06:30	41
9	43747.47	7:20	16	43619.33	06:20	12

Figure 7.2: Manual searching for the corresponding spots.

Both "intelligent pig" runs were started from the same place but unfortunately, here we encounter the first problem. For none of the spots in Pipeline A data we can find the corresponding spot in Pipeline A1 data, such that the distance between them is zero (or at least close to zero). Arduous searching for any pattern in the data failed, similarly as the automated attempt performed by a MatLab function searching for the corresponding spots in the data. Figure 7.2 shows a small sample of the data which could depict related defects. First of all the difference between the locations of the defects reported in 1999 and 2001 is almost constant and equal to 120.2 m (only for this selected group of defects). This may suggest that the reference location is shifted by 120.2 m. But for a different group of defects this difference changes. Moreover, the difference between the positions is about 30° (1 hour) in this case. Now starts a long procedure of assigning the defects from both data sets. But certainly, the result is nothing that we could rely on. For example, the maximum metal loss detected in 2001 is 54 %. With very high probability, the same defect

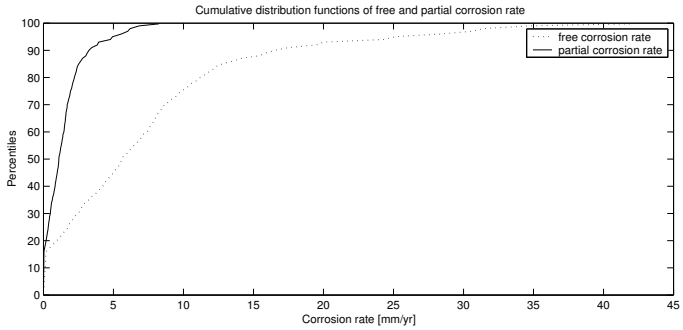

Figure 7.3: Cumulative distribution functions of free and partial corrosion rate returned by the Unicorn model for Pipeline A characteristics.

was found in 1999 and the metal loss should be close to the maximum from the observed metal losses. The maximum metal loss reported by the data from 1999 is 41 %. But the locations of these two particular defects (54 % and 41 %) are not even close to each other. The maximum reported metal loss in 1999 data at the location close to the location of 54 % metal loss defect in 2001 data is 38 %. Roughly calculating, the progress of the corrosion would be in this case at least 16 % of the pipe wall thickness, which is 1.96 mm. This gives the corrosion rate at least 1.31 mm/yr, which is 22^{nd} and 57^{th} percentile of the cumulative distribution of crf and crp respectively. These distributions were assessed by the experts.

This particular pipeline is very tough for this type of analysis, because of the defects are clustered, where two or more consecutive corrosion spots are only few centimeters from each other. We suggest that for determining the corrosion rate another pipeline should be reinspected, which need to meet the following conditions:

- defects are not clustered,
- both inspection and reinspection starts from the same reference location - all reported distances are measured from the same point,
- more accurate an same MFL-pigs are used,
- time period between the inspections should be at least 2-3 years to easier distinguish the corrosion growth

- data includes characteristics of the soil at the defects' locations (soil type, pH, resistivity),
- data includes the information on state of the cathodic protection at the defects' locations,
- data includes defects with metal loss than 0%, in contrast to the currently used 10% threshold.

The third and fourth conditions would be used to determine is we calculate *crf* or *crp* and to see the impact of the environmental factors on the corrosion rate. The last condition allows to use all information from the reinspection. Suppose there are defects with 10 % metal loss collected during the reinspection, which were not detected during the first inspection. Pipeline A data has this feature. Since we don't know what was the metal loss for these defects before the reinspection, we cannot use them to find the distribution of the corrosion rate. If we took only three first conditions into account we would recommend to reinspect pipelines D and E, especially as there is a lot of defects reported by the pipeline D and E data sets.

Chapter 8

Conclusions

Collecting corrosion data with MFL-pigs is still not a very reliable way of inspecting gas pipelines. There is an intensive development of these devices, though. The data presented and analyzed in this thesis confirm this remark. First of all, measuring the metal loss due to external corrosion is rather inaccurate and the deviation from the real value of removed wall thickness can be even more than 15 %. Currently, only excavation of the inspected pipeline allows to evaluate the quality of the measurements. Some intelligent pigs may overestimate or underestimate the metal loss. Therefore, if a pipeline is reinspected, it is very important to do this with the same device. Otherwise the results will be very hard to compare and analyze. For instance, metal loss reported during the reinspection might be less than the one collected during the previous inspection. This is the case with Pipeline A, which was inspected twice in a period of 18 months, but with two different MFL-pigs. As Gasunie stated recently, the defects with the largest metal losses found during the first inspection of Pipeline A in 1999 were repaired. Another important issue related to the MFL-pigs based inspection is accuracy of positioning of the defects. The positions we can find in the presented data are returned directly by the intelligent pig. However, before this information is used, Gasunie processes the data comparing it with the information they have on construction of the pipeline's sections. As a result, they obtain a very accurate positioning of the defects and usually, if an excavation is made for repairing a defect, they don't miss the point they are looking for. Currently, one of the pipelines owned by Gasunie is being inspected 3 times, each inspection with a different intelligent

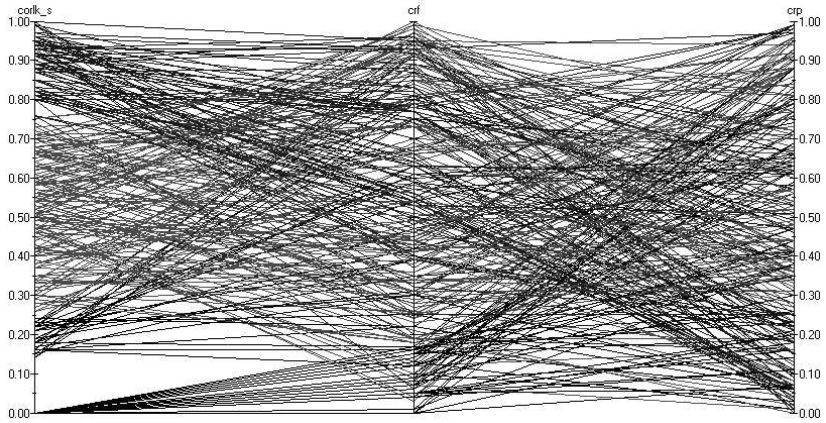

Figure 8.1: Cobweb plot of *corlk*, *crf* and *crp*.

pig. The resulting data will be very interesting obviously, since it will allow to compare the performance of the used pigs and obtain more reliable corrosion data. If, in addition, Gasunie will perform a number of excavations at some randomly chosen locations of the discovered corrosion spots in order to confirm the information provided by the pigs with the reality, then we could obtain a very nice study of the currently used inspection technology.

One possible extension of the technology applied nowadays is improving the MFL-pig by lowering the detection threshold. The data we have is reporting only the defects with metal loss more than 10 %. The exception is Pipeline E data, where the smallest metal loss defects have 5 % of removed wall thickness. However, if one look at the histogram of the data from this pipeline (Figure 6.7), he/she will immediately notice, that the number of the defects with metal loss between 5 % and 10 % is not realistic. As the metal loss approaches 0 %, the number of defects with the corresponding metal loss should converge to infinity. This is not the case here. The most likely, the data has been filtered out. To assess the number of defects with metal loss less than 10 % we can try to fit a parametric model to the corrosion data and extrapolate the information that we have on the metal losses. Under the assumption, that the data is right censored, we can find the overall distribution of the percentage of metal loss. Pipeline D data could be particularly helpful for this task, because this data set gives information on a large number of defects. Hence, the uncertainty associated with the number of defects with a given percentage of metal loss

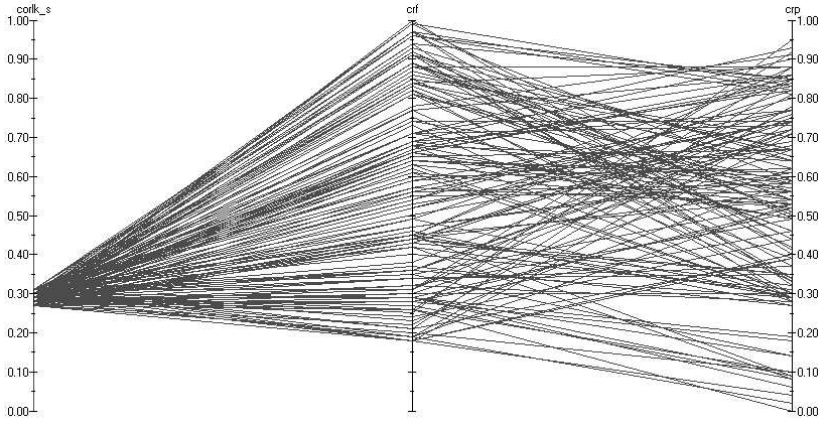

Figure 8.2: Cobweb plot of *corlk*, *crf* and *crp* conditionalized on 30$^{\text{th}}$ percentile of *corlk*.

should be the smallest among the data sets we present in this thesis. This is reflected by the histogram of this data in Figure 6.7, which depicts the most regular shape. Similarly, Pipeline E data could be used as well, but after removing the defects with metal loss less than 10 %.

Determination of the corrosion rate is a particularly tough task. Since we don't know the year in which a given corrosion spot has started to grow, the information on the percentage of metal loss gives no indication of the corrosion rate. We see that one inspection of a pipeline does not give sufficient grounds for calculation of the corrosion rate.

As it has been stated in the previous chapter, if one wants to determine the corrosion rate from the data given a twice inspected pipeline (like Pipeline A) few conditions must be met in order to have a reliable information on metal loss due to corrosion. First of all, the period of time between the inspections must be long enough such that the effect of growing corrosion is easier to detect. Moreover, the intelligent pigs used during the inspections should be accurate and, preferably, the same. A different approach to this problem involves using the UNICORN model and samples exploring tool, UNIGRAPH. Suppose, we observe a frequency of exceeding 10 % of the metal loss as equal to 0.03 per km.yr (Pipeline A data). Now we set the UNICORN model's parameters, such that the model returns the distribution of the exceeding 10 % of metal loss due to corrosion, like it has been described in Section 6.3 where we produced

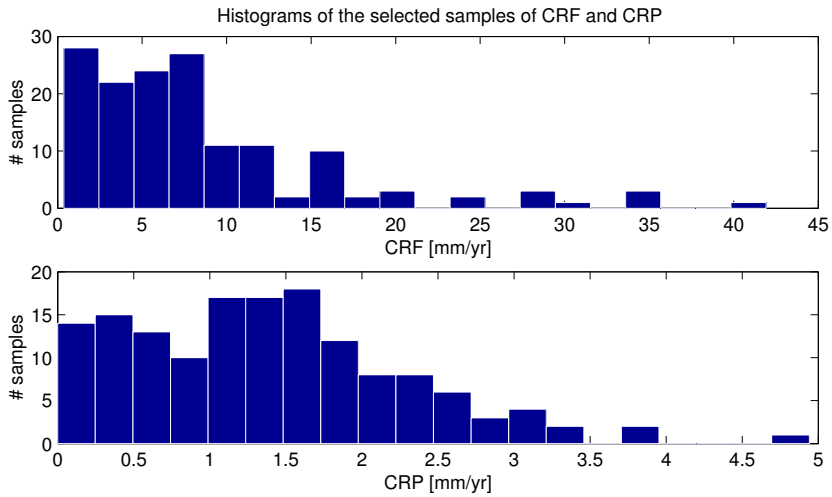

Figure 8.3: Histograms of the selected samples of *crf* and *crp*.

Figure 6.9 with the same approach. The observed frequency is equal to 30^{th} percentile of the distribution of *corlk*. We can visualize distributions of the selected variables - *corlk*, *crf* and *crp* with UNIGRAPH as in Figure 8.1. Variables *crf* and *crp* represent the corrosion rate when the cathodic protection does not work at all or works partially respectively. Values that these variables take are a direct derivative of the experts' knowledge. The only data that is used to find the distributions of *crf* and *crp* are values of the parameters *r*, *pH*, *wf* and *wu*. But if we filter the cobweb plot such that only those samples of *corlk* that are close to its 30^{th} percentile are selected, than we obtain picture like in Figure 8.2. Now, the selected samples of *crf* form an updated distribution, conditionalized on the value of *corlk*. UNIGRAPH allows to save the selected samples and work with them in an external program. Histograms of the selected samples of *crf* and *crp* are depicted in Figure 8.3. The mean *crf* is 8.55 mm/yr and the mean of *crp* is 1.39 mm/yr. These are the values of the corrosion rate that would occur if a pipeline was exposed to the same environmental conditions as Pipeline A. Of course, it is still an assessment of the experts, but conditionalized on the data. Hence, we deal here with a sort of Bayesian updating.

The UNICORN model reveals a little bit too pessimistic prediction of the gas pipeline failure frequency overestimating the data, but only if we regard

pipelines laid in sand. The situations changes completely in case of the data collected from the pipelines laid in clay. Then the model is too conservative and heavily underestimates the frequencies. Certainly, there are many factors influencing the failure frequencies not covered by the model, that could be incorporated into the model. Under some circumstances, biological organism (microbes) may influence corrosion. This influence often results in extremely accelerated rate of corrosion, but this cause of corrosion is not taken into account by the model. Peat is particularly susceptible to microbal corrosion. This soil type very often is mixed with clay. The microbal corrosion occurs mostly at the bottom of pipeline. From the existing model's parameters the critical wall thickness is relatively easy to update. The default values which are now in use might need a small adjustment based on the analysis of the experiments that many laboratories have performed. These values will change depending, for instance, on diameter of a pipeline or type of damage to pipe initiating corrosion.

The technology used in the gas industry is getting more and more sophisticated, and this is also applicable to the inspection devices such as MFL-pigs. However, data collected during inspections of gas pipelines still must be treated with caution since the measurement may vary from the true values. Using computer programs for predicting the failure frequency in combination with data will result in larger reliability of future pipelines, since this will allow to determine the factors that are the most dangerous for safe transport of liquid natural gas. UNICORN and the model introduced in this thesis are examples of a statistical tool and its application. Combination of those two with UNIGRAPH gives a system which helps to explore the statistical aspects of maintaining gas pipelines, which cannot be neglected as the information provided by uncertainty and sensitivity analysis may allow to find factors minimizing risk of failure.

Bibliography

Basalo, C. (1992), 'Water and gas mains corrosion, degradation and protection'. Ellis Horwood, New York.

Camitz, G. & Vinka, T. (1989), 'Corrosion of steel and metal-coated steel in swedish soils - effects of soil parameters'. Effects of Soil Characteristics on Corrosion ASTM STP 1013.

Chaker, V. & (eds), J. P. (1989), 'Effects of soil characteristics on corrosion'. ASTM STP 1013.

Cooke, R. (1991), 'Experts in uncertainty'. Oxford University Press, Oxford, UK.

Cooke, R., Dorrepaal, J. & Bedford, T. (1995), 'Review of ski data processing methodology, ski report 95:2'.

CPR (1999), *Guidelines for quantitative risk assessment (CPR 18E)*, Guideline, Committee for the Prevention of Disasters, The Hague, The Netherlands.

Gas Safety (Safety Case) Regulations (1999). S.R. No. 5/1999, Victoria State, Australia.

Geervliet, S. (1994), 'Modellering van de faalkans van ondergronds transportleidingen'. Report for Two Year Post Graduate Program, Department of Mathematics and Informatics, performed under contract with the Netherlands Gasunie, Delft University of Technology, Delft.

Health and Safety: The Gas Safety (Installation and Use) Regulations (1998). Statutory Instrument 1994 No. 1886, UK.

Hofer, E. & Peschke, J. (1999), 'Bayesian modeling of failure rates and initiating event frequencies', *Safety and Reliability* pp. 887–887.

Homma, T. I. T. (1990), 'An importance quantification technique in uncertainty analysis for computer models', *Proceedings of the ISUMA '90 First International Symposium on Uncertianty Modelling and Analysis* pp. 398–403.

Hopkins, P., Corder, I. & Corbin, P. (1992), 'The resistance of gas transmission pipelines to mechanical damage'. European Pipeline Research Group.

Hora, S. & Iman, R. (1990), 'Bayesian modelling of initiating event frequencies at nuclear power plants', *Risk Analysis* **10**(1), 102–109.

Kiefner, J., Vieth, P. & Feder, P. (1990), 'Methods for prioritizing pipeline maintenance and rehabilitation'. American Gas Association, Washington.

Lewandowski, D. & Cooke, R. (2001), 'Bayesian sensitivity analysis', *System and bayesian reliability - Essays in honor of professor Richard E. Barlow on his 70th birthday* **19**, 315–331.

Lewandowski, D., Cooke, R. & Jager, E. (2002), 'The failure frequency of underground gas pipelines: A model based on field data and expert judgement'. to be published in *Case Studies in Reliability and Maintenance* by W.R. Blischke and D.N.P. Murthy (eds).

Lukezich, S., Hancock, J. & Yen, B. (1992), 'State-of-the-art for the use of anti-corrosion coatings on buried pipelines in the natural gas industry'. topical report 06-3699, Gas Research Institute.

Meyer, W. & Hennings, W. (1999), 'Prior distributions in two-stage bayesian estimation of failure rates', *Safety and Reliability* pp. 893–899.

Pörn, K. (1990), 'On empirical bayesian inference applied to poisson probability models', *Linkoping Studies in Science and Technology* (Dissertation No. 234).

Wegman, E. (1990), 'Hyperdimensional data analysis using parallel coordinates', *Journal of the American Statistical Analysis* **90**(411).

Whittle, P. (1992), 'Probability via expectation', *Springer Verlag* .

Appendix A

Help file for GasUnicorn

GasUnicorn

Authors: Valery Kritchallo - core, Daniel Lewandowski - interface

Overview

The full model consists of 3 submodels:

- 3rd Party - HITPIP
- Environment
  - ENVSAND - for sand
  - ENVCLAY - for clay
  - ENVPEAT - for peat
- Corrosion
  - CORRSAND - for sand
  - CORRCLAY - for clay
  - CORRPEAT - for peat

Environment and *Corrosion* use different experts' distributions for different soil type. *Corrosion* submodel uses outputs of *3rd Party* and *Environment* models as input variables (see figure A.1). It is advisable to run the whole model in one of the following orders:

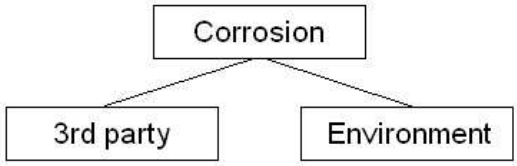

Figure A.1: Structural organization of the model.

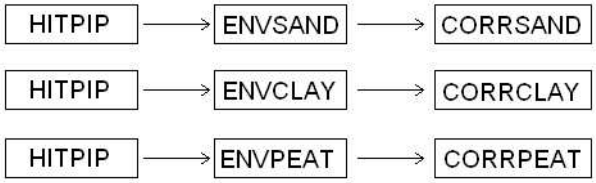

Environment model creates distributions with indices "s", "c" or "p" (crfs.dis for instance) indicating the soil type sand, clay and peat respectively. *Corrosion* model reads appropriate data, hence you can run, for example, first ENVCLAY and then CORRSAND. This will not affect the results of CORRSAND because this model reads only distributions with index "s", whereas ENVCLAY creates distribution files with index "c".

Organization of the program files

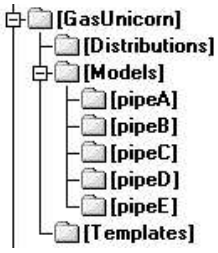

The program files are stored in predefined directories. The main program is called GasUnicorn.exe and is placed in folder *GasUnicorn*. In the same directory you will find

- Delpht.dll - program library, core of Unicorn
- Unigraph.exe - program for visualization of results (cobweb plots, density functions, scatter plots, etc)
- GasUnicorn.ini, Unigraph.ini - files with program settings

Subdirectory *Distributions* contains all experts' distributions; hence there is no need to copy them to each directory with GasUnicorn models. Subdirectory *Models* contains files with some example models. This is the main working directory upon first start of the program. There are also five folders

PipeA,...,*PipeE* containing models with parameters corresponding to characteristics of the inspected pipelines. Running a submodel will result in creating a distribution files (extension .dis) of output variables which will be used in the next submodel. Only those distribution files that are required at the next stage of the simulation process are produced. Files Cdc.dis, Cdo.dis, Dlc.dis, Dlo.dis, Ldlc.dis, Ldlo.dis, Ldsc.dis, Ldso.dis must be copied to all directories with files containing parameters for *3rd Party* (HITPIP) submodel. Folder *Templates* stores ExcelTemplate.xlt - template file used during exporting the report to Excel, and files with default values of parameters for all submodels.

The working directory can be changed. It is strongly recommended to

work only with files from directories added from within the program. This will assure removing by the program all of the intermediate files produced during the simulation.

Running the model

After the application has been started, you can load a file with models' parameters. The file can be load either by clicking one of the buttons in *Assign files to submodels* frame or appropriate menu entry.

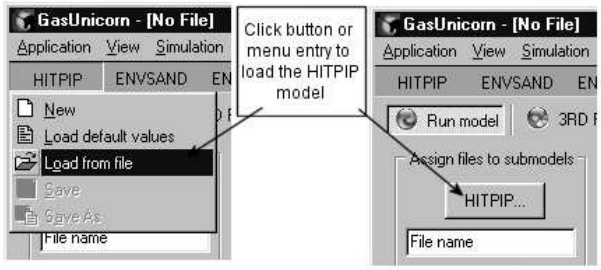

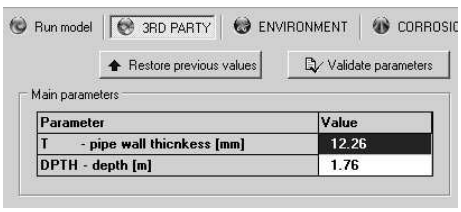

Content of the file is displayed in *3rd Party* tab. Parameters can be changed. Click *Validate parameters* to perform simple validation of the parameters (not required). This action checks whether the filled numbers and experts'

distributions file names are correct. If you want to restore values, that were there when you entered the *3rd Party* tab, click *Restore previous values* button. Keep in mind that as soon as you go to another tab, the information on previous values of parameters in tab *3rd Party* are lost.

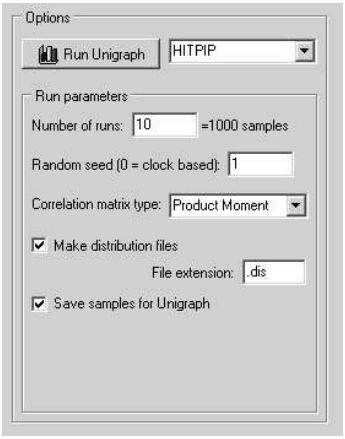

Run settings can be changed too:

- Number of runs - set number of samples you want to produce (1 run = 100 samples)
- Random seed - set the random seed which will be used to produce samples
- Correlation matrix type - set output correlation matrix type
- Make distribution type - checking this feature will produce distribution files needed to run correctly next submodels
- Save samples for Unigraph - checking this feature will make sample file with samples of all variables existing in current model. This is mandatory to enable Unigraph.

Creating report

Once the submodel has been run, we can go to *REPORT* tab and create the report by clicking button *Generate Report*. The report can be exported to Excel (requires Excel installed, preferably Excel 2000 or XP) by clicking *Excel file report*. This operation is rather time-consuming. Excel file will be saved in the same directory as the run submodel model and with the same name except the extension. You can also save text version of the report by clicking the menu bar Report → Save Report. The saved report will have extension "rep". Figure A.2 presents an exemplary report created by GasUnicorn.

New file, loading default values

To create a new set of values of parameters click *New* from the menu. However, most of the parameters, like path to experts' distribution files, do

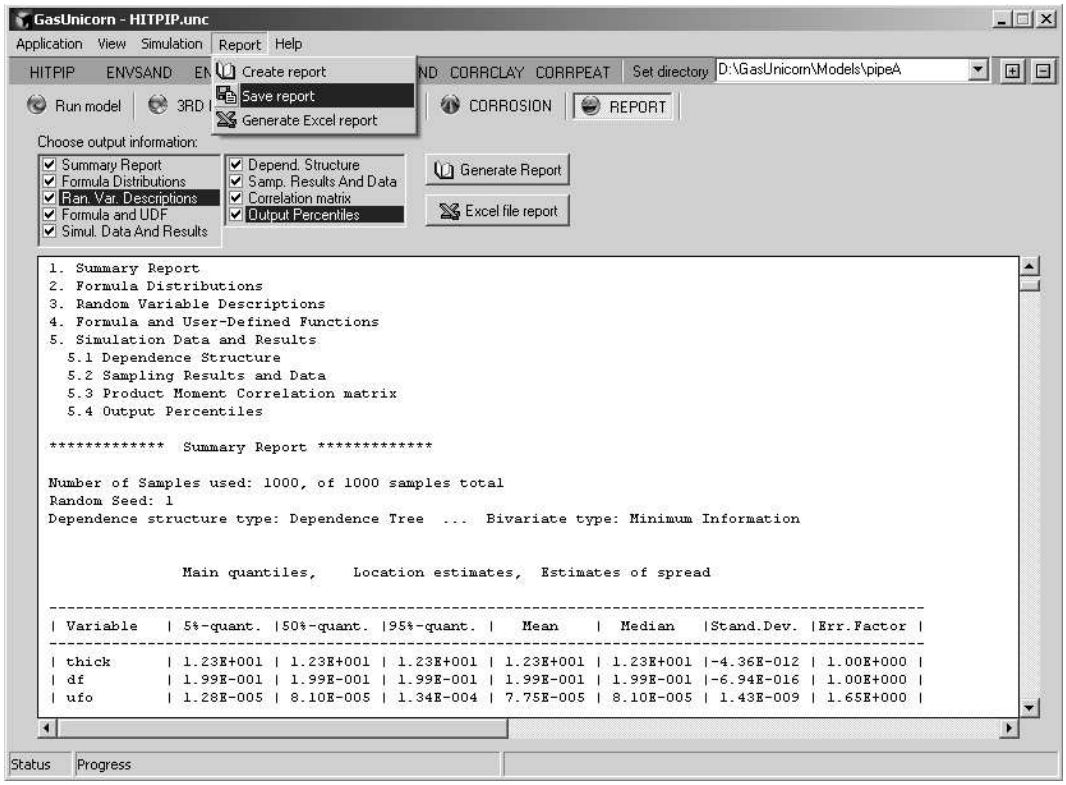

Figure A.2: Report generated by GasUnicorn.

not have to be changed. Hence it may be useful to load default values of the parameters and adjust only the most important ones. For each submodel there exists a file with default values for parameters. The names are:

- NF3RD.unc
- NFENVSAND.unc
- NFENVCLAY.unc
- NFENVPEAT.unc
- NFCORRSAND.unc
- NFCORRCLAY.unc
- NFCORRPEAT.unc

You can load these files, change values of the parameters and save. To load default values click *Load default values* from the menu.

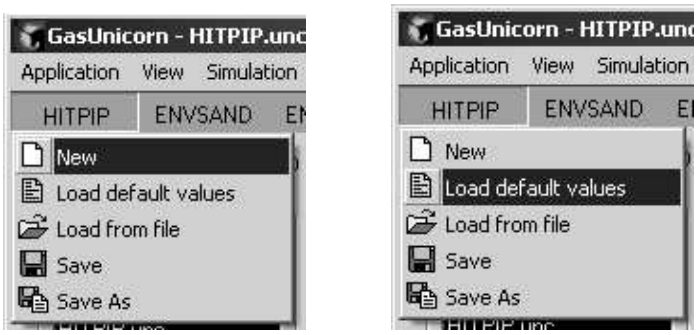

The same approach holds for the rest of the submodels.

Appendix B

Unicorn model implementation

HITPIP

Inputs:

Random variable	Value	Interpretation	Source
t	12.26	pipe wall thickness [mm]	user
dpth	1.76	depth [m]	user
fop	0.155	frequency of open digs per kmyr	user
fcl	0.052	frequency of closed digs per kmyr	user
hooyz	0.00044	freq. of hitting per kmyr; open dig, oversight, 0th order	user
hoonz	0.0008	freq. of hitting per kmyr; open dig, no oversight, 0th order	user
hcoyz	0.000166	freq. of hitting per kmyr; closed dig, oversight, 0th order	user
hconz	0.000491	freq. of hitting per kmyr; closed dig, no oversight, 0th order	user
fopz	0.155	freq. of open digs per kmyr; 0th order	user
fclz	0.052	freq. of closed digs per kmyr; 0th order	user
rcoy	26.dis	perc. of repaired damages due to hits during closed digs with oversight	experts
rcon	27.dis	perc. of repaired damages due to hits during closed digs without oversight	experts
rooy	28.dis	perc. of repaired damages due to hits during open digs with oversight	experts

Random variable	Value	Interpretation	Source
roon	29.dis	perc. of repaired damages due to hits during open digs without oversight	experts
rup71	24.dis	perc. of direct leak which will be ruptures per kmyr; 7.1 mm wt	experts
rup54	23.dis	perc. of direct leak which will be ruptures per kmyr; 5.4 mm wt	experts
hooye	01.dis	freq. of hitting per kmyr; open dig, oversight	experts
hoone	02.dis	freq. of hitting per kmyr; open dig, no oversight	experts
hcoye	03.dis	freq. of hitting per kmyr; closed dig, oversight	experts
hcone	04.dis	freq. of hitting per kmyr; closed dig, no oversight	experts

Outputs:

Formula name	Formula
thick	t
df	exp(5.43-7.31*dpth+1.88*dpthˆ2)
ufo	fop*((1-rooy)*(hooyz+(fop-fopz)*(hooye/11000-hooyz)/fopz)+ (1-roon)*(hoonz+(fop-fopz)*(hoone/11000-hoonz)/fopz))
ufc	fcl*((1-rcoy)*(hcoyz+(fcl-fclz)*(hcoye/11000-hcoyz)/fclz)+ (1-rcon)*(hconz+(fcl-fclz)*(hcone/11000-hconz)/fclz))
cd3rn	df*(ufo*cdo(t)+ufc*cdc(t))
ldsrn	df*(ufo*ldso(t)+ufc*ldsc(t))
ldlrn	df*(ufo*ldlo(t)+ufc*ldlc(t))
dl	(dlo(t)*(hooyz+(fop-fopz)*(hooye/11000-hooyz)/fopz+hoonz+ (fop-fopz)*(hoone/11000-hoonz)/fopz)+ dlc(t)*(hcoyz+(fcl-fclz)*(hcoye/11000-hcoyz)/fclz+hconz+ (fcl-fclz)*(hcone/11000-hconz)/fclz))*df
rup	dl*(rup71+(rup71-rup54)*(t-7.1)/1.7)* i1{0.00000000001,dl*(rup71+(rup71-rup54)*(t-7.1)/1.7),1}

ENVSAND

Inputs:

Random variable	Value	Interpretation	Source
%bit	1	%km with bitumen coating	user
dia	36	diameter	user
wf	0	%km with fluctuation under and above water table	user
rt	0	%km with heavy roots growth	user
ch	0	%km with heavy industrial contamination	user
ph	5.7	pH value	user
wu	0.95	% km under water table	user
crfz	0.13	default free corrosion rate	user
r	10000	resistivity	user
grb	255	rate of occurrence of bitumen defects (per 100 km)	user
grp	33	rate occurrence of polyethylene defects (per 100 km)	user
%ebe	33.dis	% of coating damages due to ground movement, root growth or chemical contamination; bitumen	experts
%epe	34.dis	% of coating damages due to ground movement, root growth or chemical contamination; polyethylene	experts
xbde	37.dis	#defects per 100 km if diameter = 36"; bitumen	experts
xbwfe	39.dis	#defects per 100 km if water table fluctuates; bitumen	experts
xbrte	41.dis	#defects per 100 km if heavy root growth; bitumen	experts
xbche	43.dis	#defects per 100 km if chemical contamination; bitumen	experts
xpde	38.dis	#defects per 100 km if diameter = 36"; polyethylene	experts
xpwfe	40.dis	#defects per 100 km if water table fluctuates; polyethylene	experts
xprte	42.dis	#defects per 100 km if heavy root growth; polyethylene	experts
xpche	44.dis	#defects per 100 km if chemical contamination; polyethylene	experts

Random variable	Value	Interpretation	Source
xre	51.dis	pit corrosion rate if resistivity is a factor 10 lower	experts
xphe	69.dis	pit corrosion rate if pH is raised by 2.3	experts
xwfe	63.dis	pit corrosion rate if water table fluctuates	experts
xwue	57.dis	pit corrosion rate if water table is above pipe lines	experts
crpe	0.0256	pit corrosion rate if the pipe ground potential is -700 mV	experts

Outputs:

Formula name	Formula
crp	crf*crpe/crfz
xbd	(xbde-grb)/(2400*(1994-1968))
xbwf	(xbwfe-grb)/(100*(1994-1968))
xbrt	(xbrte-grb)/(100*(1994-1968))
xbch	(xbche-grb)/(100*(1994-1968))
xpd	(xpde-grb)/(2400*(1994-1973))
xpwf	(xpwfe-grb)/(100*(1994-1973))
xprt	(xprte-grb)/(100*(1994-1973))
xpch	(xpche-grb)/(100*(1994-1973))
xr	(crfz-xr)/18000
xph	(xphe-crfz)/2.3
xwu	(xwue-crfz)
udfb	grb/(100*(1994-1968))+xbd*(dia-12)+xbwf*wf+xbrt*rt+xbch*ch
udfp	grp/(100*(1994-1973))+xpd*(dia-12)+xpwf*wf+xprt*rt+xpch*ch
fcde	%bit*udfb+(1-%bit)*udfp
pcde	1-exp(-fcde)
xwf	xwfe-crfz
crf	crfz+xr*(r-200000)+xph*(pH-5,7)+xwf*wf+xwu*wu
condition	i1{0,00001,crf,>>}

CORRSAND

Inputs:

Random variable	Value	Interpretation	Source
b	1967	birthyear	user
yb	1998	begin year for cumulative frequency of corrosion	user
ye	1999	end year for cumulative frequency of corrosion	user
cps	1970	year of cathodic protection (CP) installment	user
ts	0.5	material removed by small line damage [mm]	user
tl	2	material removed by large line damage [mm]	user
t	thick.dis	pipe wall thickness [mm]	user
xc	0.9	critical thickness fraction; coating damage	user
xs	0.7	critical thickness fraction; small damage	user
xl	0.6	critical thickness fraction; large damage	user
crse	87.dis	corrosion rate if there are unprotected stray currents	experts
bs	0.8	%1km pipe near bond site	user
pspe	0.93	prob. that stray current protection fails at bond site	experts
pcpfe	91.dis	prob. that CP fails completely	experts
pcppe	96.dis	prob. that CP fails partially	experts
pc3	cd3rn.dis	prob. of coating damage from 3rd parties	cd3rn.dis
ps	ldsrn.dis	prob. of small pipe damage	ldsrn.dis
pl	ldlrn.dis	prob. of large pipe damage	ldlrn.dis
dl	dl.dis	prob. of direct leak from 3rd parties	dl.dis
crf	crf_s.dis	free corrosion rate	crf.dis
pcen	pcde_s.dis	prob. of coating damage from environment	pcde.dis
crp	crp_s.dis	corrosion rate when CP partially functional	crp.dis

Outputs:

Formula name	Formula
leak	3leak+corlk-3leak*corlk
psp	pspe/600
pcpf	pcpfe/150000
pcpp	pcppe/150000
pc	min{pc3+pcen,.999}
j	vary{yb+1,ye+0.5,1}
elcf	xc*t/crf
leak	3leak+corlk-3leak*corlk
elsf	xs*(t-ts)/crf
ellf	xl*(t-tl)/crf
elcp	i1{1970,j-xc*t/crp,>>}*xc*t/crp+(1-i1{1970,j-xc*t/crp,>>})*(xc*t-(j-1970)*crp)/crf+j-1970
elsp	i1{1970,j-xs*(t-ts)/crp,>>}*xs*(t-ts)/crp+(1-i1{1970,j-xs*(t-ts)/crp,>>})*(xs*(t-ts)-(j-1970)*crp)/crf+j-1970
ellp	i1{1970,j-xl*(t-tl)/crp,>>}*xl*(t-tl)/crp+(1-i1{1970,j-xl*(t-tl)/crp,>>})*(xl*(t-tl)-(j-1970)*crp)/crf+j-1970
elcs	i1{1970,j-xc*t*24/crse,>>}*xc*t*24/crse+(1-i1{1970,,j-xc*t*24/crse,>>})*(xc*t-(j-1970)*crse/24)/crse+ j-1970
elss	i1{1970,j-xs*(t-ts)*24/crse,>>}*xs*(t-ts)*24/crse+(1-i1{1970,,j-xs*(t-ts)*24/crse,>>})*(xs*(t-ts)-(j-1970)*crse/24)/crse+j-1970
ells	i1{1970,j-xl*(t-tl)*24/crse,>>}*xs*(t-tl)*24/crse+(1-i1{1970,,j-xl*(t-tl)*24/crse,>>})*(xl*(t-tl)-(j-1970)*crse/24)/crse+j-1970
qcf	min{max{j-elcf-b, .00009}, y-yb}
qsf	min{max{j-elsf-b, .00009}, y-yb}
qlf	min{max{j-ellf-b, .00009}, y-yb}
qcp	min{max{j-elcp-b, .00009}, y-yb}
qsp	min{max{j-elsp-b, .00009}, y-yb}
qlp	min{max{j-ellp-b, .00009}, y-yb}
qcs	min{max{j-elcs-b, .00009}, y-yb}
qss	min{max{j-elss-b, .00009}, y-yb}
qls	min{max{j-ells-b, .00009}, y-yb}
pcrf	sum((1-pcˆ2)ˆmax{qcf-1,0}*(1-ps)ˆqsf*(1-pl)ˆqlf*i1{1,qcf,>>}*(1-(1-pcpf)ˆ(-ln(1-pc)))+((1-pc)ˆqcf*(1-ps)ˆmax{qsf-1,0}*(1-pl)ˆqlf*ps*i1{1,qsf,>>}+(1-pc)ˆqcf*(1-ps)ˆqsf*(1-pl)ˆmax{qlf-1,0}*pl*i1{1,qlf,>>})*pcpf)

Formula name	Formula
pcrp	sum((1-pc^2)^max{qcp-1,0}*(1-ps)^qsp*(1-pl)^qlp*i1{1,qcp,>>}*(1-(1-pcpp)^(-ln(1-pc)))+((1-pc)^qcp*(1-ps)^max{qsp-1,0}*(1-pl)^qlp*ps*i1{1,qsp,>>}+(1-pc)^qcp*(1-ps)^qsp*(1-pl)^max{qlp-1,0}*pl*i1{1,qlp,>>})*pcpp)
pcrs	sum((1-pc^2)^max{qcs-1,0}*(1-ps)^qss*(1-pl)^qls*i1{1,qcp,>>}*(1-(1-bs)^(-ln(1-pc)))+((1-pc)^qcs*(1-ps)^max{qss-1,0}*(1-pl)^qls*ps*i1{1,qss,>>}+(1-pc)^qcs*(1-ps)^qss*(1-pl)^max{qls-1,0}*pl*i1{1,qls,>>})*psp)
3leak	sum((1-dl)^(j-yb-1)*dl)
corlk	pcrf+pcrp+pcrs-pcrf*pcrp-pcrf*pcrs*pcrp*pcrs+pcrf*pcrp*pcrp

Appendix C

MatLab code performing preliminary analysis

Main code of the program.

```
1  function varargout = CorRate(varargin)
2  % CORRATE Application M-file for CorRate.fig
3  % Performs extensive visualization of the corrosion data
4  % from 4 pipelines.
5  %    FIG = CORRATE launch CorRate GUI.
6  %    CORRATE('callback_name', ...) invoke the named callback.
7  %
8  % Last Modified by GUIDE v2.0 26-May-2002 14:42:42
9
10 global fi
11
12 if nargin == 0  % LAUNCH GUI
13
14     fig = openfig(mfilename,'reuse');
15
16     scrsz = get(0,'ScreenSize');
17     fi = figure('Units','pixels','ToolBar','figure','Name',...
18     'Analysis Screen','NumberTitle','off','Position',...
19     [191 32 scrsz(3)-193 scrsz(4)-104]);
20
21     % Generate a structure of handles to pass to callbacks,
22     % and store it.
23     handles = guihandles(fig);
24     guidata(fig, handles);
```

```
25
26      pop = 0;
27
28      if nargout > 0
29          varargout{1} = fig;
30      end
31
32  elseif ischar(varargin{1}) % INVOKE NAMED SUBFUNCTION OR CALLBACK
33
34      try
35          [varargout{1:nargout}] = feval(varargin{:}); % FEVAL switchyard
36      catch
37          disp(lasterr);
38      end
39
40  end
```

Total number of corrosions vs distance from the starting point.

```
41  % --------------------------------------------------------------------
42  function varargout = pushbutton1_Callback(h, eventdata, handles,...
43      varargin)
44  % Stub for Callback of the uicontrol handles.pushbutton1.
45  global fi
46
47  subplot(1,1,1);
48  [p1, p2, name1, name2] = determine_data(handles);
49  set(fi,'Name','TOTAL NUMBER OF OBSERVED CORROSIONS');
50  if ~isempty(name1)
51      stairs(p1.stationary, [1:length(p1.stationary)]);
52      text(max(p1.stationary)*.95,length(p1.stationary)+1.5,name1);
53      hold on;
54  end
55  if ~isempty(name2)
56      stairs(p2.stationary, [1:length(p2.stationary)],'r');
57      text(max(p2.stationary)*.95,length(p2.stationary)+1.5,name2);
58  end
59
60  hold off;
61  title('Total number of corrosions vs distance from the starting point');
62  xlabel('Distance [m]');
63  ylabel('Total number of corrosions');
64
```

```
65  if isequal(name1,'pipeA') & isequal(name2,'pipeA1')
66      legend('October 1999','August 2001',4);
67      set(handles.text1,'Visible','on','String',...
68          [{' OBSERVATIONS:';'Length of the pipeline - 66 km';...
69          'October 1999 - 65 events';'August 2001 - 74 events';}]);
70  end
```

Quantile-quantile plot of both corrosion data sets.

```
71  % --------------------------------------------------------------------
72  function varargout = pushbutton2_Callback(h, eventdata, handles,...
73      varargin)
74  % Stub for Callback of the uicontrol handles.pushbutton2.
75  global fi
76
77  subplot(1,1,1);
78  [p1, p2, name1, name2] = determine_data(handles);
79  set(fi,'Name','QUANTILE-QUANTILE PLOT OF BOTH DATA SETS');
80  subplot(1,1,1);
81  qqplot(p1.ml,p2.ml);
82  title('Quantile-quantile plot of both corrosion data sets');
83  xlabel([name1,' data quantiles']);
84  ylabel([name2,' data quantiles']);
```

Empirical distribution functions.

```
85  % --------------------------------------------------------------------
86  function varargout = pushbutton3_Callback(h, eventdata, handles,...
87      varargin)
88  % Stub for Callback of the uicontrol handles.pushbutton3.
89  global fi
90
91  [p1, p2, name1, name2] = determine_data(handles);
92  set(fi,'Name','EMPIRICAL CDF');
93  subplot(1,1,1);
94  if ~isempty(name1)
95      cdfplot(p1.ml);
96      hold on;
97  end
98  if ~isempty(name2)
99      hand = cdfplot(p2.ml);
100     set(hand,'Color','r');
101 end
102 hold off;
```

```
103  title('Empirical distribution functions');
104  xlabel('Metal loss [\%]');
105  ylabel('CDF');
106  if ~isempty(name1) | ~isempty(name2)
107      if ~isempty(name1) & ~isempty(name2)
108          legend(name1,name2,4);
109      end
110      if ~isempty(name1) & isempty(name2)
111          legend(name1,4);
112      end
113      if isempty(name1) & ~isempty(name2)
114          legend(name2,4);
115      end
116  end
117  axis([5 60 0 1.1])
118
119  % Kolmogorov-Smirnoff test
120  if ~isempty(name1) & ~isempty(name2)
121      [thesis,p,ksstat] = kstest2(p1.ml,p2.ml);
122      if thesis == 0
123          rej = '   NOT REJECTED';
124      else
125          rej = '   REJECTED';
126      end
127
128      set(handles.text1,'Visible','on','String',[{' KS TEST:';...
129         'H0 - two independent random samples are drawn
130         from the same underlying continuous population';...
131         [' 1) H0: ', rej]; [' 2) p-value: ', num2str(p)];...
132         [' 3) ks-statistics: ', num2str(ksstat)]}]);
133  end
```

Length vs Width of corrosion events.

```
134  % --------------------------------------------------------------------
135  function varargout = pushbutton4_Callback(h, eventdata, handles,...
136      varargin)
137  % Stub for Callback of the uicontrol handles.pushbutton4.
138  global fi
139
140  [p1, p2, name1, name2] = determine_data(handles);
141  set(fi,'Name','LENGTH/ WIDTH SCATTER PLOT');
142  subplot(1,1,1);
```

```
143  if ~isempty(name1)
144      loglog(p1.length,p1.width,'o','MarkerEdgeColor','b',...
145          'MarkerFaceColor','b','MarkerSize',5)
146      hold on;
147  end
148  if ~isempty(name2)
149      loglog(p2.length,p2.width,'o','MarkerEdgeColor','m',...
150          'MarkerFaceColor','m','MarkerSize',5)
151  end
152  hold off;
153  title('Length vs Width of corrosion events');
154  xlabel('Length [mm]');
155  ylabel('Width [mm]');
156  if ~isempty(name1) | ~isempty(name2)
157      if ~isempty(name1) & ~isempty(name2)
158          legend(name1,name2,4);
159      end
160      if ~isempty(name1) & isempty(name2)
161          legend(name1,4);
162      end
163      if isempty(name1) & ~isempty(name2)
164          legend(name2,4);
165      end
166  end
```

Distance at which corrosion was observed.

```
167  % --------------------------------------------------------------------
168  function varargout = pushbutton5_Callback(h, eventdata, handles,...
169      varargin)
170  % Stub for Callback of the uicontrol handles.pushbutton5.
171  global fi
172
173  load pipeA;
174  load pipeA1;
175  subplot(1,1,1);
176  set(fi,'Name','DISTANCE');
177  subplot(1,1,1);
178  plot(pipeA.stationary,ones(length(pipeA.stationary)),...
179     'o','MarkerEdgeColor','b','MarkerFaceColor','b','MarkerSize',5);
180  hold on;
181  plot(pipeA1.stationary,ones(length(pipeA1.stationary))*2,...
182     'o','MarkerEdgeColor','b','MarkerFaceColor','b','MarkerSize',5);
```

```
183  hold off;
184  set(gca,'YLim',[-1,4]);
185  set(gca,'YTick',[1:2],'YTickLabel',{'1999','2001'});
186  set(gca,'XGrid','on');
187
188  title('Distance at which corrosion was observed');
189  xlabel('Distance [m]');
190  ylabel('Inspection year [calendar year]');
```

Histogram of the corrosion data.

```
191  % --------------------------------------------------------------------
192  function varargout = pushbutton6_Callback(h, eventdata, handles,...
193      varargin)
194  % Stub for Callback of the uicontrol handles.pushbutton6.
195  global fi
196
197  [p1, p2, name1, name2] = determine_data(handles);
198  set(fi,'Name','HISTOGRAMS');
199  if ~isempty(name1) | ~isempty(name2)
200      if ~isempty(name1) & ~isempty(name2)
201          subplot(2,1,1);
202          hist(p1.ml,15);
203          title(['Histogram of the ', name1, ' data']);
204          xlabel('Metal loss [%]');
205          ylabel('Number of corrosion events');
206
207          subplot(2,1,2);
208          hist(p2.ml,15);
209          title(['Histogram of the ', name2, ' data']);
210          xlabel('Metal loss [%]');
211          ylabel('Number of corrosion events');
212      else if ~isempty(name1)
213          subplot(1,1,1);
214          hist(p1.ml,15);
215          title(['Histogram of the ', name1, ' data']);
216          xlabel('Metal loss [%]');
217          ylabel('Number of corrosion events');
218      else
219          subplot(1,1,1);
220          hist(p2.ml,15);
221          title(['Histogram of the ', name2, ' data']);
222          xlabel('Metal loss [%]');
```

```
223           ylabel('Number of corrosion events');
224       end
225       end
226   end
```

Destroy figure and quit program.

```
227   % --------------------------------------------------------------------
228   function varargout = figure1_DeleteFcn(h, eventdata, handles,...
229       varargin)
230   % Stub for DeleteFcn of the figure handles.figure1.
231   global fi
232
233   delete(fi);
```

Minimum distance between corrosion events given by both data sets.

```
234   % --------------------------------------------------------------------
235   function varargout = popupmenu1_Callback(h, eventdata, handles,...
236       varargin)
237   % Stub for Callback of the uicontrol handles.popupmenu1.
238   global fi
239
240   load pipeA;
241   load pipeA1;
242   set(fi,'Name','1:1 PROJECTION');
243   subplot(1,1,1);
244
245   g = zeros(length(pipeA.stationary));
246
247   for i=1:length(pipeA.stationary)
248       g(i) = min(abs(pipeA1.stationary-pipeA.stationary(i)));
249   end
250
251   for i=1:length(pipeA.stationary)
252       d(i).ind = find(pipeA1.stationary-pipeA.stationary(i)==g(i));
253   end
254
255   switch get(handles.popupmenu1,'Value')
256   case 2
257       stem(pipeA.stationary,g);
258       xlabel('Distance [m]');
259   case 3
260       stem(g);
```

```
261       xlabel('Index of the corrosion event in the pipeA data');
262   end
263   hold off;
264   title('Minimum distance between corrosion events...
265       given by both data sets');
266   ylabel('Minimum distance [m]');
```

Positions of the corrosion spots on the surface of pipelines.

```
267   % --------------------------------------------------------------------
268   function varargout = popupmenu2_Callback(h, eventdata, handles,...
269       varargin)
270   % Stub for Callback of the uicontrol handles.popupmenu2.
271   global fi
272
273   set(fi,'Name','POSITIONS');
274   switch get(handles.popupmenu2,'Value')
275   case 2
276       load pipeA;
277       MyData = pipeA;
278   case 3
279       load pipeA1;
280       MyData = pipeA1;
281   case 4
282       load pipeB;
283       MyData = pipeB;
284       clear pipeB;
285   case 5
286       load pipeC;
287       MyData = pipeC;
288       clear pipeC;
289   case 6
290       load pipeD;
291       MyData = pipeD;
292       clear pipeD;
293   case 7
294       load pipeE;
295       MyData = pipeE;
296       clear pipeE;
297   end subplot(1,1,1);
298   if get(handles.popupmenu2,'Value')>1
299       i = [0:0.025:0.5];
300       N = histc(MyData.position,i);
```

```
301       [XX,YY] = stairs(i,N);
302       XX = XX * 4 * pi;
303       N = N/sum(N);
304       XX = 2*pi - XX;
305       max(YY)
306       YY = YY/sum(YY);
307       YY = YY*0.1957/max(YY);
308       area(max(YY)*2*cos([0:0.01:2*pi]),...
309           max(YY)*2*sin([0:0.01:2*pi]),'FaceColor','red',...
310           'LineStyle','none');
311       hold on;
312       area((max(YY)*2 - YY).*cos(XX+pi/2),...
313           (max(YY)*2-YY).*sin(XX+pi/2),'FaceColor','white',...
314           'LineStyle','none');
315       plot(max(YY)*cos([0:0.01:2*pi]),max(YY)*sin([0:0.01:2*pi]),...
316           'LineStyle',':');
317       axis([-max(YY)*2 max(YY)*2 -max(YY)*2 max(YY)*2]);
318       hold on;
319       pbaspect([1 1 1]);
320       text(0,max(YY)*2 + 0.02,'0^{o}');
321       text(max(YY)*2 + 0.01,0,'90^{o}');
322       text(0,-(max(YY)*2+0.02),'180^{o}');
323       text(-(max(YY)*2+0.05),0,'270^{o}');
324       set(gca,'YTick',[]);
325       set(gca,'XTick',[])
326       hold off;
327   end
```

Determine data set to load.

```
328   % --------------------------------------------------------------------
329   function [p1, p2, name1, name2] = determine_data(handles)
330
331   name1 = '';
332   name2 = '';
333
334   switch get(handles.popupmenu3,'Value') case 1
335       load pipeA;
336       p1 = pipeA;
337       clear pipeA;
338   case 2
339       load pipeA;
340       p1 = pipeA;
```

```
341       clear pipeA;
342       name1 = 'pipeA';
343   case 3
344       load pipeA1;
345       p1 = pipeA1;
346       clear pipeA1;
347       name1 = 'pipeA1';
348   case 4
349       load pipeB;
350       p1 = pipeB;
351       clear pipeB;
352       name1 = 'pipeB';
353   case 5
354       load pipeC;
355       p1 = pipeC;
356       clear pipeC;
357       name1 = 'pipeC';
358   case 6
359       load pipeD;
360       p1 = pipeD;
361       clear pipeD;
362       name1 = 'pipeD';
363   case 7
364       load pipeE;
365       p1 = pipeE;
366       clear pipeE;
367       name1 = 'pipeE';
368   end
369
370   switch get(handles.popupmenu4,'Value') case 1
371       p2check = 0;
372       load pipeA;
373       p2 = pipeA;
374       clear pipeA;
375   case 2
376       load pipeA;
377       p2 = pipeA;
378       clear pipeA;
379       name2 = 'pipeA';
380   case 3
381       load pipeA1;
382       p2 = pipeA1;
```

```
383       clear pipeA1;
384       name2 = 'pipeA1';
385   case 4
386       load pipeB;
387       p2 = pipeB;
388       clear pipeB;
389       name2 = 'pipeB';
390   case 5
391       load pipeC;
392       p2 = pipeC;
393       clear pipeC;
394       name2 = 'pipeC';
395   case 6
396       load pipeD;
397       p2 = pipeD;
398       clear pipeD;
399       name2 = 'pipeD';
400   case 7
401       load pipeE;
402       p2 = pipeE;
403       clear pipeE;
404       name2 = 'pipeE';
405   end
```

Display comparison of the data with the model output.

```
406   % --------------------------------------------------------------------
407   function varargout = popupmenu5_Callback(h, eventdata, handles,...
408       varargin)
409   % Stub for Callback of the uicontrol handles.popupmenu5.
410   global fi
411
412   MyData = 0;
413   x = [0.25 1:99 99.75];
414   set(fi,'Name','UNICORN''s DATA');
415   switch get(handles.popupmenu5,'Value')
416   case 2
417       load pipeAunc;
418       MyData = pipeAunc;
419       clear pipeAunc;
420       name = 'A';
421   case 3
422       load pipeA1unc;
```

```
423       MyData = pipeA1unc;
424       clear pipeA1unc;
425       name = 'A1';
426   case 4
427       load pipeBunc;
428       MyData = pipeBunc;
429       clear pipeBunc;
430       name = 'B';
431   end
432   subplot(1,1,1);
433   semilogx(MyData.d10,x,'b');
434   hold on;
435   semilogx(MyData.d15,x,'r');
436   semilogx(MyData.d20,x,'k');
437   semilogx(MyData.d25,x,'g');
438   semilogx(MyData.d30,x,'y');
439   semilogx(MyData.d35,x,'m');
440   semilogx(MyData.d40,x,'c');
441   perc = find(abs(MyData.d10 - MyData.unic(1)) == ...
442       min(abs(MyData.d10 - MyData.unic(1))));
443   semilogx(MyData.d10(perc),x(perc),'s','MarkerEdgeColor',...
444      'b','MarkerFaceColor','b','MarkerSize',5);
445   perc = find(abs(MyData.d15 - MyData.unic(2)) == ...
446       min(abs(MyData.d15 - MyData.unic(2))));
447   semilogx(MyData.d15(perc),x(perc),'s','MarkerEdgeColor',...
448       'r','MarkerFaceColor','r','MarkerSize',5);
449   perc = find(abs(MyData.d20 - MyData.unic(3)) == ...
450       min(abs(MyData.d20 - MyData.unic(3))));
451   semilogx(MyData.d20(perc),x(perc),'s','MarkerEdgeColor',...
452       'k','MarkerFaceColor','k','MarkerSize',5);
453   perc = find(abs(MyData.d25- MyData.unic(4)) == ...
454       min(abs(MyData.d25 - MyData.unic(4))));
455   semilogx(MyData.d25(perc),x(perc),'s','MarkerEdgeColor',...
456       'g','MarkerFaceColor','g','MarkerSize',5);
457   perc = find(abs(MyData.d30 - MyData.unic(5)) == ...
458       min(abs(MyData.d30 - MyData.unic(5))));
459   semilogx(MyData.d30(perc),x(perc),'s','MarkerEdgeColor',...
460       'y','MarkerFaceColor','y','MarkerSize',5);
461   perc = find(abs(MyData.d35 - MyData.unic(6)) == ...
462       min(abs(MyData.d35 - MyData.unic(6))));
463   semilogx(MyData.d35(perc),x(perc),'s','MarkerEdgeColor',...
464       'm','MarkerFaceColor','m','MarkerSize',5);
```

```
465  perc = find(abs(MyData.d40 - MyData.unic(7)) == ...
466      min(abs(MyData.d40 - MyData.unic(7))));
467  semilogx(MyData.d40(perc),x(perc),'s','MarkerEdgeColor',...
468      'c','MarkerFaceColor','c','MarkerSize',5);
469  hold off;
470  axis([10^(-12) 10^0 0 100]);
471  legend('10\%','15\%','20\%','25\%','30\%','35\%','40\%',2);
472  xlabel('Frequency corrosion per kmyr');
473  ylabel('Percentiles');
474  title(['Frequency of exceeding a certain percentage of ...
475      corrosion based on pipe ', name, ' data.']);
476  text(10^(-10), 95, 'Squares mark the data from the pipelines');
```

Vita

Daniel Lewandowski was born in Poland in 1977. In 1997 he began mathematical studies at the Technical University of Zielona Góra, Poland. During the studies he completed a course in *Risk and Uncertainty Analysis* at the Delft University of Technology and in 2000 he became a regular MSc student at this university.